GEORG-AUGUST-UNIVERSITÄT
GÖTTINGEN IN PUBLICA COMMODA SEIT 1737

The evolution of the head appendages in marine bristle worms

Dissertation

for the award of the degree

"Doctor rerum naturalium" (Dr.rer.nat.)

of the Georg-August-Universität Göttingen

within the doctoral program “Biodiversity and Ecology”

of the Georg-August University School of Science (GAUSS)

submitted by

Paul Kalke

from Berlin, Germany

Göttingen, 2023

Thesis Committee

Prof. Dr. Christoph Bleidorn
(Johann-Friedrich-Blumenbach-Institute for Zoology & Anthropology, Dpt. of Animal Evolution and Biodiversity, University of Goettingen, Goettingen)

Prof. Dr. Andreas Stumpner
(Schwann-Schleiden Research Centre, Dept. Cellular Neurobiology, University of Goettingen, Goettingen)

Dr. Conrad Helm
(Johann-Friedrich-Blumenbach-Institute for Zoology & Anthropology, Dpt. of Animal Evolution and Biodiversity, University of Goettingen, Goettingen)

Members of the Examination Board

1st Reviewer: Prof. Dr. Christoph Bleidorn
(Johann-Friedrich-Blumenbach-Institute for Zoology & Anthropology, Dpt. of Animal Evolution and Biodiversity, University of Goettingen, Goettingen)

2nd Reviewer: Prof. Dr. Andreas Stumpner
(Schwann-Schleiden Research Centre, Dept. of Cellular Neurobiology, University of Goettingen, Goettingen)

Further members of the Examination Board:

Prof. Dr. Susann Boretius
(Functional Imaging Unit, German Primate Center, Goettingen)

Dr. Nico Posnien
(Johann-Friedrich-Blumenbach-Institute for Zoology & Anthropology, Dpt. of Developmental Biology, University of Goettingen, Goettingen)

Prof. Dr. Daniel J. Jackson
(Dpt. of Geobiology, University of Goettingen, Goettingen)

Prof. Dr. Mark Maraun
(Johann-Friedrich-Blumenbach-Institute for Zoology & Anthropology, Dpt. of Animal Ecology, University of Goettingen, Goettingen)

Date of the oral examination: November 17, 2023

to Ronja and Marie -

my beloved family.

Table of Contents

Acknowledgements

First and foremost, I would like to express my gratitude to Conrad Helm, my supervisor and friend, who instilled in me a deep passion for fluorescence microscopy and, of course, annelids during my bachelor's degree in Leipzig. You are the mentor I had always hoped for. I genuinely hope that our collaboration will continue beyond this chapter, allowing us to work together on the subjects we are so passionate about in an engaging manner.

I extend my heartfelt thanks to Christoph Bleidorn. Without your belief in the project and in me, this endeavor would not have materialized without external funding. I am immensely grateful for granting me the opportunity to delve into this incredibly exciting topic within our esteemed research group, and for providing us with the exceptional coffee machine.

Special recognition is also due to Andreas Stumpner, who served as my second examiner and a member of the thesis committee. His guidance, precise questioning, and insightful advice have been invaluable. Additionally, I wish to express my gratitude to Prof. Dr. Daniel J. Jackson, Prof. Dr. Susann Boretius, Dr. Nico Posnien, and Prof. Dr. Mark Maraun for generously participating in my defense as members of the examination committee.

I want to convey my appreciation to all the members and colleagues in our department, particularly Yegi, Sarah, Rabea, Marco, Sven, and Moni. Their words of encouragement, attentive listening, and the camaraderie we shared over beers and conversations contributed significantly to the positive atmosphere at work.

This work is dedicated to the family I have found here, my beloved Marie, and our precious daughter, Ronja Mathilda. Both of you have defied the skeptics who claimed that pursuing a doctorate and raising a child were incompatible. Without your unwavering support, I might have faltered during these past few years, and I wouldn't have successfully navigated this stage so swiftly and unscathed. You are my pillars of strength and have illuminated my life with more beauty than worm brains could ever offer. Thank you for the wonderful life we have built together.

I must express my gratitude, no less profound, to my mother, Andrea, who is the most resilient person I've ever known, and to my perceptive and warm-hearted father, Bernd, who, unfortunately, did not live to witness the conclusion of this chapter but profoundly influenced my journey. I also wish to thank my sister, Karoline, her partner, Carl, and their son, Levi, for the cherished moments we have shared and will continue to enjoy, as we collectively embrace the experience of building and growing with our own families.

Lastly, but certainly not least, I want to extend my appreciation to friends like Leo and Phil from Göttingen, who have transitioned from being flatmates to becoming friends, babysitters, sled builders, fellow gardeners, and even godparents. Many thanks are also owed to the friends who have remained steadfast from other cities such as Berlin, Leipzig, and Rostock. Reuniting after months apart feels like we said goodbye just yesterday. Thank you for being such exceptional, intriguing, and warm-hearted individuals in my life.

Summary

Annelida can be found in all kind of habitats and thus show a huge diversity in form, size, and colour. A key structure for their evolutionary success and adaptability to their individual lifestyles are the head appendages. The sheer diversity and the baffling distribution of palps, antennae, buccal lips, and tentacular cirri among annelid families have fascinated researchers over decades. Lars Orrhage, a pioneer in the field of annelid comparative morphology, started to unravel the evolutionary history of head appendages in polychaetes by the systematic investigation of the anterior nervous system. However, recent studies question his findings. By using an integrative morphological approach including immunohistochemistry and confocal laser scanning microscopy in combination with Azan-stained serial histology sections, and subsequent 3D-visualization, I comparatively investigated the innervation patterns of head appendages in annelid key taxa in different ontogenetic stages. Chapter II presents an examination concerning a century-old debate regarding the Terebelliformia, a subgroup within the Sedentaria. A proposal is presented regarding the homology of their numerous buccal tentacles with feeding-palps found in other annelid taxa. Chapter III, which is primarily methodological in nature, emphasizes the necessity of employing 3D visualizations through open-source software. This chapter furnishes a modular workflow and a comprehensive, step-by-step guide for conducting morphological research using image stack-based datasets. Chapter IV involves a comparative study of the larval and adult anterior nervous systems of Magelonidae, Amphinomidae, and Spionidae. As a result of this investigation, homologies were identified between the feeding-palps in both distantly related groups, Paleo- and Pleistoannelida. Chapter V centres on the investigation of members of the errant Nereididae, ultimately culminating in the proposition that feeding-palps and short sensorial palps, collectively referred to as "palps," in Annelida exhibit homology across the entirety of their phylogenetic tree.

My thesis challenges established knowledge about the evolution of annelid head appendages and answers old questions by using a combination of microscopic methods. I discuss the changes of the understanding about the evolutionary origin and history of head appendages induced by recent research, and show the benefits of open-source software solutions. Additionally, I stress the importance of the integration of different ontogenetic stages into analyses of old morphological traits.

Zusammenfassung

Annelida kommen in den verschiedensten Lebensräumen vor und weisen daher eine große Vielfalt an Formen, Größen und Farben auf. Eine Schlüsselstruktur für ihren evolutionären Erfolg und ihre Anpassungsfähigkeit an ihre individuelle Lebensweise sind ihre Kopfanhänge. Die schiere Vielfalt und die verblüffende Verteilung von Palpen, Antennen, Bukkallippen und Tentakelzirren unter den Ringelwürmern hat die Forschung über Jahrzehnte fasziniert. Lars Orrhage, ein Pionier auf dem Gebiet der vergleichenden Morphologie der Ringelwürmer, begann, die Evolutionsgeschichte der Kopfanhänge bei Polychaeten durch die systematische Untersuchung des vorderen Nervensystems zu entschlüsseln. Neuere Studien stellen seine Ergebnisse jedoch in Frage. Mit Hilfe eines integrativen morphologischen Ansatzes, der Immunhistochemie und konfokale Laser-Scanning-Mikroskopie in Kombination mit Azan-gefärbten seriellen Histologieschnitten und anschließender 3D-Visualisierung umfasst, habe ich die Innervationsmuster von Kopfanhängen bei Schlüsseltaxa in verschiedenen ontogenetischen Stadien vergleichend untersucht. In Kapitel II wurde eine jahrhundertealte Debatte über die Terebelliformia, eine Untergruppe innerhalb der Sedentaria, untersucht, wobei die Homologie ihrer zahlreichen bukkalen Tentakel mit den langen Fress-Palpen anderer Anneliden-Taxa aufgezeigt wurde. Kapitel III, das in erster Linie methodischer Natur ist, unterstreicht die Notwendigkeit des Einsatzes von 3D-Visualisierungen durch Open-Source-Software. In diesem Kapitel werden ein modularer Arbeitsablauf und eine umfassende Schritt-für-Schritt-Anleitung für die Durchführung von morphologischen Untersuchungen anhand von Bildstapeldatensätzen präsentiert. Kapitel IV beinhaltet eine vergleichende Studie des vorderen Nervensystems von Larven und erwachsenen Tieren der Magelonidae, Amphinomidae und Spionidae. Als Ergebnis dieser Untersuchung wurden Homologien zwischen den Fress-Palpen der beiden entfernt verwandten Gruppen Paleo- und Pleistoannelida festgestellt. Kapitel V konzentriert sich auf die Untersuchung von Mitgliedern der Nereididae und gipfelt schließlich in der These, dass die Fresspalpen und die kurzen sensorischen Palpen, die zusammen als "Palpen" bezeichnet werden, bei den Annelida über den gesamten Stammbaum hinweg homolog sind.

Meine Dissertation stellt das etablierte Wissen über die Evolution der Kopfanhänge von Anneliden in Frage und beantwortet alte Fragen mit einer Kombination von mikroskopischen Methoden. Ich diskutiere die Veränderungen des Verständnisses über den evolutionären Ursprung und die Geschichte der Kopfanhänge, die durch die jüngste Forschung ausgelöst wurden, und zeige die Vorteile von Open-Source-Softwarelösungen auf. Ebenso betone ich die Wichtigkeit der Integration verschiedener ontogenetischer Stadien in Analysen alter morphologischer Merkmale.

Overview of publications

This is a publication-based, cumulative dissertation. The following chapters have been accepted by or submitted to peer-reviewed scientific journals:

Chapter II:

Kalke, P., Beckers, P., & Helm, C. (2021). May the palps be with you–new insights into the evolutionary origin of anterior appendages in Terebelliformia (Annelida). *BMC zoology*, *6*, 1-14. https://doi.org/10.1186/s40850-021-00094-6

Chapter III:

Kalke, P., & Helm, C. (2023). No cost but high performance–An alternative open source solution for 3D-visualizations in morphology. *Microscopy Research and Technique*, *86*(2), 193-197. https://doi.org/10.1002/jemt.24250

Chapter IV:

Kalke, P., Linder, S. S., Beckers, P., & Helm, C. (2023). Palps across the tree – the neuronal innervation and development of sensory head appendages in Annelida. Submitted to *Frontiers of Neuroscience*.

Chapter V:

Kalke, P., Wietoska, N., Beckers, P., & Helm, C. (2023). *Palps are homologous among Annelida – Lessons from Nereididae*. Manuscript in preparation.

Chapter I: General Introduction

Lophotrochozoa and Annelida

The phylum Annelida is part of the puzzling taxon Lophotrochozoa, the putative sister group to Ecdysozoa (Telford, Budd and Philippe, 2015; Kocot *et al.*, 2016; Marlétaz *et al.*, 2019). Lophotrochozoa, as suggested by (Bleidorn, 2019) and used as a synonym for Spiralia, comprises an intriguingly diverse group of taxa with profoundly different bodyplans, such as predatory chaetognaths with a centralised and complex nervous system, sessile shell-bearing filter feeders such as Mollusca and Brachiopoda, microscopic Gastrotricha and Rotifera, acoelomate Nemertea and Platythelminthes as well as Annelida. Recent phylogenetic approaches resulted in a Lophotrochozoan phylogeny without consistent sister group relationships between the involved taxa (Telford, Budd and Philippe, 2015; Kocot *et al.*, 2016; Bleidorn, 2019; Marlétaz *et al.*, 2019). Owing to ongoing discrepancies concerning the internal lophotrochozoan topology, Bleidorn (2019) suggested the importance of the integration of morphological as well as fossil record data and/or the inclusion of rare genomic changes into the analyses, although its integration is challenging. However, the systematic of Lophotrochozoa, with this huge diversity including a variety of taxa with anterior sensory or feeding appendages, is still under lively discussion – a fact which makes it even more interesting to take a closer look at one of the iconic phyla of this fascinating group, the Annelida.

Annelida resemble an evolutionary old (Parry, Vinther and Edgecombe, 2015; Parry and Caron, 2019; Chen *et al.*, 2020), invertebrate taxon that can be found in nearly all habitats (Struck, 2011; Struck *et al.*, 2011; Purschke, Bleidorn and Struck, 2014). Hence, their evolutionary adaptations have led to a wide range of body plans among different families. Consequently, various adaptations can be observed within Annelida, such as filter-feeding organisms, predatory species with impressive jaws, such as the bobbit-worm *Eunice aphrotois*, tube-dwelling groups featuring slender head appendages, and even ground-dwelling taxa devoid of any discernible appendages (Fauchald and Rouse, 1997; Rouse and Fauchald, 1997; Rouse and Pleijel, 2001; Purschke, Bleidorn and Struck, 2014). Phylogenetic reconstructions of the annelid tree of life based solely on morphological characters was proven to be of little help for our understanding of annelid evolution and resulted in the today rejected sister group

relationship of Clitellata and Polychaeta and their division in Scolecida – without head appendages- and Palpata – bearing various appendages at the anterior end (Rouse and Fauchald, 1997). Nevertheless, the shear diversity and baffling distribution of the array of sometimes similar looking head appendages hampered the determination of phylogenetic relationships in the past (Fauchald and Rouse, 1997; Rouse and Pleijel, 2001, 2003; Purschke, Bleidorn and Struck, 2014). However, thanks to the first phylogenomic investigations, the current topology dividing Annelida into the basally-branching Paleoannelida, with Magelonidae and Owenidae as sister group to all other annelids, Chaetopteriformia as well as Amphinomidae (fireworms), and Sipuncula as part of the basally-branching clades, and the Pleistoannelida, comprising the sister groups Errantia and Sedentaria, was established (see Fig. 1) (Struck *et al.*, 2011; Weigert *et al.*, 2014; Weigert and Bleidorn, 2016; Helm *et al.*, 2018). As a result, formerly separated phyla such as the unsegmented Sipuncula or Echiura and the deep-sea taxon Siboglinidae could be integrated into the annelid tree of life (Weigert *et al.*, 2014). Furthermore, the entire annelid phylogeny became reshaped based on a solid molecular backbone. Other enigmatic taxa, such as Orthonectida, Myzostomida, or Spintheridae, could be assigned to Annelida, but their position is still under debate (Weigert and Bleidorn, 2016; Bleidorn, 2019).

Head appendages in Annelida

Although annelids differ in general size, colour and shape, one of their key features helped them to adapt to all kinds of ecological niches and ensured their evolutionary success - the head appendages. Head appendages in Annelida appear in a huge variability reaching from so-called antennae over several types of tentacular cirri towards elongated feeding-palps (e.g. in Magelonidae and Spionidae (Chapter IV)), feather-like tentacular crowns (Sabellaridae and Serpulidae) as well as impressive multiplications head structures in e.g. Terebellifomia (Chapter II) and Cirratulidae, and a lack of the latter structures in other taxa (e.g., Orbiniidae) (Rouse and Pleijel, 2001; Purschke, Bleidorn and Struck, 2014; Purschke, 2015; Stiller *et al.*, 2020; Kalke, Beckers and Helm, 2021) (Fig 1).

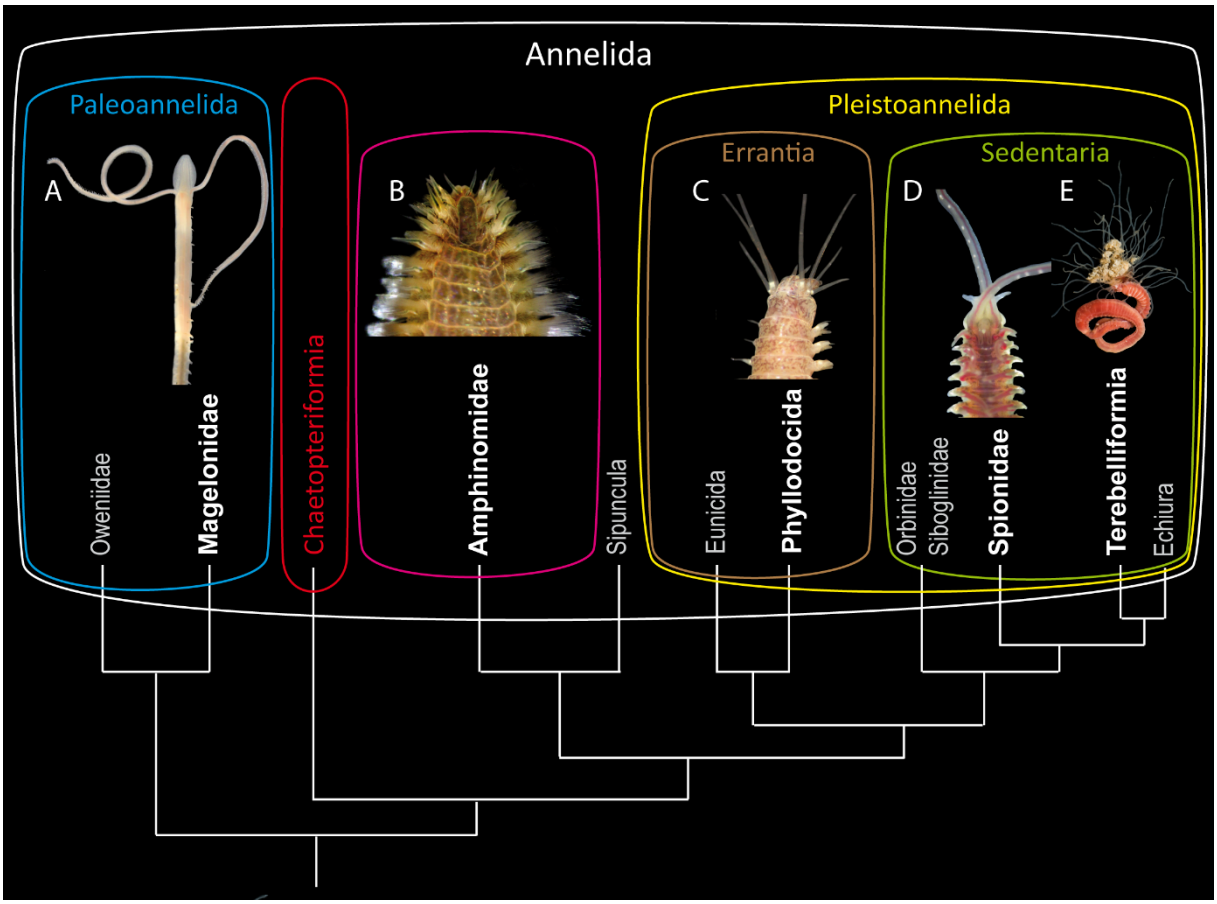

Figure 1. Annelid phylogeny modified after Helm 2018. All taxa investigated in this thesis are highlighted in bold letters, and their representatives are shown. (A) Anterior end of *Magelona mirabilis* (Paleoannelida, Magelonidae) with two elongated feeding-palps. (B) Anterior end of *Eurythoe complanata* (Amphinomidae), with a pair of buccal lips and five antennae. (C) Anterior end of *Nereis spec.* (Errantia, Nereididae) with two lateral antennae, a pair of sensorial palps, and four pairs of tentacular cirri. (D) Anterior end of *Malacoceros fuliginosus* (Sedentaria, Spionidae) with two elongated feeding palps. (E) *Terebella spec.* (Terebellidae) with numerous head appendages catching food. Images taken by Patrick Beckers (Bonn).

Generations of scientists have attempted to unravel the mystery behind these important sensory and feeding structures (Nilsson, 1912; Hanström, 1927; Binard and Jeener, 1928; Wilson, 1936, 1982; Keßler, 1963; Bhaud, 1988) and have used them to systemize and order polychaete taxa (Fauchald and Rouse, 1997; Rouse and Pleijel, 2001, 2003). Lars Orrhage, a pioneer in the field of polychaete morphology, made significant contributions to our understanding of head appendage distribution and homology in polychaetes, and his theory dealing with `the 12 palps nerve roots` had a huge impact on our understanding of annelid evolution. His systematic investigations of the anterior nervous system of polychaetes provided a valuable framework for a discrimination between palps, antennae, and tentacular cirri and complemented the external morphological features that had been used traditionally

(Purschke, Bleidorn and Struck, 2014). Resulting definitions of antennae and palps were thus based on the neuronal innervation pattern caused by the dorsal and ventral root of the circumoesopageal connectives (cc) and their commissures, which culminated in this mentioned theory about `the 12 palp roots` (summarized in (Orrhage and Müller, 2005) (see Fig. 2). The underlying impressively detailed morphological descriptions of the anterior nervous system of Annelida focus on a majority of annelid taxa such as Paleoannelida (Chapter IV), Chaetopteriformia, Amphinomidae (Chapter IV), Errantia (Chapter V) like Eunicida and Phyllodocida as well as Sedetaria like Terebelliformia (Chapter II), Serpulidae, Sabellidae and Spionidae (Chapter IV) (Orrhage, 1966, 1980, 1990, 1991, 1993, 1995, 1999, 2001; Orrhage and Eibye-Jacobsen, 1998; Orrhage and Müller, 2005).

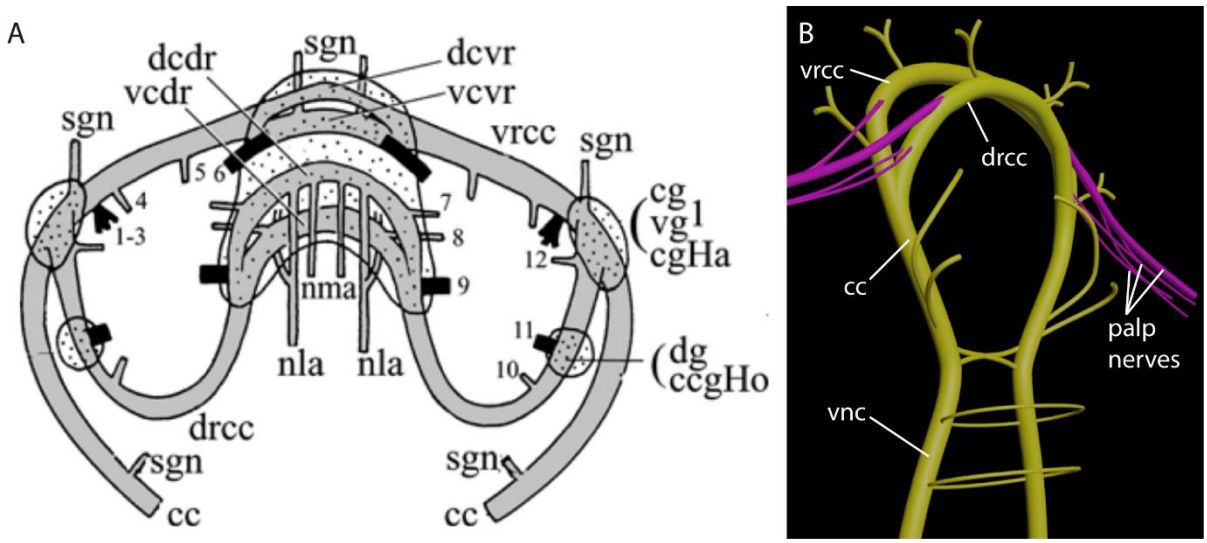

Figure 2. Comparison of visualisations of Orrhage´s theory of 12 palp roots and the recent innervation pattern of larval anterior nervous system and feeding-palps in *Malacoceros fuliginosus* (Sedentaria, Spionidae, see Chapter V). (A) Synopsis of all potential palp nerve roots (1-12) investigated by Orrrhage and Co-workers (Orrhage and Müller, 2005), in dorsal view. (B) Dorso-lateral 3D-schematic drawing of the anterior nervous system of *Malacoceros*, palp nerves are highlighted in pink (Kalke et al. submitted). **Abbreviations:** cc – circumoesophageal connectives, ccgHo – Holmgren´s cerebral commissural ganglion, cgHa – Hanmaker´s commissural ganglion, dcdr – dorsal commissure of drcc, dcvr – dorsal commissure of vrcc, drcc – dorsal root of cc, nla – nerves of lateral antennae, nma – nerves of median antennae, sgn – stomatogastric nerves, vcdr – ventral commissure of drcc, vcvr – ventral commissure of vrcc, vrcc – ventral root of cc

Unfortunately, the previous lack of a proper phylogeny and Orrhage´s dogmatic ´12 palp nerve roots´ theory and the lack of other morphological analyses lead to misinterpretations and baffled generations of scientists. Fortunately, an increasing number of researchers raised questions about the previous detailed morphological descriptions and prompted a re-evaluation of Orrhage's findings. Hence, (Beckers, Helm and Bartolomaeus, 2019) could reveal/demonstrate the discrepancies in Orrhage´s observations. As a consequence, further studies on the paleoannelid family Oweniidae (Beckers *et al.*, 2019) and Chaetopteriformia (Helm, Schwarze and Beckers, 2022) followed and therefore built a highly needed backbone for a re-evaluation of existing knowledge (Struck *et al.*, 2011; Weigert *et al.*, 2014; Weigert and Bleidorn, 2016).

Thesis Aims

Orrhage's theory of `the 12 palp nerve roots` and the lack of further comparative datasets still has a huge impact on the understanding and ongoing discussion of annelid evolution and hampers the dialogue. After the rise of an increasing number of observations showing discrepancies in previous findings and interpretations, it is time to challenge old knowledge and take a fresh look at old questions (Beckers *et al.*, 2019; Beckers, Helm and Bartolomaeus, 2019; Schmidbaur *et al.*, 2020; Kalke, Beckers and Helm, 2021).

In this dissertation, I therefore intend to elucidate the homology and evolution of anterior head appendages in Annelida. Focussing on innervation patterns and morphological characteristics of head appendages in polychaete key taxa, my investigations aim to compare different ontogenetic stages intra- and interspecifically to:

(1) *define and re-evaluate the knowledge concerning the composition of head appendages in marine bristle worms (Annelida)*,

(2) *clarify the homology of so-called feeding-palps of distantly related Palaeoannelida and Sedentaria*,

And, finally, (3) *answer the question about the evolutionary origin of short sensorial palps and their putative homology with feeding-palps of other taxa.*

To tackle this main research questions and shed new light on the evolutionary history of head appendages in polychaetes in general, I employ an integrative and comparative morphological approach that combines latest immunohistochemistry, immunohistological sections, Azan-stained serial histology sections, and subsequent 3D visualization (Fig. 3).

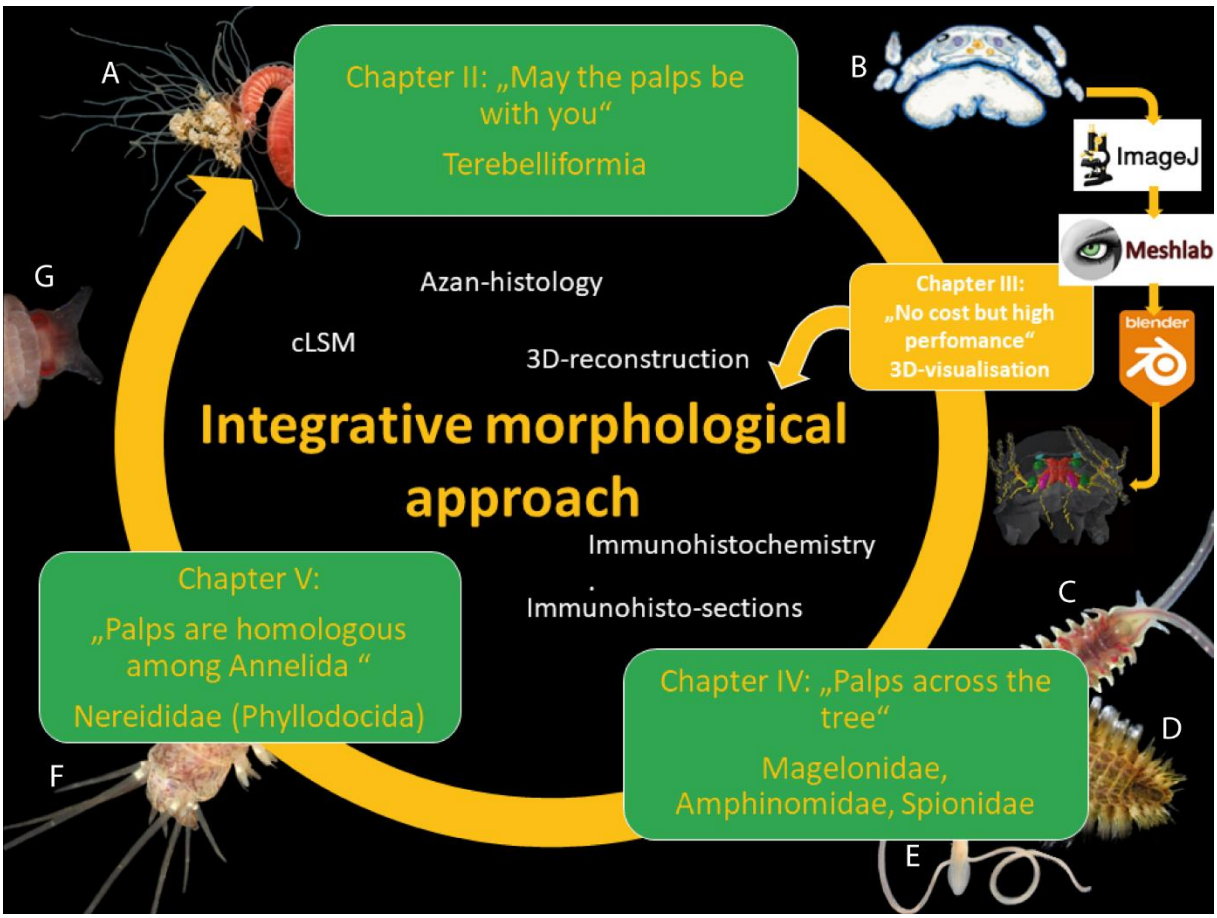

Figure 3. Graphic summarizing the four chapters of this thesis (shown in boxes) and investigated key taxa. (A) *Terebella spec.* (Terebellidae) with numerous head appendages catching food. (B) Flow chart of our open-source 3D visualization workflow for image stack-based datasets. (C) Anterior end of *Malacoceros fuliginosus* (Sedentaria, Spionidae) with two elongated feeding palps. (D) Anterior end of *Eurythoe complanata* (Amphinomidae), with a pair of buccal lips and five antennae. (E) Anterior end of *Magelona mirabilis* (Paleoannelida, Magelonidae) with two elongated feeding-palps. (F) Anterior end of *Nereis spec.* (Errantia, Nereididae) with two lateral antennae, a pair of sensorial palps, and four pairs of tentacular cirri. (G) Anterior end of *Scalibregma celticum* (Sedentaria, Scalibregmatidae). Images made by Patrick Beckers (Bonn).

Thesis Outline

To elucidate the question concerning the homology of anterior head appendages across the annelid tree of life, this thesis is composed of four main chapters. The chronological order corresponds to the chronology of preparation, and each chapter, excluding the solely

methodological Chapter III, is built on the knowledge and insights of the previous chapter. All chapters either tackle different annelid key taxa and therefore provide insight into the taxon-specific neuronal innervation patterns of the respective head appendages. Although this thesis mainly focuses in particular on the palp evolution and homology across polychaetes, all types of head appendages being present in the respective groups are part of investigations.

In chapter II, we discuss a more than 100-year-old debate on whether the buccal tentacles in Terebelliformia - a clade deeply nested in the sedentary Pleistoannelida - are homologous to feeding-palps recently described for Paleoannelida or if these appendages represent parts of the anterior alimentary canal in the respective taxon, as proposed by Orrhage and co-workers.

The necessity of proper 3D-visualizations based on image stacks and the advantages of a rising number of open-source software solutions and their communities inspired Chapter III. Here, we advertise the need and benefits of open-source software for up-to-date morphological research and deliver a modular workflow, together with a step-by-step-guide, for all types of image stack-based datasets and their subsequent 3D-visualization.

In Chapter IV, we compare the innervation of larval feeding-palps with the adult character states of members of three annelid key taxa - the Magelonidae (Paleoannelida), Amphinomidae (together with Sipuncula, the sister group to the derived Pleistoannelida (Errantia and Sedentaria)), and Spionidae (a deeply nested within sedentary Pleistoannelida). The aim of this study is to determine whether feeding-palps of the Paleoannelida are homologous to so-called feeding palps observed in derived Sedentaria.

Finally, Chapter V focuses on the head appendages in Errantia, the sister group of Sedentaria. With focus on nectochaete larvae of *Platynereis dumerilii* and adult specimens of *Platynereis massiliensis*, the homology of the diverse head appendages observed in errant polychaetes is discussed and helps to answer our main research question: Are annelid feeding-palps and short sensorial palps homologous?

References

Beckers, P. *et al.* (2019) 'The central nervous system of Oweniidae (Annelida) and its implications for the structure of the ancestral annelid brain', *Frontiers in Zoology*, 16(1), pp. 1–21. Available at: https://doi.org/10.1186/s12983-019-0305-1.

Beckers, P., Helm, C. and Bartolomaeus, T. (2019) 'The anatomy and development of the nervous system in Magelonidae (Annelida) – insights into the evolution of the annelid brain', *BMC Evolutionary Biology*, 19, p. 173. Available at: https://doi.org/10.1186/s12862-019-1498-9.

Bhaud, M. (1988) 'Change in setal pattern during early development of Eupolymnia nebulosa (Polychaeta: Terebellidae) grown in simulated natural conditions', *Journal of the Marine Biological Association of the United Kingdom*, 68(4), pp. 677–687. Available at: https://doi.org/10.1017/S0025315400028794.

Binard, A. and Jeener, R. (1928) *Morphologie du lobe préoral des polychètes*.

Bleidorn, C. (2019) 'Recent progress in reconstructing lophotrochozoan (spiralian) phylogeny', *Organisms Diversity & Evolution*, 19, pp. 557–566. Available at: https://doi.org/10.1007/s13127-019-00412-4.

Chen, H. *et al.* (2020) 'A Cambrian crown annelid reconciles phylogenomics and the fossil record', *Nature*, 583, pp. 249–252. Available at: https://doi.org/10.1038/s41586-020-2384-8.

Fauchald, K. and Rouse, G. (1997) 'Polychaete systematics: Past and present', *Zoologica Scripta*, 26(2), pp. 71–138. Available at: https://doi.org/10.1111/j.1463-6409.1997.tb00411.x.

Hanström, B. (1927) 'DAS ZENTRALE UND PERIPHERE NERVENSYSTEM DES KOPFLAPPENS EINIGER POLYCHÄTEN', *Zeitschrift für Morphologie und Ökologie der Tiere*, 7(4), pp. 543–596. Available at: https://www.jstor.org/stable/43261104.

Helm, C. *et al.* (2018) 'Convergent evolution of the ladder-like ventral nerve cord in Annelida', *Frontiers in Zoology*, 15(1). Available at: https://doi.org/10.1186/s12983-018-0280-y.

Helm, C., Schwarze, G. and Beckers, P. (2022) 'Loss of complexity from larval towards adult nervous systems in Chaetopteridae (Chaetopteriformia , Annelida) unveils evolutionary patterns in Annelida', *Organisms Diversity & Evolution*, 22, pp. 631–647. Available at: https://doi.org/10.1007/s13127-022-00553-z.

Kalke, P., Beckers, P. and Helm, C. (2021) 'May the Palps Be With You – New Insights Into the Evolutionary Origin of Anterior Appendages in Terebelliformia (Annelida)', *BMC Zoology*, 6(30), pp. 1–16. Available at: https://doi.org/10.1186/s40850-021-00094-6.

Keßler, M. (1963) 'Die Entwicklung von Lanice conchilega (Pallas) mit besonderer Berücksichtigung der Lebensweise', *Helgoländer Wissenschaftliche Meeresuntersuchungen*, 8(4), pp. 425–476. Available at: https://doi.org/10.1007/BF01610572.

Kocot, K.M. *et al.* (2016) 'Phylogenomics of Lophotrochozoa with Consideration of Systematic Error', *Systematic Biology*, p. syw079. Available at: https://doi.org/10.1093/sysbio/syw079.

Marlétaz, F. *et al.* (2019) 'A New Spiralian Phylogeny Places the Enigmatic Arrow Worms among Gnathiferans', *Current Biology*, 29(2). Available at: https://doi.org/10.1016/j.cub.2018.11.042.

Nilsson, D. (1912) *Beiträge zur Kenntnis des Nervensystems der Polychaeten*. Almquist & Wiksells.

Orrhage, L. (1966) ‘Über die Anatomie des zentralen Nervensystems der sedentaren Polychaeten’, *Arkiv för Zoologi*, 19(3), pp. 99–133.

Orrhage, L. (1980) ‘On the structure and homologues of the anterior end of the polychaete families sabellidae and serpulidae’, *Zoomorphology*, 96(1–2), pp. 113–167. Available at: https://doi.org/10.1007/BF00310081.

Orrhage, L. (1990) ‘On the Microanatomy of the Supraoesophageal Ganglion of Some Amphinomids (Polychaeta Errantia), with Further Discussion of the Innervation and Homologues of the Polychaete Palps’, *Acta Zoologica*, 71(1), pp. 45–59. Available at: https://doi.org/10.1111/j.1463-6395.1990.tb01180.x.

Orrhage, L. (1991) ‘On the Innervation and Homologues of the Cephalic Appendages of the Aphroditacea (Polychaeta)’, *Acta Zoologica*, 72(4), pp. 233–246. Available at: https://doi.org/10.1111/j.1463-6395.1991.tb01201.x.

Orrhage, L. (1993) ‘On the Microanatomy of the Cephalic Nervous System of Nereidae (Polychaeta), with a Preliminary Discussion of Some Earlier Theories on the Segmentation of the Polychaete Brain’, *Acta Zoologica*, 74(2), pp. 145–172.

Orrhage, L. (1995) ‘On the Innervation and Homologues of the Anterior End Appendages of the Eunicea (Polychaeta), with a Tentative Outline of the Fundamental Constitution of the Cephalic Nervous System of the Polychaetes’, *Acta Zoologica*, 76(3), pp. 229–248. Available at: https://doi.org/10.1111/j.1463-6395.1995.tb00996.x.

Orrhage, L. (1999) ‘On the morphological value of the glycerid-goniadid prostomium and its appendages (Polychaeta)’, *Acta Zoologica*, 80(3), pp. 251–264. Available at: https://doi.org/10.1046/j.1463-6395.1999.00025.x.

Orrhage, L. (2001) ‘On the anatomy of the central nervous system and the morphological value of the anterior end appendages of Ampharetidae, Pectinariidae and Terebellidae (Polychaeta)’, *Acta Zoologica*, 82(1), pp. 57–71. Available at: https://doi.org/10.1046/j.1463-6395.2001.00070.x.

Orrhage, L. and Eibye-Jacobsen, D. (1998) ‘On the Anatomy of the Central Nervous System of Phyllodocidae (Polychaeta) and the Phylogeny of Phyllodocid Genera: a New Alternative’, *Acta Zoologica*, 79(3), pp. 215–234. Available at: https://doi.org/10.1111/j.1463-6395.1998.tb01160.x.

Orrhage, L. and Müller, M.C.M. (2005) ‘Morphology of the nervous system of Polychaeta (Annelida)’, *Hydrobiologia*, 535(1), pp. 79–111. Available at: https://doi.org/10.1186/s40850-021-00094-6.

Parry, L. and Caron, J.B. (2019) ‘Canadia spinosa and the early evolution of the annelid nervous system’, *Sience Avances*, 5(9), pp. 1–8. Available at: https://doi.org/10.1126/sciadv.aax5858.

Parry, L., Vinther, J. and Edgecombe, G.D. (2015) ‘Cambrian stem-group annelids and a metameric origin of the annelid head’, *Biology letters*, 11(10), p. 20150763.

Purschke, G. (2015) ‘24 Annelida: basal groups and Pleistoannelida’, *Structure and evolution of invertebrate nervous systems*, p. 254.

Purschke, G., Bleidorn, C. and Struck, T. (2014) ‘Systematics, evolution and phylogeny of Annelida – A morphological perspective’, *Memoirs of Museum Victoria*, 71, pp. 247–269. Available at: https://doi.org/10.24199/j.mmv.2014.71.19.

Rouse, G.W. and Fauchald, K. (1997) 'Cladistics and Polychaetes', *Zoologica Scripta*, 26(2), pp. 139–204. Available at: https://doi.org/10.1111/j.1463-6409.1997.tb00412.x.

Rouse, G.W. and Pleijel, F. (2001) *Polychaetes*. Oxford, New York: Oxford University Press. Available at: https://doi.org/10.1111/j.1439-0469.2004.00263.x.

Rouse, G.W. and Pleijel, F. (2003) 'Problems in polychaete systematics', *Hydrobiologia*, 496, pp. 175–189. Available at: https://doi.org/10.1023/A:1026188630116.

Schmidbaur, H. *et al.* (2020) 'Within-family plasticity of nervous system architecture in Syllidae (Annelida, Errantia)', *Frontiers in Zoology*, 17(20), pp. 1–44. Available at: https://doi.org/10.1186/s12983-020-00359-9.

Stiller, J. *et al.* (2020) 'Spaghetti to a Tree: A Robust Phylogeny for Terebelliformia (Annelida) Based on Transcriptomes, Molecular and Morphological Data', *Biology*, 9(73), pp. 1–28. Available at: https://doi.org/10.3390/biology9040073.

Struck, T.H. (2011) 'Direction of evolution within Annelida and the definition of Pleistoannelida', *Journal of Zoological Systematics and Evolutionary Research*, 49(4), pp. 340–345. Available at: https://doi.org/10.1111/j.1439-0469.2011.00640.x.

Struck, T.H. *et al.* (2011) 'Phylogenomic analyses unravel annelid evolution', *Nature*, 471(7336), pp. 95–98. Available at: https://doi.org/10.1038/nature09864.

Telford, M.J., Budd, G.E. and Philippe, H. (2015) 'Phylogenomic Insights into Animal Evolution', *Current Biology*, 25(19), pp. R876–R887. Available at: https://doi.org/10.1016/j.cub.2015.07.060.

Weigert, A. *et al.* (2014) 'Illuminating the base of the Annelid tree using transcriptomics', *Molecular Biology and Evolution*, 31(6), pp. 1391–1401. Available at: https://doi.org/10.1093/molbev/msu080.

Weigert, A. and Bleidorn, C. (2016) 'Current status of annelid phylogeny', *Organisms Diversity and Evolution*, 16(2), pp. 345–362. Available at: https://doi.org/10.1007/s13127-016-0265-7.

Wilson, D.P. (1936) 'Memoirs: The Development of the Sabellid Branchiomma vesiculosum', *Journal of Cell Science*, 2(312), pp. 543–603.

Wilson, D.P. (1982) 'The larval development of three species of Magelona (Polychaeta) from localities near Plymouth', *Journal of the Marine Biological Association of the United Kingdom*, 62(2), pp. 385–401.

Kalke *et al. BMC Zoology* (2021) 6:30
https://doi.org/10.1186/s40850-021-00094-6

BMC Zoology

RESEARCH Open Access

May the palps be with you – new insights into the evolutionary origin of anterior appendages in Terebelliformia (Annelida)

Paul Kalke[1*], Patrick Beckers[2] and Conrad Helm[1*]

Abstract

Background: Head appendages in Annelida contribute significantly to the immense morphological diversity in this spiralian taxon. Nevertheless, the evolutionary origin of annelid antennae, palps, cirri and tentacles are part of vast theories and debates that took place over decades. One of these heavily discussed groups are the Terebelliformia, which bear numerous anterior tentacles originating from different regions of the head. The question, whether these tentacles are homologous to feeding palps in other annelids or if these structures evolved convergently in terebellids and the remaining taxa, has been highly debated in the past.

Results: By using morphological methods including immunohistochemistry, confocal microscopy, Azan-stained serial sections and 3D-visualisation, we are able to shed new light and a fresh look on the old question of the evolutionary origin of the buccal tentacles and their associated head structures in Terebelliformia. Our investigations show that the brains of the ampharetid *Hypania invalida* and the aulophora larvae of *Lanice conchilega* (Terebellidae) consist of a dorsal, more prominent and a more slender, ventral brain region. Neurite bundles innervating the buccal tentacles split off from the ventral and dorsal root within the ventral brain region and thus originate from the dorsal and ventral root of the circumoesophageal connectives. Hence, the observed neurite bundles fulfil the morphological criteria for the innervating neurite bundles of feeding palps known from Paleoannelida.

Conclusions: We disagree with former conclusions that buccal tentacles are part of the alimentary canal. Based on the presented data, the buccal tentacles of terebelliform taxa are innervated by neurite bundles and can be homologized with peristomial feeding palps of other Annelida.

Our comparative investigations reveal important insights into morphological changes during the evolution of anterior head appendages in Terebelliformia and Annelida in general. Nevertheless, our analyses also illustrate the gaps in knowledge and that more investigations throughout the annelid tree are necessary to explain and understand the huge diversity of annelid anterior appendages.

Keywords: Segmented worms, Morphology, Nervous system, Tentacles, Comparative approach, Histology, cLSM

Background

Annelida represent a fascinating and diverse group of invertebrates. In particular, the frontal end shows a variety of head appendages in terms of shape, function and number, and contributes to this immense diversity of forms within segmented worms. A remarkable and highly discussed annelid taxon in this respect is Terebelliformia.

*Correspondence: paul.kalke@uni-goettingen.de; chelm@uni-goettingen.de
[1] Department of Animal Evolution and Biodiversity, University of Goettingen, Goettingen, Germany
Full list of author information is available at the end of the article

The exact phylogenetic position of terebelliform lineages and the topology within the taxon were under persistent discussion for a long time [1–3]. However, phylogenomic approaches placed Terebelliformia confidently within the Sedentaria and hence they represent the sister taxon to the Maldanomorpha (Maldanidae + Arenicolidae) [4, 5]. Recently, new analyses uncovered the phylogenetic relations within the group, and suggest a taxon arrangement of Ampharetidae + Alvinellidae and Trichobranchidae + Terebellidae (including Melinnidae) [6]. Furthermore, the authors present Pectinariidae as sistergroup to all other Terebelliformia and therefore recover the idea of an "archaeoterebellomorph" with four pairs of branchiae and a large prostomium [1].

Deeply nested within the sedentary annelids [5], see also Fig. 1), most members of the Terebelliformia bear numerous, well-developed anterior head appendages.

Besides highly diverse branchial structures, numerous slender buccal tentacles can be observed throughout the family. Notably, these buccal tentacles and their evolutionary origin are part of a long-lasting and still ongoing discussion [1, 8–14].

The position of these buccal tentacles differs inside Terebelliformia and reaches from tentacles surrounding the mouth opening in an arc-like frame (in Pectinariidae), over appendages originating from an eversible pharynx (in Ampharetidae) to tentacles located in a dorsal position on the anterior end (in Terebellidae and Trichobranchidae) [6, 12]. So far, two contradictory theories about the evolutionary origin of these buccal tentacles in Terebelliformia are debated:

1) the buccal tentacles are homologous to feeding palps observed in other annelids [8, 9, 11, 12] or
2) the buccal tentacles evolved from buccal structures and therefore represent a convergently evolved structure non-homologous to sensory or feeding palps of other Annelida [1, 13, 14].

In the early twentieth century, these terebelliform buccal tentacles and their associated structures were homologised with almost any kind of anterior appendage, even being rudiments of antennae [8, 9]. On the other hand, Orrhage [13] described a ribbon-like, simple brain for Terebelliformia and suggested the buccal tentacles as being an outgrowth of the upper lip. According to his descriptions, the tentacular nerves are closely associated with nerves of the alimentary canal, thus being part of it. In contrast, Rouse and Fauchald [11] suggested that the buccal tentacles of Terebelliformia are homologous to the palps of e.g., Sabellidae and Spionidae - a statement which also follows their Canalipalpata-Aciculata theory. Other authors used the buccal morphology to accentuate the homology to palps by the absence of pharyngeal ciliated fields on tentacles and their area of attachment [12]. Based on these investigations, the terebelliform tentacles

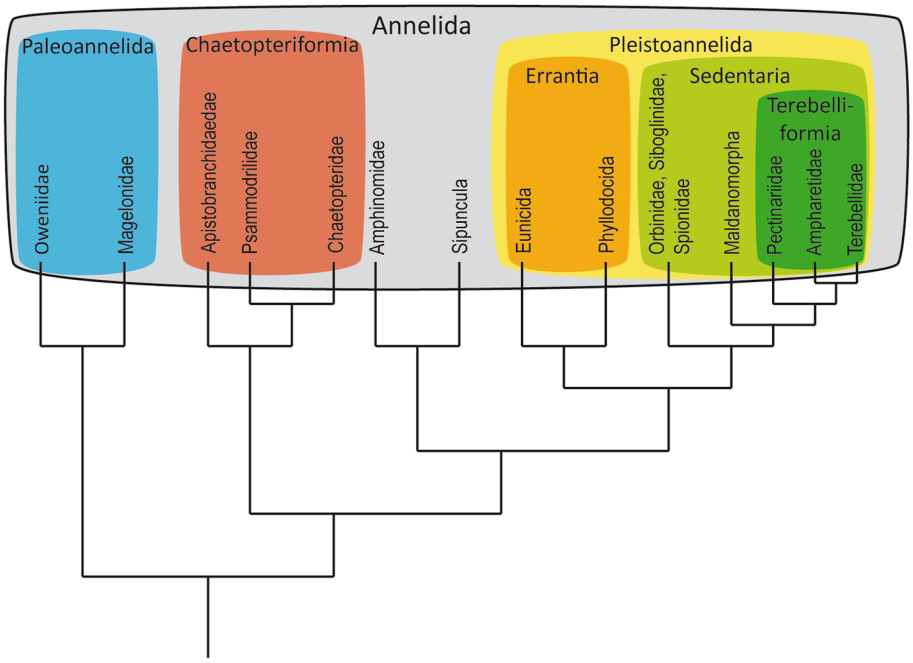

Fig. 1 Combined and simplified topology showing recent hypotheses concerning relationships within Annelida. The scheme is based on different sources [5–7]

are not part of the alimentary canal. Furthermore, developmental studies favour the homology with feeding palps due to the independent maturation of pharyngeal structures and buccal tentacles [15–17].

To shed new light on this long-lasting discussion, and to unveil further details helpful for our understanding of the evolutionary origin of terebelliform anterior appendages, we used a comparative and integrative approach. Our analyses include a variety of morphological methods such as immunohistochemistry, serial, Azan-stained, sections and 3D-visualization. Our comprehensive investigations provide a fresh look on a more than a hundred years ongoing discussion and uncover the evolutionary origin and homology hypotheses for anterior body appendages in terebellids and allies. Additionally, our data will critically challenge existing knowledge dealing with this topic and contribute to our understanding concerning the evolution of character complexes in annelid worms.

Results

To understand the development and anatomy of the head appendages in Terebelliformia, we used aulophora larvae of *Lanice conchilega* (Pallas, 1766) for immunohistochemistry (Fig. 2) and *Terebella labidaria* (Linnaeus, 1767) for Azan-histology (Fig. 3) (as members of the Terebellidae). Furthermore, we investigated adult *Hypania invalida* (Grube, 1860) as a member of the Ampharetidae with both methods (Figs. 4, 5) and summarized all findings in schematic drawings (Fig. 6). In our descriptions of the nervous system, we refer to [18] for used terms and annotations. The description of the head parts follows, if not stated otherwise, [12].

Central nervous system

Aulophora larvae of Lanice conchilega and adult Terebella lapidaria (Terebellidae)

The aulophora larvae of *Lanice conchilega* already show all features of adult Terebellidae, although the number of anterior tentacles is much less (Fig. 2A). The brain of *L. conchilega* consists of one more prominent dorsal brain region and the delicate anlage of the ventral one (Figs. 2C-F; 6D, E). Both are connected to both roots of the circumoesophageal connective (*cc*) (Figs. 2C, E, F). The ventral brain region protrudes slightly anteriorly from the dorsal one, which is well shown by confocal data but hardly perceptible in Azan-sections. Additionally, several thin longitudinal prostomial nerves connect the dorsal to the ventral region of the brain (Fig. 2F). The subepidermal ventral nerve cord is composed of two longitudinal neurite bundles. Furthermore, four pairs of serotonergic neurite bundles are visible within the ventral nerve cord (*vnc*) of aulophora larvae (Figs. 2A, B). Ventrally, in particular where the *cc* originate, groups of serotonergic cell somata form prominent aggregations (Figs. 2C, D). At regular intervals, two pairs of lateral nerves originate from the *vnc* and proceed in dorsal direction. Although, we could not trace these nerves to their final destination they seems to innervate regular emerging dorsal notopodial structures, such as chaetal muscles or branchiae (in posterior segments). Similar to *H. invalida*, four pair of nerves emerge from the *cc* and proceed in lateral direction (Fig. 2D). They branch off and innervate two lateral epidermal, serotonergic protrusions next to the heavily ciliated lateral lips (Fig. 2B). Glandular cells often catch antibodies. Hence, a strong serotonergic signal without a nervous system specific pattern in huge epidermal cells hints towards the presence of glandular structures in this region (Figs. 3C, G). The stomatogastric nervous system is composed of a lateral lip nerve (Figs. 2C; 6D, E) and a lower lip nerve (Fig. 6D, E). Both are connected to a loop-like stomatogastric nerve (Figs. 2C, D; 6D, E). The lateral lip nerve is connected to the ventral region of the brain via several thin stomatogastric nerves (Figs. 2C; 6E). Along the nerves of the lateral lip, a dense meshwork of slender neurite bundles is coating the upper mouth region (see Fig. 2C). Additionally, numerous delicate neurite bundles originate at the lateral lip nerve and proceed along the dorsal side of the pharynx as found for the ventral side of the stomatogastric loop-like nerve as well (see Figs. 6D, E). The lip nerves and the stomatogastric loop-like nerve are connected to the *cc* via few thin neurite bundles (see Figs. 6D, E).

Hypania invalida (Ampharetidae)

The brain of *Hypania invalida* is located subepidermally. It consists of a dorsal and ventral region similarly arranged as described for *L. conchilega* (Figs. 4A-C; 6A-C). The dorsal region of the brain (dpbr) is the more prominent part (Figs. 4A-C), linked with numerous cell bodies located dorsally to the brain. The more delicate ventral region of the brain (vpbr), better perceptible in confocal data than in Azan-sections, show a more advanced protrusion from the dorsal region compared to *L. conchilega*. It is connected to the circumesophageal connectives (cc) via a ventral brain connective (cvbr) (Fig. 4D). Additionally, it is connected to the dorsal brain region by a dorsal brain connective (cdbr) (Figs. 4D; 6B). Both parts are connected to the ventral nerve cord (vnc) (Figs. 4A, C; 5E; 6A) by the *cc* (Figs. 4A-C; 5A-C; 6A-C). The latter is composed of two major nerve strands (roots) - the ventral and the dorsal one (visible via serotonin staining, Fig. 4A). The subepidermal *vnc* is composed of two pairs of distinct serotonergic neurite bundles with cell soma concentrated in ganglia (Figs. 5E, G). Anteriorly of the transition from *vnc* to the *cc,* three pairs of

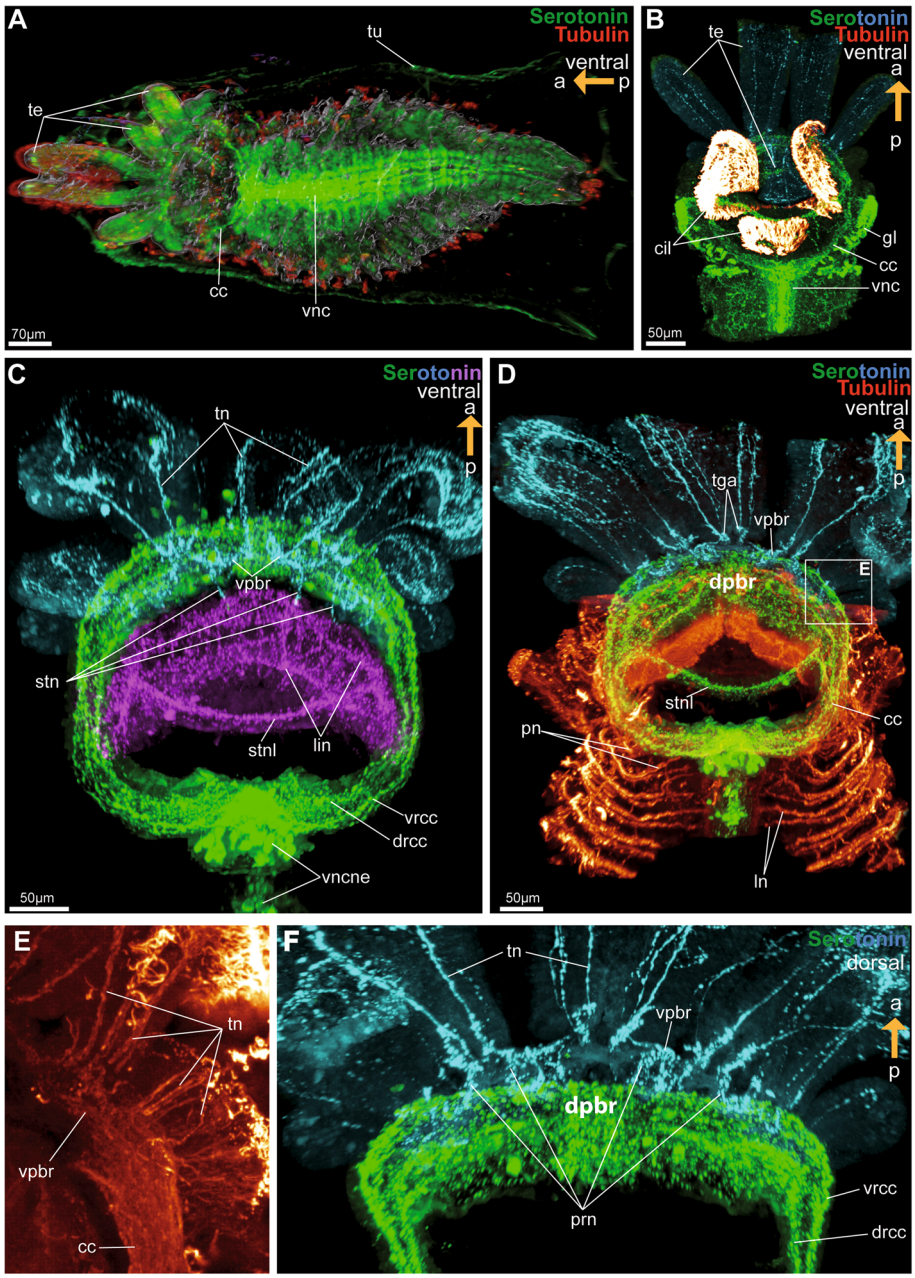

Fig. 2 Nervous system of the anterior region of aulophora larvae of *Lanice conchilega*, cLSM micrographs. **A**. General anatomy of aulophora larvae sitting in its tube, overall serotonergic nervous system highlighted in green and α-tubulinergic setae in red. **B**. Serotonergic nervous system anterior region. Central nervous system like brain and vnc are highlighted in green, tentacular nerves in cyan and α-tubulinergic cilia on the lateral and lower lips in red. **C**. Close-up of the serotonergic nervous system of the head region. Ventral region of the brain and tentacular nerves are highlighted in cyan, dorsal region of the brain, cc and vnc in green and stomatogastric nerves including lip nerves in magenta. **D**. General anatomy of the serotonergic and α-tubulinergic nervous system of the anterior region. Ventral region of the brain and tentacular nerves are highlighted in cyan, central and stomatogastric nervous system in green and α-tubulinergic nervous system in red. **E**. Close-up of micrograph D. α-tubulinergic nervous system in red. On the right side innervation of a developing palp is shown. Additionally, displayed is the transition of cc to the ventral brain region. **F**. Close-up of the brain region, showing the prostomial nerves connecting the dorsal with the ventral brain region. cc – circumoesophageal connectives; cil – cilia of lips; dpbr – dorsal region of brain; drcc – dorsal root of cc; gl – glandular cells; ln – lateral nerves; pn – peripheral nerves; prn – prostomial nerves; stnl – stomatogastric nerve loop; te – buccal tentacles; tga – tentacular ganglion; tn – tentacular nerves; tu – tube; vncne – neurons of vnc, vpbr – ventral region of brain, vrcc – ventral root of cc

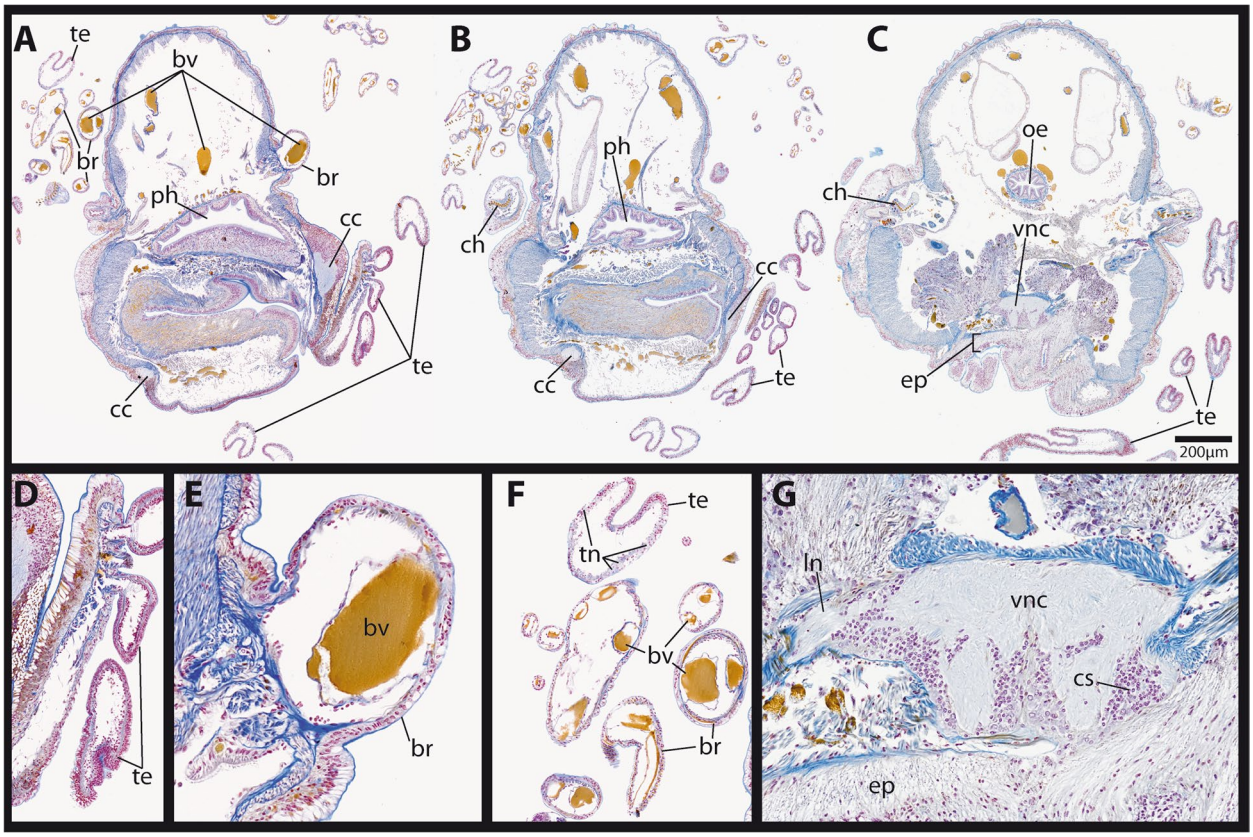

Fig. 3 General anatomy of the anterior end of adult *Terebella lapidaria* (Linnaeus 1767), 5 µm sections, Azan-staining, light microscopic images. **A.** Cross-section through anterior head region from which tentacles and branchiae emerge. **B.** Cross-section through middle head region. **C.** Cross-section through posterior head region, cc united to the vnc and anterior oesophageal cavity is identifiable. **D.** Close-up of the cross-section through the lateral origin of buccal tentacles. **E.** Close-up of the cross-section of the dorsal origin of the branchiae. **F.** Close-up of the cross-section through tentacles and branchiae. **G.** Close-up of the cross-section through the ventral nerve cord, huge glandular epidermal cells and the subepidermal vnc are shown. br – branchiae; bv – blood vessel; cc – circumoesophageal connectives; ch – chaete; cs – cell soma; ep – epidermis; ln – lateral nerve; oe – oesophagus; ph – pharynx; te – buccal tentacles; tn – tentacular nerves; vnc – ventral nerve cord

neurite bundles (Fig. 4C: pn) emerge from each side of the *cc* and proceed laterally. There they branch off and become part of the intraepidermal peripheral nervous system (Fig. 4C). Anteriorly, a pair of stomatogastric nerve bundles (Figs. 4C; 6A-C) originates medially of the *cc* and fuses with the ventral root of the ventral brain region (Figs. 4B-C; 6A-C). From that point of fusion, two nerves connect a prominent stomatogastric loop-like neurite bundle which proceeds ventrally along the pharynx (Figs. 4C-E; 6A-C). Numerous delicate neurite bundles emerge from that loop-like structure and innervate the anterior stomatogastric system. The dorsal branch of the *vpbr* is connected to the brain via several minute nerves, which run along the prostomium of adult *Hypania invalida* (prn) (Figs. 4B-E; 6A-C).

Anterior appendages

Aulophora larvae of Lanice conchilega and adult Terebella lapidaria (Terebellidae)

The most prominent structure observable in aulophora larvae of *L. conchilega* are the tentacles at the anterior end (Figs. 2A, B; 3A-D; 6D). The latter are located dorsally to the mouth opening. Cross-sections of the tentacles of adult *Terebella lapidaria* exhibit a prominent longitudinal invagination along the entire tentacle. This prominent structure, which is also present in the tentacles of *L. conchilega,* represents the food rim (see Figs. 3A-C, F), which are not present in the branchiae with their prominent blood vessels (Fig. 3A,E, F). The (buccal) tentacles in *L. conchilega* are innervated by numerous neurite bundles (Figs. 2C, D; 6D, E), which originate in the delicate anlage of the ventral region of the brain (Figs. 2C, E, F; 6E). The

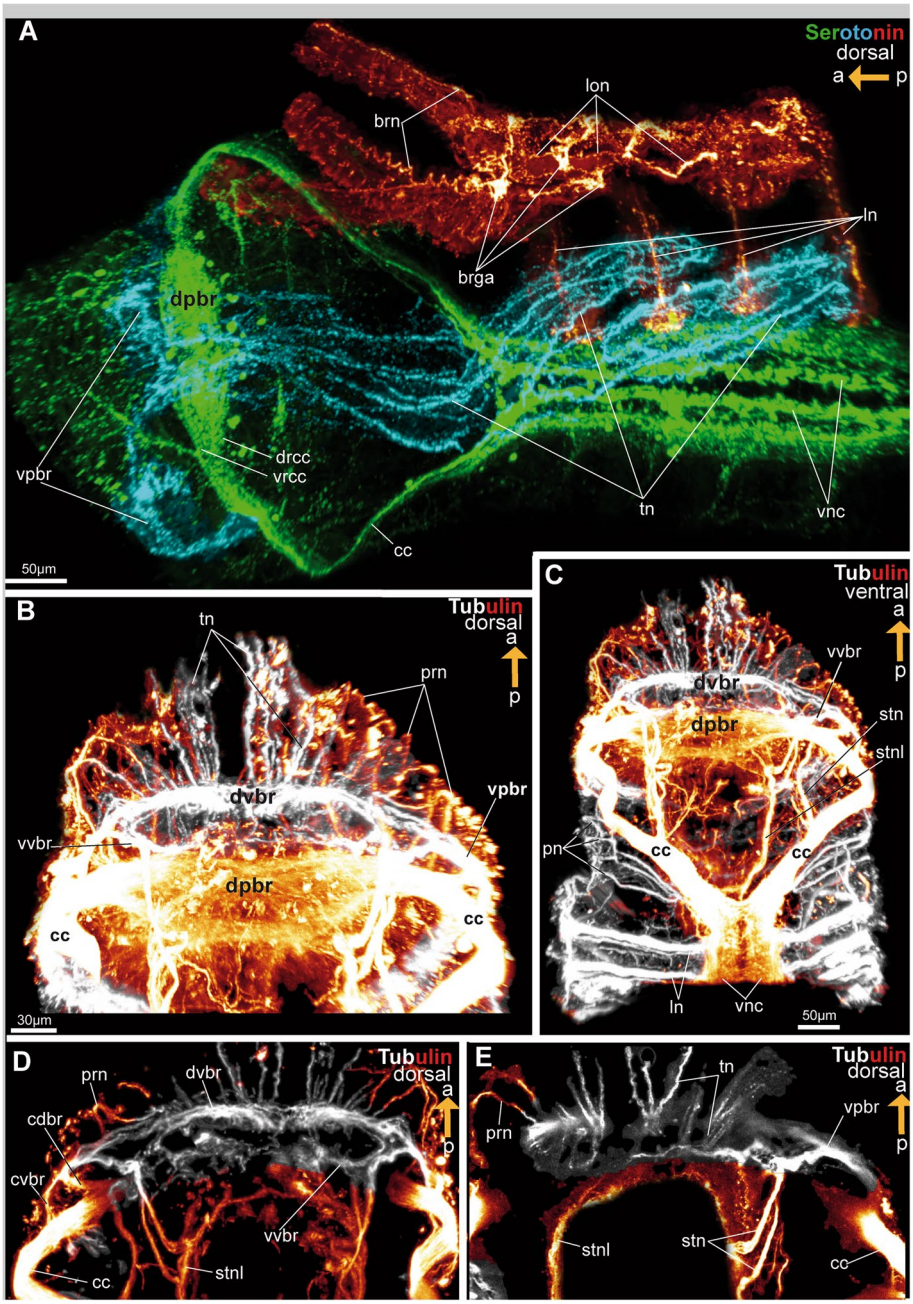

Fig. 4 Anterior nervous system of adult *Hypania invalida*, cLSM micrographs. **A.** General anatomy of the serotonergic nervous system. The central nervous is highlighted in green, ventral region of brain and tentacle nerves in blue and branchial neurites in red. **B.** Close-up of brain region stained against acetylated α-tubulin. Ventral region of brain and tentacular nerves highlighted in white. **C.** General anatomy of the tubulinergic nervous system. Ventral region of brain, tentacular nerves and laterally branching nerves are highlighted in white. **D.** Close-up of the ventral brain region stained against α-tubulin, ventral brain region highlighted in white. Connectives of the ventral brain region to the dorsal brain region, the *cc* and the stomatogastric nerve loop are shown. **E.** Close-up of the ventral brain region stained against α-tubulin, ventral brain region highlighted in white. Tentacular nerve originate from both roots of the ventral brain region. Brga – ganglion of branchiae; brn – branchae nerves; cc – circumoesophageal connective; cdbr – connective of dpbr; cvbr – connective of vpbr; dpbr – dorsal region of brain; drcc – dorsal root of cc; dvbr – dorsal root of vpbr; ln – lateral nerves; lon – lateral organ nerve; pn – peripheral nerves; prn – prostomial nerves; stn – stomatogastric nerve; stnl – stomatogastric nerve loop; tn – tentacular nerves; vnc – ventral nerve cord; vpbr – ventral region of brain; vrcc – ventral root of cc; vvbr – ventral root of vpbr

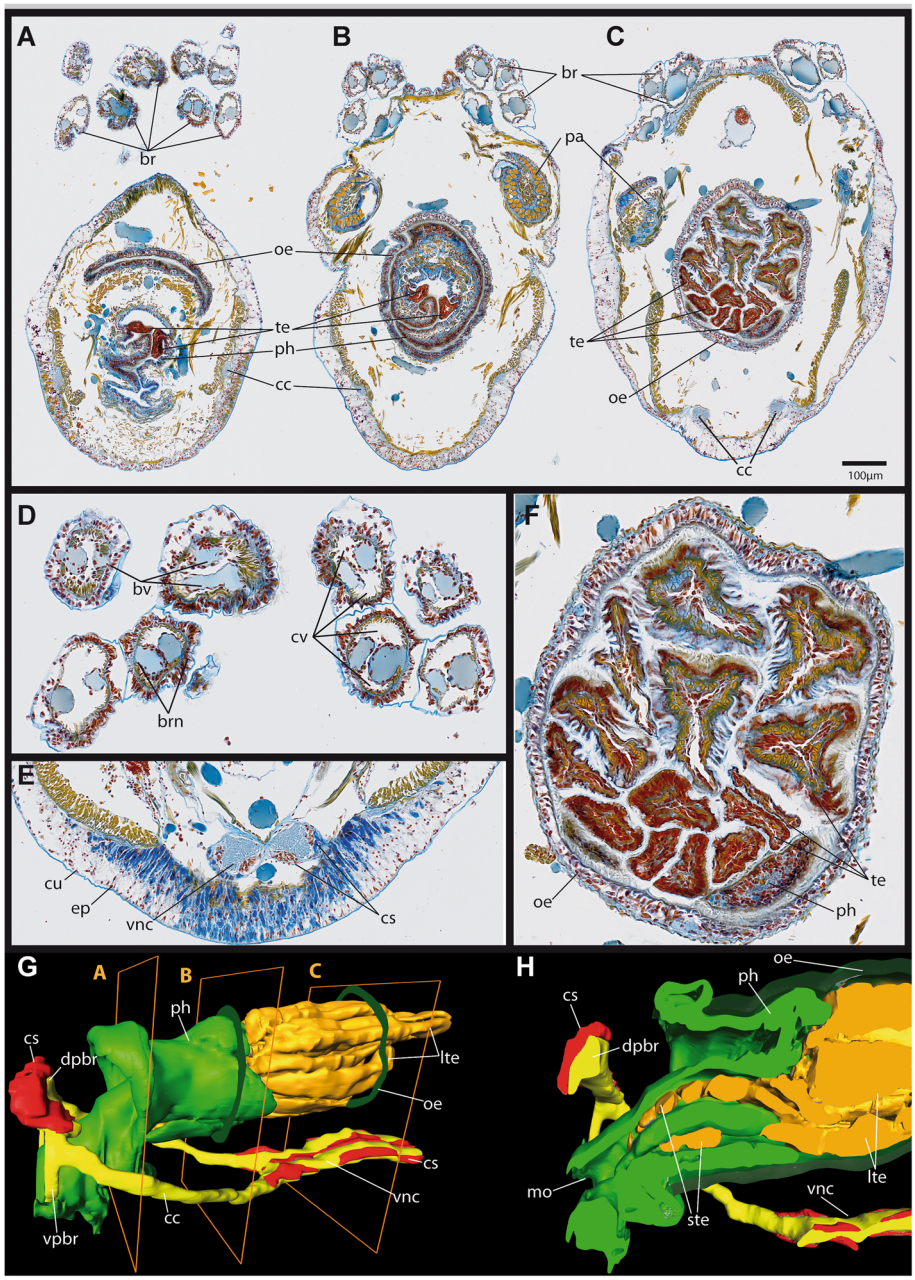

Fig. 5 General anatomy of the anterior end of adult *Hypania invalida*, 5 µm sections, Azan-staining, light microscopic images. **A.** Cross-section through anterior part of inverted pharynx, see Fig. G. Short buccal tentacles situated inside the pharyngeal cavity. **B.** Cross-section through the posterior part of the inverted pharynx, see Fig. G. Folded pharynx located inside the oesophageal cavity associated with short tentacles. **C.** Cross-section through the posterior part of the oesophageal cavity, see Fig. G. Long buccal tentacles filling the whole cavity of the oesophagus. **D.** Close-up of a cross-section through the branchiae with two prominent blood vessels, see Fig. A. **E.** Close-up of the anterior region of the subepidermal ventral nerve cord and ganglionic cell somata. **F.** Close-up of the posterior part of the oesophagus, see Fig. C, with numerous long tentacles located inside the oesophageal cavity. **G.** 3D-visualization of the anterior central nervous system and stomatogastric region, long distal buccal tentacle associated with the pharynx, oesophagus omitted. Frames show area of Parafin-sections of Fig. A, B and C. **H.** Digital sagittal section through the 3D-visualisation of the anterior central nervous system and the short buccal tentacles located in the middle part of the pharynx. br – branchiae; brn – branchiael nerves; bv – blood vessel; cc – circumoesophageal connectives; cs – cell soma; cu – cuticle; cv – coelom cavity; dpbr – dorsal region of brain; ep – epidermis; lte – long buccal tentacles; mo – mouth opening; oe – oesophagus; pa – palae bristles; ph – pharynx; ste – short buccal tentacles; te – buccal tentacles; vnc – ventral nerve cord; vpbr – ventral region of brain

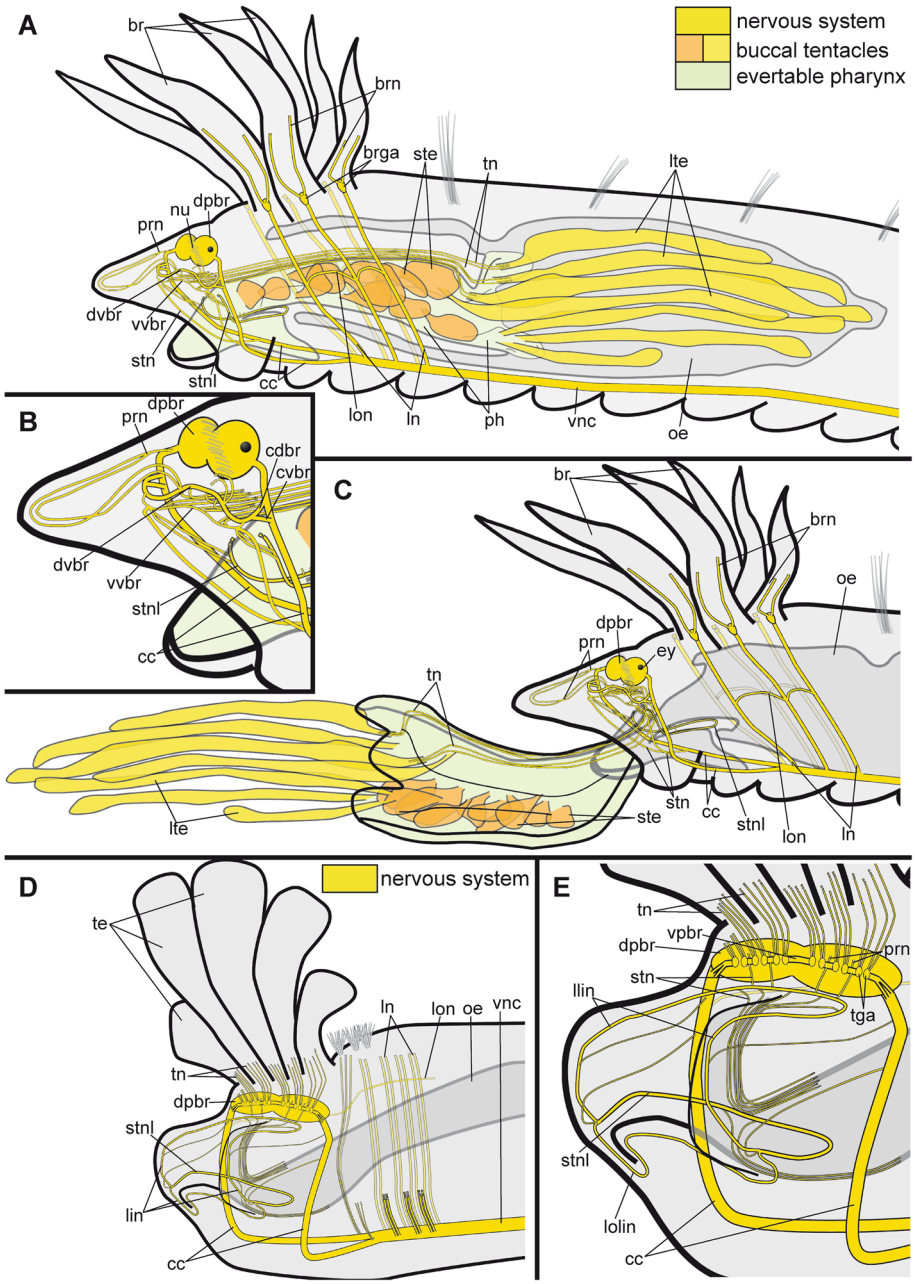

Fig. 6 Comparative schematic drawings of the overall nervous system of adult *Hypania invalida* (a-c) and aulophora larvae of *Lanice conchilega* (d, e). Nervous system is yellow, short buccal tentacles are orange and long buccal tentacles are colored in light yellow, the evertable pharynx is colored in mint green, see legend. **A.** Drawing of the anterior region of adult *Hypania invalida*, pharynx in inverted position. **B.** Close-up of the head region, see Fig. A. **C.** Drawing of the anterior region of adult *Hypania invalida*, pharynx in everted position. **D.** Drawing of the anterior region of aulophora larvae of *Lanice conchilega*. **E.** Close-up of the head region, see Fig. D. brga – ganglion of branchiae; br – branchiae; brn – branchiael nerves; cc – circumoesophageal connectives; cdbr – connective of dpbr; cvbr – connective of vpbr; dpbr – dorsal region of brain; ey – eye; llin – lateral lip nerves; lin – lip nerves; ln – lateral nerves; lolin – lower lip nerve; lon – lateral organ nerve; lte – long buccal tentacles; nu – nuchal organ; oe – oesophagus; ph – pharynx; prn – prostomial nerves; ste – short buccal tentacles; stnl – stomatogastric nerve loop; te - buccal tentacle; tn – tentacle nerves; tga – tentacular ganglion; vnc – ventral nerve cord, dvbr – dorsal root of vpbr; vvbr – ventral root of vpbr

ventral region of the brain is connected to both strands (roots) of the *cc* (Figs. 2C-F; 3A; 6D, E). In particular the chaplet-like appearance is obvious in serotonin-like immunoreactivity (Figs. 2C, F; 6D, E). Each anterior appendage is innervated by two pairs of neurite bundles originating from two distinct ganglia located at the base of the tentacle (Figs. 2D, F; 6D, E). The latter nerves run along the entire structure and form a prominent loop at the tentacular tip. Notably, the connection between these ganglia is not direct. Although the respective structures are laying side by side, they are interconnected via the mentioned nerve loop of the tentacles (see Fig. 6E).

Hypania invalida (Ampharetidae)

Dorsally - at the anterior end of *H. invalida* - four pairs of tentacle-like head appendages with two prominent blood vessels are present (Fig. 5A-D). These appendages are innervated by the first four pairs of lateral neurite bundles, in every case a thick and a slender one, originating from the *vnc* and proceed dorsally (Figs. 4A, C; 6A, C). Along their course - about half way - they are connected to a crossing neurite bundle innervating the lateral organ (Figs. 4A; 6B, C). Afterwards, the lateral neurite bundles terminate in a ganglion (Figs. 4A; 6A, B). From that terminal ganglion, two main branchial neurite bundles emerge and proceed along each branchial structure forming a loop by getting interconnected by numerous ring-shaped neurite bundles (Figs. 4A; 6A).

Additionally, a second type of head appendages – normally exhibited in inverted position inside the pharynx – is present within the oesophageal cavity (see Figs. 4A; 5A-C, 5F-H; 6A, B). These so-called buccal tentacles are innervated by four neurite bundles originating from the ventral and dorsal root of the ventral region of the brain (Figs. 4A-E; 6A-C). These tentacles can be stretched out for food uptake (shown in Figs. 4B, C; 6C).

A combination of all datasets allows for a proximation concerning the most probable location and appearance of these head appendages in everted position and their respective neuronal innervation (Fig. 6C). The assumed position and differentiation between short more proximal tentacles (Figs. 5A, B, H; 6A, C) and long distal tentacles (Figs. 5F-H; 6A, C) is mainly based on the Azan stained-sections and the 3D-reconstruction.

Discussion

The brain and major neuroanatomical properties in Terebelliformia

Based on our comprehensive investigations, the terebellid *Lanice conchilega* and the ampharetid *Hypania invalida* possess circumoesophageal connectives (*cc*) which are similarly connected to the brain by two strands (roots), a ventral and a dorsal one. These strands or roots of the *cc* show a clear serotonin-like immunoreactive signal but cannot be seen in Azan-sections. Due to their general location and the patterning in anti-serotonin-staining, we assume them as being homologous to the two roots previous authors described using histological sections [14]. Anatomical differences, in terms of course and extension of the mentioned roots in both investigated taxa, are caused by morphological transitions related to adaptive changes of the entire anterior end in Terebelliformia. Although both roots of the *cc* are closer associated in *H. invalida* than in *L. conchilega*, the transition of the latter into the two paired neurite bundles of the ventral nerve cord is comparable when observing their serotonin-like immunoreactivity. A closer examination of the neuroanatomical characteristics of both taxa shows many similarities in this respect. In anterior direction, the *cc* fuses with the dorsal, more prominent region of the brain. Anteroventral to the dorsal brain region, two connectives - one splitting from the *cc* (connective of ventral brain region-*cvbr*) and another proceeding from the dorsal brain region (*cdbr*) - fuse by forming the ventral, more slender region of the brain. Thereby, the ventrally oriented brain region splits up distally and forms a distinct ventral and dorsal root, which both innervate the buccal tentacles in *H. invalida* and *L. conchilega*.

Contradictory, earlier investigations focussing on Terebelliformia describe a unified, ribbon-like brain [13] and postulate the ventral and dorsal connective (*cvbr* and *cdbr*) as the two roots of the "common tract" – the latter not being part of the brain. Instead, both roots were described to innervate the lateral part of the "tentacular membrane" and the buccal tentacles.

Nevertheless, our data reveal a protrusion of a slender brain region in ventral direction. This ventral region exhibits two neuronal roots and innervates the buccal tentacles in Terebelliformia. The investigations presented herein demonstrate that nerves of the so-called "tentacular membrane" (see [13]) are in fact loop-like neurite bundles, which connect the dorsal brain region with the dorsal root of the ventral brain region (*prn*). Caused by a hypothesized evolutionary transition of the dorsal lip and associated buccal tentacles from the mouth region towards dorsal in Terebellidae (as summarized in [12]), these prostomial nerves are comparable with those in the ampharetid *H. invalida*. Nevertheless, they are much shorter. The same loop-like nerves innervate the ampharetid buccal tentacles as well as the "dorsal ridge" in Terebellidae (according to [13]) and potentially even the "cephalic veil" in Pectinariidae.

Due to the comparable position of the brain in Terebelliformia [12] and similar innervation patterns – including prostomial loop-like nerves connecting the dorsal to the ventral brain region – our data generally confirm

previous assumptions [12–14]. Accordingly, the "cephalic veil" of Pectinariidae, the "dorsal ridge" of Terebellidae and the hood-like "tentacular membrane" of Ampharetidae should be treated as being homologous structures.

In contrast, our conclusions concerning the potential prostomial or peristomial origin of these structures differ from earlier hypotheses. [19] suggested the pectinariid cephalic veil as a fusion of pro- and peristomium. Furthermore, developmental studies support the tentacles of Terebellidae as being part of the prostomium [20], whereas others suggested a peristomial origin of the latter [12]. Only for Ampharetidae developmental and morphological studies both suggest a peristomial origin of the buccal tentacles [12, 15]. Nevertheless, these assumptions concerning the tissue origin of palps in various terebelliform taxa are mainly based on the final position of the latter and the ability to retract the palp-like structures into the mouth opening. Anatomical data including innervation patterns were missing so far.

The question whether the buccal tentacles are of prostomial or peristomial origin can now partly be answered, based on our morphological data. Hence, our comparative investigations do not support a prostomial origin of the tentacles in Terebelliformia. The prostomium and all associated structures are innervated by loop-like nerves connecting the anterior-most ventral and dorsal brain region. Notably, they are limited to the prostomial hood in Ampharetidae as well as the prostomial and very short dorsal ridge in Terebellidae. In contrast, the buccal tentacles in all investigated taxa are associated with the peristomial upper lip and show a differing and much more complex peristomial innervation. Concluding, our data support a peristomial origin of the buccal tentacles in Terebelliformia. A similar pattern can be hypothesized for Pectinariidae, but needs further investigation.

The combination of potentially homologous innervation patterns described for Pectinariidae [13] and our observation concerning terebellid and ampharetid taxa, homologous structures such as the "cephalic veil", the "dorsal ridge" and the "tentacular membrane" should be defined as prostomial structures.

The earlier interpretation of terebellid tentacles as being of prostomial origin might have been caused by the developmental transition of character complexes involved into the cephalisation processes and obscurities about their ontogenetic origin. This cephalisation is obvious for the ontogenetic transition of branchiae and their inclusion in the formation of the anterior end in Ampharetidae, Alvinellidae, Melinnidae and Terebellidae [6], but is not responsible for the localization of terebelliform tentacles. The latter are characterized by a steady lateral addition of tentacles during ontogenesis. Both processes are independent. Nonetheless, additional detailed morphological as well as comprehensive developmental analyses are necessary for a better understanding of the role of cephalisation and multiplication processes in the formation of morphological features in Annelida.

Branchiae – anterior transition during cephalisation

The ampharetid *Hypania invalida* bears four pairs of digitate branchiae grouped dorsally on the head, while the two terebellid species *Lanice conchilega* and *Terebella lapidaria* show three pairs of dichotomous branchiae serially arranged along the trunk [6, 21]. The putative sister group of all other Terebelliformia - the Pectinariidae - also exhibit four pairs of branchiae along the segments II-V like shown for many other Terebelliformia [3, 22]. For all species investigated herein, the branchiae were easily identifiable in histological sections by the appearance of an afferent and an efferent blood vessel surrounded by the coelomic cavity.

In Terebelliformia, an ancestral number of four branchiae is assumed, while several reductions, transitions and even multiplication processes took place [6]. Due to developmental studies e.g. [15] the branchiae in larval Ampharetidae occur from segment II-VI and shift towards anterior during ontogenesis. Therefore, branchia in adults are located at segment II and III [6]. All branchial appendages in Terebelliformia are innervated by a more prominent anterior and a slender posterior, segmentally arranged lateral neurite bundle originating from the anterior end of the *vnc*. They proceed in dorsal direction along the trunk musculature and terminate in a branchial ganglion, situated at the base of each branchia. Notably, this observed pattern is comparable to the neuronal innervation pattern known from parapodial appendages in the errant annelids *Neanthes arenaceodentata* (Moore, 1903) and *Platynereis dumerilii* (Audouin & Milne Edwards, 1833) (see [23, 24]). Therefore, an evolutionary scenario including a parapodia-linked origin of the branchial structures and the later involvement in cephalization events has to be assumed. Notably, cephalisation seems to be a widespread evolutionary phenomenon in annelids, and is described for several errant as well as sedentary taxa [25, 26]. Such an ontogenetic transition of larval trunk-associated appendages towards anterior in adult specimens seems to represent an important mechanism. Cephalisation seem to represent one major evolutionary process responsible for the diversity of the sensorial apparatus and even physiological adaptations of the anterior end in Terebelliformia and Annelida in general. Unfortunately, we were not able to compare our observation with the neuronal innervation of the branchiae in adult Terebellidae. The branchiae in the investigated aulophora larvae of *L. conchilega* were

still not fully developed and can therefore not be used for detailed interpretations.

The anterior-most appendages – a multiplications of palps?

In the ampharetid *H. invalida* each tentacle is innervated by four neurite bundles, whereas in total eight prominent neurite bundles proceed along each tentacle in late larvae of *L. conchilega*. However, in both species the tentacles are similarly innervated by neurite bundles, which originate from the ventral and dorsal root of the circumoesophageal connectives. In *H. invalida,* tentacular nerves originate from the ventral root of the more delicate ventral brain region, which is connected to the circumoesophageal connectives (*cc*) by the ventral brain region commissure (*cvbr*). Additionally, they always originate from the dorsal root of the ventral brain region, which is connected to the dorsal, prominent region of the brain by the dorsal brain region commissure (*cdbr*). In *L. conchilega,* nerves of the buccal tentacles originate from neurons arranged arc-like on the ventral region of the brain. They are innervated by neurite bundles of both roots of the *cc*. These neurite bundles split up directly before entering the more prominent dorsal brain region. Such an arc-like set of innervating ganglia (tga) was never described for terebellids so far.

According to various authors, annelid feeding palps are defined as being innervated by nerves originating from the ventral and dorsal main neurite bundles (roots) of the *cc* [13, 14, 19, 27, 28]. As described for the terebellid *Pista cristata* (Müller, 1776) and the ampharetid *Amphicteis* cf. *gunneri* (M. Sars, 1835) [13] a quite similar peristomial innervation pattern of the buccal tentacles can be assumed. Furthermore, they seem closely associated with the nerves of the alimentary canal [13, 14]. By comparing earlier investigations of Orrhage (see [14]) and our results, the branching pattern of all involved neurite bundles is similar. It is shown that stomatogastric nerves only originate from the *cc* or/and its ventral root and thus belong to the ventral brain region. A pattern we can observe in *H. invalida* and *L. conchilega* as well. Accordingly, the ventral strand (root) of the *cc* and the innervation of the entire stomatogastric system are closely associated. A close neuroanatomical connection of the "common tract"/ ventral region of the brain and the stomatogastric neurite bundles seems to be a widespread phenomenon. An alimentary origin of the buccal tentacles is therefore unreasonable based on the presented data.

Furthermore, no obvious developmental connection of the pharynx and the buccal tentacles can be observed for terebelliform taxa so far [15, 17, 20].

According to the current knowledge [13] and our presented data, a similar neuroanatomy can be assumed for Pectinariidae as being the sister taxon of all other Terebelliformia [6]. Many authors also support the homology of the buccal tentacles in all Terebelliformia investigated so far [1, 12, 13]. In conclusion, our data strongly promote a homologization of the buccal tentacles in Terebelliformia with the feeding palps in the remaining Annelida. Accordingly, in Oweniidae (exemplarily shown for *Owenia fusiformis* (Delle Chiaje, 1844) and *Myriowenia sp.* (Hartmann, 1960)), two main neurite bundles innervate the palps or the tentacular crown. These prominent neurite bundles originate dorso-laterally and medio-dorsally from the brain [29]. Together with data from Magelonidae - which show a much more structured brain with a clear interpretation of the palp neurite bundles coming from the ventral and the dorsal region of the brain - a homologization of the feeding palps in Paleoannelida (Oweniidae and Magelonidae) and Terebelliformia is plausible [30] with respect of multiple losses that might have happened in non-sedentarian families. In Sedentaria, comparable palps and palp nerves fulfilling these neuroanatomical criteria can also be found in Orbiniidae [31], Siboglinidae [32, 33], Cirratuliformia [14] and Spionidae/Sabellidae [10, 14, 34]. A detailed comparison of the neuroanatomy of all mentioned taxa highly supports our hypothesis concerning the terebelliform anteriormost head appendages as sharing the same evolutionary (peristomial) origin like the feeding palps of other taxa. Comparable investigations for errant annelids are still pending.

During the ontogenetic formation of the anterior end, a clear differentiation has to be made in respect of "cephalisation" and "multiplication" – not only in Terebelliformia.

In contrast to adult Terebellidae, the aulophora larvae of *L. conchilega* possesses only a few tentacles, which are arranged antero-dorsally on the head. During ontogenesis, multiplication – an increase in the number of similar structures – in this case of the tentacles, leads to a lateral increase of tentacles until adulthood. Inside the tentacular bud, loop-like nerves originate from the ventral brain region and differentiate from lateral in median direction. This multiplication process is also known from other sedentary polychaetes, such as Sabellariidae and Sabellidae [26, 35] and results in an anterior concentration of numerous identical structures, like e.g. feeding palps, which are therefore involved into the formation of the anterior end. In contrast, the anterior clustering of other structures – such as branchiae – is shown to be the result of ontogenetic transition of parapodia-associated structures during cephalisation (see above). Although the result of both processes – multiplication and cephalisation – highly contributes to the formation of the anterior

end in annelids (or at least the realisation of the sensorial peculiarities of the head), they have to be considered as independent processes that should be interpreted separately.

Conclusion

Our comparative and comprehensive approach including various morphological methods and a detailed literature revision sheds new light on the evolutionary origin of anterior head appendages in Terebelliformia.

The brains of the ampharetid *Hypania invalida* and the aulophora larvae of *Lanice conchilega* (Terebellidae) consist of a dorsal, more prominent and a more slender, ventral brain region, which seems to be the result of a brain protrusion. Neurite bundles innervating the buccal tentacles split off from the ventral and dorsal root within the ventral brain region and thus originate from the dorsal and ventral root of the circumoesophageal connectives. In this respect, the observed neurite bundles fulfil the morphological criteria for the innervating neurite bundles of feeding palps known from Palaeoannelida. Furthermore, we confirm a close association of the neurite bundles of the buccal tentacles and neurite bundles of the alimentary tract. Nevertheless, the innervation of parts of the alimentary canal by the ventral strand (root) of the circumoesophageal connectives seems to be the rule and not the exception in Annelida. Thus, we disagree with former conclusions that buccal tentacles are part of the alimentary canal. Accordingly, the buccal tentacles of terebelliform taxa can be homologized with peristomial feeding palps of other Annelida. Hence, multiple losses in non-sedentarian families have to be assumed. Additionally, our data uncover two important and independent processes during the formation and localisation of head appendages in Terebelliformia - cephalisation and multiplication. Hence, both processes result in a concentration of appendages and sensory structures around the head. Unfortunately, there is a huge lack of morphological data concerning these key features of annelid evolution and further investigations are needed to investigate both processes in related families. Furthermore, to gather a comprehensive picture concerning the evolution of head appendages in Annelida in general, additional comparative investigations of anterior appendages in other families are strongly/urgently needed.

Methods

Specimen collection

Adult specimens of *Hypania invalida* (Grube, 1860) were collected from the river Rhein near Bonn in summer 2018. Specimens were maintained together with the collected sediment in a freshwater aquarium with a 12 h:12 h light regime at 17 °C at the University of Göttingen. Adult specimen of *Terebella lapidaria* Linnaeus, 1767 were found in crevices on the beach of Le Cabellou, close to the city of Concarneau (Brittany, France) in September 2018.

Aulophora larvae of *Lanice conchilega* (Pallas, 1766) were caught around the island of Helgoland with a plankton net and fixed by employees of the Biological Station Helgoland according to our protocols in autumn 2019.

Immunohistochemistry

Anatomical details of adult *H. invalida* and aulophora larvae of *L. conchilega* were investigated using standard immunohistochemical staining protocols. Specimens of both species were relaxed in 7% $MgCl_2$ and subsequently fixed in 4% paraformaldehyde (PFA) in 1x phosphate buffered saline with Tween (PTW = 1x PBS: 0.05 M PB / 0.3 M NaCl / 0.6% Tween20 (0.4% Tween20 for *L. conchilega*, pH 7,4). Fixation was performed at room temperature (RT) for 2 h for *H. invalida* and 1 h for *L. conchilega*. After fixing, the specimens were washed and stored in PTW containing 0,005% NaN_3 until usage at 4 °C.

For antibody staining, specimens were rinsed 2 × 5 min in PTW at RT and permeabilized in 10 µg proteinase K/ml PTW (10 min for *H. invalida* and 15 min for *L. conchilega*). After 2 short rinses in glycine (2 mg glycine/ml PTW), and 3 × 5 min washes in PTW, the specimens were re-fixed using 4% PFA in PTW containing 0.6/0.4% Tween for 20 min at RT. Subsequently, the samples were rinsed 2 × 5 min in PTW, 2 × 5 min in THT (0.1 M TrisCl, 0.1% Tween, pH 8,5) and blocked with 5% goat serum (Sigma-Aldrich Chemie GmbH, Steinheim, 25 µl goatserum in 500 µl THT) for 2 h. Afterwards, specimens were incubated with the primary antibodies against α-tubulin (Anti-acetyl α -tubuline, clone 6-11B-1, Merck, Darmstadt, 2 µl tubulin in 500 µl incl. 5% goat serum) and serotonin (5-HT (serotonin), ImmunoStar Inc.,Hudson, USA, 1 µl in 500 µl incl. 5% goat serum) in THT for 48-72 h at 4 °C.

Afterwards, samples were rinsed 2 × 10 min in 1 M NaCl and washed 5 × 30 min in THT.

Subsequently, the samples were incubated in the secondary antibodies goat-anti-mouse 633 (Alexa Fluor® 633 goat-anti- mouse IgG (H + L), Thermo Fisher Scientific Inc., Waltham, USA, 1 µl in 500 µl inlc. 5% goat serum) and goat-anti-rabbit 488 (Alexa Fluor® 488 goat-anti-rabbit IgG (H + L), Thermo Fisher Scientific Inc., Waltham, USA, 1 µl in 500 µl incl. 5% goat serum) in THT for 48-72 h at 4 °C.

After the staining, specimens were rinsed 5 × 30 min in THT and 2 × 5 min in PTW. Additionally, samples were incubated in DAPI (DAPI, Thermo Fisher Scientific Inc., Waltham, USA, 5 µl in PTW) in PTW overnight at 4 °C.

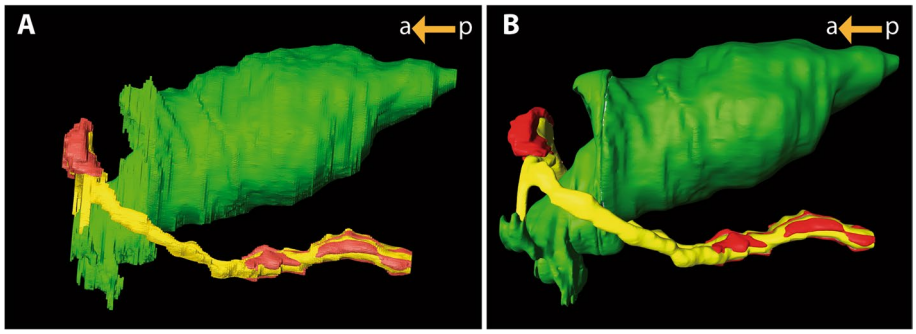

Fig. 7 3D-reconstruction based on Azan-stained -sections of *Hypania invalida*. **A.** 3D-reconstruction of the brain, circumoesophageal connectives, ventral nerve cord (yellow), cell soma (red) and inverted pharynx and oesophagus (green) using Fiji and Amira. **B.** Same reconstruction using workflow including Blender

Subsequently, the specimens were dehydrated in an ascending isopropanol series, cleared using Murray's clear (benzyl alcohol & benzyl benzoate, 1:2) and embedded between two cover slips using DPX mounting medium (Merck, Darmstadt, Germany). The specimens were analysed with a confocal laser-scanning microscope Leica TCS SP8 (Leica Microsystems, Wetzlar, Germany). The confocal image stacks were processed with Leica AS AF v2.3.5 (Leica Microsystems) and Imaris ×64 9.2.1 (Bitplane AG, Zurich, Switzerland).

Azan staining, histological sections and 3D-reconstruction

For semi-thin sections and AZAN-staining specimens of *Hypania invalida* and *Terebella lapidaria* were processed as described in [36]. Accordingly, specimens were relaxed in 7% $MgCl_2$ and then fixed in Bouin's fluid for 12 h, dehydrated in an ethanol series and incubated in methylbenzoat and butanol. Afterwards the samples were pre- incubated in Histoplast (Thermo Scientific, Dreieich, Germany) and embedded in Paraplast (McCormick Scientific, Richmond, USA). 5 µm thick sections were made using a Reichert-Jung Autocut 2050 microtome (Leica, Wetzlar, Germany). The sections were transferred to albumen-glycerin coated glass slides. Afterwards sections were stained with Carmalaun, differentiated with sodium phosphotungstate (5%), washed in distilled water, stained in aniline blue orange G and subsequently embedded with Malinol (Waldeck, Münster, Germany). In Azan staining, the neuropil of the nervous system stains gray, the nuclei of cell somata stain red, the extracellular matrix stains blue and the musculature stains orange [36]. Each section was digitalized at 40x magnification using a slide scanner (Olympus dotslide (2.2 Olympus, Hamburg)) and aligned using IMOD [37] and imodalign (http://www.q-terra.de/biowelt/3drekon/guides/imod_first_aid.pdf).

For the 3D-visualization we used Amira 2019.1, Meshlab_64bit_fp v2020.6, Blender 2.83 and deep exploration 5.5. Due to the unavoidable artefacts occurring during physical sectioning and the problems coming with it to reconstruct a smooth 3D-model (see Fig. 7A) we used a new combination of freeware resulting in a much more satisfactory result for the eye (Fig. 7B).

Abbreviations

cc: Circumoesophageal connectives; *cdbr*: Connective of dpbr; *cvbr*: Connective of vpbr; *dpbr*: Dorsal region of the brain; PB: Phosphate buffer saline; PFA: Paraformaldehyde; *prn*: Prostomial nerves; RT: Room temperature; THT: TrisCl buffer; *vnc*: Ventral nerve cord; *vpbr*: Ventral region of the brain.

Acknowledgments

The authors want to thank the working group "Animal Evolution and Biodiversity" and "Evolutionary Biology and Ecology" for the financial and technical support. We want to thank Dr. Georg Becker from The Ecological Rhine Station, University of Cologne for providing adult *Hypania invalida* and Ute Kieb from the Alfred-Wegner-Institute Helgoland for providing larvae of *Lanice conchilega*. Finally, we want to thank the reviewers for help and constructive suggestions improving an earlier version of this manuscript.

Authors' contributions

PK and CH designed the project and conducted immunohistochemical experiments and CLSM-analyses. PB conducted the paraffin histology and Azan-staining. PK created the schematic drawings and 3D-visualizations. CH and PK drafted the manuscript and PB counselled in data presentation and writing. All authors read, commented on and agreed to the final version of the manuscript.

Funding

This work was financially supported by the group "Animal Evolution and Biodiversity" of the University of Goettingen. No third party funding was used in addition. Open Access funding enabled and organized by Projekt DEAL.

Availability of data and materials

All data analysed in this study are used in figures of this article. The original 3D confocal image stacks can be made available after personal contact with the corresponding authors.

Declarations

Ethics approval and consent to participate

Not applicable.

Consent for publication
Not applicable.

Competing interests
The authors declare that they have no competing interests.

Author details
[1]Department of Animal Evolution and Biodiversity, University of Goettingen, Goettingen, Germany. [2]Institute of Evolutionary Biology and Ecology, University of Bonn, Bonn, Germany.

Received: 2 February 2021 Accepted: 19 October 2021
Published online: 16 November 2021

References

1. Holthe T. Evolution, systematics, and distribution of the Polychaeta Terebellomorpha, with a catalogue of the taxa and a bibliography. Gunneria. 1986;55:1–236.
2. Glasby CJ, Hutchings PA, Hall K. Assessment of monophyly and taxon affinities within the polychaete clade Terebelliformia (Terebellida). J. Mar. Biol. Assoc. United Kingdom. Oct. 2004;84(5):961–71.
3. Nogueira JMDM, Fitzhugh K, Hutchings P. The continuing challenge of phylogenetic relationships in Terebelliformia (Annelida : Polychaeta). Invertebr Syst. 2013;27:186–238.
4. C. Helm et al., "Convergent evolution of the ladder-like ventral nerve cord in Annelida," Front. Zool., vol. 15, no. 1, 2018.
5. Weigert A, et al. Illuminating the base of the annelid tree using transcriptomics. Mol Biol Evol. 2014;31(6):1391–401.
6. Stiller J, Tilic E, Rousset V, Pleijel F, Rouse GW. Spaghetti to a tree: a robust phylogeny for Terebelliformia (Annelida) based on Transcriptomes, molecular and morphological data. Biology (Basel). 2020;9(73):1–28.
7. A. Weigert and C. Bleidorn, "Current status of annelid phylogeny," Organisms Diversity and Evolution, vol. 16, no. 2. 2016.
8. Binard A, Jeener R. Morphologie du lobe préoral des polychètes; 1928.
9. D. Nilsson, Beiträge zur Kenntnis des Nervensystems der Polychaeten, vol. 1. Almquist & Wiksells, 1912.
10. Orrhage L. On the structure and homologues of the anterior end of the polychaete families sabellidae and serpulidae. Zoomorphology. 1980;96(1–2):113–67.
11. Rouse GW, Fauchald K. Cladistics and Polychaetes. Zool Scr. 1997;26(2):139–204.
12. Zhadan AE, Tzetlin AB. Comparative morphology of the feeding apparatus in the Terebellida (Annelida: Polychaeta). Cah Biol Mar. 2002;43(2):149–64.
13. Orrhage L. On the anatomy of the central nervous system and the morphological value of the anterior end appendages of Ampharetidae, Pectinariidae and Terebellidae (Polychaeta). Acta Zool. 2001;82(1):57–71.
14. Orrhage L, Müller MCM. Morphology of the nervous system of Polychaeta (Annelida). Hydrobiologia. 2005;535(1):79–111.
15. C. Cazaux, "Developpement larvaire de l'ampharetidae lagunaire Alkmaria romijni Horst 1919. Cahiers de Biologie Marine, 23: 143–157,7figures.," no. 1, pp. 143–157, 1982.
16. Bhaud M. Change in setal pattern during early development of Eupolymnia nebulosa (Polychaeta: Terebellidae) grown in simulated natural conditions. J Mar Biol Assoc United Kingdom. 1988;68(4):677–87.
17. Eckelbarger KJ. Population biology and larval development of the terebellid polychaete Nicolea zostericola. Mar Biol. 1974;27(2):101–13.
18. Richter S, et al. Invertebrate neurophylogeny : suggested terms and definitions for a neuroanatomical glossary. Front Zool. 2010;7(1):1–49.
19. Fauchald K, Rouse G. Polychaete systematics: past and present. Zool Scr. 1997;26(2):71–138.
20. BHAUD M, GREMARE A. Larval development of theterebellid polychaete Eupolymnia nebulosa (Montagu) in the Mediterranean Sea. Zool Scr. Oct. 1988;17(4):347–56.
21. CAPA M, HUNTCHINGS PA. Terebellidae (Polychaeta) from Coiba National Park, Panamanian Pacific, including description of four new species and synonymy of the genus Paraeupolymnia with Lanicola. Zootaxa. 2006;29(1375):1–29.
22. Nogueira JMDM, Hutchings PA, Fukuda MV. Morphology of terebelliform polychaetes (Annelida: Polychaeta: Terebelliformia), with a focus on Terebellidae. Zootaxa. 2010;2460:1–185.
23. Winchell CJ, Valencia JE, Jacobs DK. Confocal analysis of nervous system architecture in direct-developing juveniles of Neanthes arenaceodentata (Annelida, Nereididae). Front Zool. 2010;7(1):1–19.
24. Starunov VV, Voronezhskaya EE, Nezlin LP. Development of the nervous system in Platynereis dumerilii (Nereididae, Annelida). Front Zool. 2017;14(1):1–20.
25. Åkesson B. The embryology of Tomopteris helgolandica (Polychaeta). Acta Zool. 1962;43(2–3):135–99.
26. Faroni-Perez L, Helm C, Burghardt I, Hutchings P, Capa M. Anterior sensory organs in Sabellariidae (Annelida). Invertebr Biol. 2016;135(4):423–47.
27. Rouse GW, Pleijel F. Polychaetes. Oxford, New York: Oxford University Press; 2001.
28. Purschke G, Bleidorn C, Struck T. Systematics, evolution and phylogeny of Annelida – a morphological perspective. Mem Museum Victoria. 2014;71:247–69.
29. Beckers P, Helm C, Purschke G, Worsaae K, Hutchings P, Bartolomaeus T. The central nervous system of Oweniidae (Annelida) and its implications for the structure of the ancestral annelid brain. Front Zool. 2019;16(1):1–21.
30. Beckers P, Helm C, Bartolomaeus T. The anatomy and development of the nervous system in Magelonidae (Annelida) - Insights into the evolution of the annelid brain. BMC Evol. Biol. 2019;19:1.
31. Wilkens V, Purschke G. Pigmented eyes, photoreceptor-like sense organs and central nervous system in the polychaete Scoloplos armiger (Orbiniidae, Annelida) and their phylogenetic importance. J Morphol. 2009;270(11):1296–310.
32. K. Worsaae, N. N. Rimskaya-Korsakova, and G. W. Rouse, "Neural reconstruction of bone-eating Osedax spp. (Annelida) and evolution of the siboglinid nervous system," BMC Evol. Biol., vol. 16, no. 1, 2016.
33. N. N. Rimskaya-Korsakova, S. V. Galkin, and V. V. Malakhov, The neuroanatomy of the siboglinid *Riftia pachyptila* highlights sedentarian annelid nervous system evolution, vol. 13, no. 12. 2018.
34. G. Purschke, "A n n e l i d a : B asa l G roups A n d P l e i s toa n n e l i d a," in Structure and Evolution of Invertebrate Nervous System, G. P. Andreas Schmidt-Rhaesa, Steffen Harzsch, Ed. Oxford University Press, 2016, pp. 254–312.
35. Wilson DP. Memoirs: the development of the Sabellid Branchiomma vesiculosum. J Cell Sci. 1936;2(312):543–603.
36. P. Beckers, R. Loesel, and T. Bartolomaeus, "The Nervous Systems of Basally Branching Nemertea (Palaeonemertea)," PLoS One, vol. 8, no. 6, 2013.
37. Kremer JR, Mastronarde DN, McIntosh JR. Computer visualization of three-dimensional image data using IMOD. J Struct Biol. 1996;116(1):71–6.

Publisher's Note

Received: 17 June 2022 | Revised: 30 September 2022 | Accepted: 6 October 2022

DOI: 10.1002/jemt.24250

RESEARCH ARTICLE

MICROSCOPY RESEARCH & TECHNIQUE WILEY

No cost but high performance–An alternative open source solution for 3D-visualizations in morphology

Paul Kalke | **Conrad Helm**

Johann-Friedrich-Blumenbach-Institute for Zoology & Anthropology, Department of Animal Evolution and Biodiversity, Georg-August-University Göttingen, Göttingen, Germany

Correspondence
Paul Kalke, Johann-Friedrich-Blumenbach-Institute for Zoology & Anthropology, Department of Animal Evolution and Biodiversity, Georg-August-University Göttingen, Untere Karspuele 2, 37073 Göttingen, Germany.
Email: paul.kalke@uni-goettingen.de

Funding information
University of Goettingen, Department of Animal Evolution and Biodiversity

Review Editor: Alberto Diaspro

Abstract

3D-visualization has become common courtesy in science and also found its way into teaching in schools and universities. Nevertheless, the way to high performance 3D-visualization and analyses remains difficult and is often also a matter of budget. Due to the obvious advantages of presenting morphological and anatomical datasets with the help of 3D-figures, all in one software solutions usually come along with high rental and maintenance fees. For that reason, it is more than overdue to establish and use open source software solutions with all their obvious advantages - as other disciplines already do. Here we provide a modular, highly adaptive and freely available software pipeline for high performance 3D-visualizations of (not only) morphological datasets by combining features of ImageJ, MeshLab and Blender, without any additional costs. Exemplarily using serial-block face SEM data as well as serial AZAN-stained histological sections, the herein presented step-by-step protocol allows for a fast and efficient analysis, visualization and animation of large, anatomical datasets. Regardless which type of serial, morphological datasets needs to be analyzed, our open source guide provides an easy to handle and promptly adaptable solution. Therefore, our pipeline for 3D-visualization represents a valuable alternative to conventional, commercial packages.

Research Highlights

We provide a highly modular and easy to learn open source solution for multiple 3D-visualizations. The step-by-step-guide make it easy to start, and advanced users can replace software, add others and such build your own individual software pipeline.

KEYWORDS
Amira, blender, ImageJ, MeshLab, step-by-step guide, workflow

1 | INTRODUCTION

3D-visualization becomes more and more important, in science (Murienne et al., 2008; Ravi et al., 2015; Richter & Wirkner, 2014; Smalley et al., 2006; Wirkner & Richter, 2010) and teaching (Dere et al., 2010; Huk, 2006; Nasir et al., 2018; Verdes et al., 2021). Not only in times of the corona pandemic, digital tools such as for example, virtual classrooms, online learning platforms (https://outschool.com/#abkvuyn38n) and digital dissecting tools (https://biosphera3d.com/product-category/software/; https://www.digitalfrog.com/products/frog.html; Zilverschoon et al., 2017) get into focus of universities and schools. Furthermore, 3D-models became standard for data

presentations and visualizations, especially–but not exclusively - in morphological/anatomical studies in biology and medicine (Handschuh et al., 2013; Kehl et al., 2022; Noever et al., 2016; Runge & Wirkner, 2016). The use of non-destructive morphological methods, free manipulation and visualization, and output formats like videos and 3D-Pdfs revolutionized the way, how morphology can be understood and imparted without leaving the third dimension (Murienne et al., 2008; Richter & Wirkner, 2014; Wirkner & Richter, 2010). Consequently, 3D-visualization has become common courtesy in many biological disciplines. Despite that, comprehensible and high quality 3D-visualizations are no small matter.

Therefore, an intuitive or good usability is irreplaceable next to accessibility and high performance. Furthermore, it has to allow for all kinds of manipulations, data refinement and visualizations. In this respect several commercial software solutions, such as for example, Amira (Stalling et al., 2005) and Imaris (https://imaris.oxinst.com/) are available, which combine most of the needs of the scientific community, but come along with high renting and maintenance fees. Amira became kind of a standard in most publications focussed on zoological approaches (Allentoft-Larsen et al., 2021; Bibermair et al., 2021; Melzer et al., 2021; Wipfler et al., 2021) and beyond.

In other biological disciplines, many often used software solutions are already open source. Popular examples are BEAST (Drummond & Rambaut, 2007), Mesquite (Maddison & Maddison, 2021) and MorphoBank (O'Leary & Kaufman, 2011). In bioinformatics packages such as Weka ([Markov & Russell, 2006] [https://www.udemy.com/course/weka-data-mining-with-open-source-machine-learning-tool/], R [https://www.r-project.org/], [Dwivedi et al., 2016], a whole array of tools for analyzing molecular data and KNIME [Berthold et al., 2006; Dwivedi et al., 2016] are used, while in ecology GIS-software and R [https://www.r-project.org/] [Dwivedi et al., 2016]) are part of the daily work.

When it comes to open source software, the advantages seem quite obvious. Besides the unlimited accessibility in combination with low costs and higher safety, the additional space for individual solutions and the easily possible cooperation with peers should be underlined.

In the context of zoology-focussed approaches several open source software packages like ImageJ (Abràmoff et al., 2004; Collins, 2007; Schindelin et al., 2012), MeVisLab (https://www.mevislab.de/), Ilastik (Sommer et al., 2011), MeshLab (Cignoni et al., 2008), SlicerMorph (Rolfe et al., 2021), online platforms such as Biomedisa (Lösel et al., 2020) or Morphosource (Boyer et al., 2016) are available and find their way into scientific publications and data presentation. Additionally, software of originally non-scientific purposes, like Blender, get used to improve the appearance and quality of 3D-content in science (Durrant, 2019; Kadam et al., 2012; Naiman, 2016; Nasir et al., 2018; Zoppè et al., 2008). Nevertheless, handling and combination of the latter tools is still very time consuming and badly realizable–in particular when it comes to different data types and large datasets.

Therefore, a modular open source solution for high performance 3D-visualizations with unlimited access and no costs is highly needed. Hence, we provide a digital workflow combining three open source software packages (Image J, MeshLab and Blender, Figure 1) suitable for almost all kinds of morphological or anatomical datasets. Our pipeline combines easy handling and usability with all advantages of an open source community. Additionally, we supply a step-by-step guide through the entire workflow exemplarily shown for a serial-block face Scanning Electron Microscopy (SEM) dataset of the larval nuchal organ of the annelid *Paramphinome jeffreysii* (McIntosh, 1868) (Amphinomidae, Annelida). Additionally, the workflow outcome is shown for serial histological azan-sections of the anterior nervous system of the adult annelid *Hypania invalida* (Grube, 1860) (Ampharetidae, Annelida).

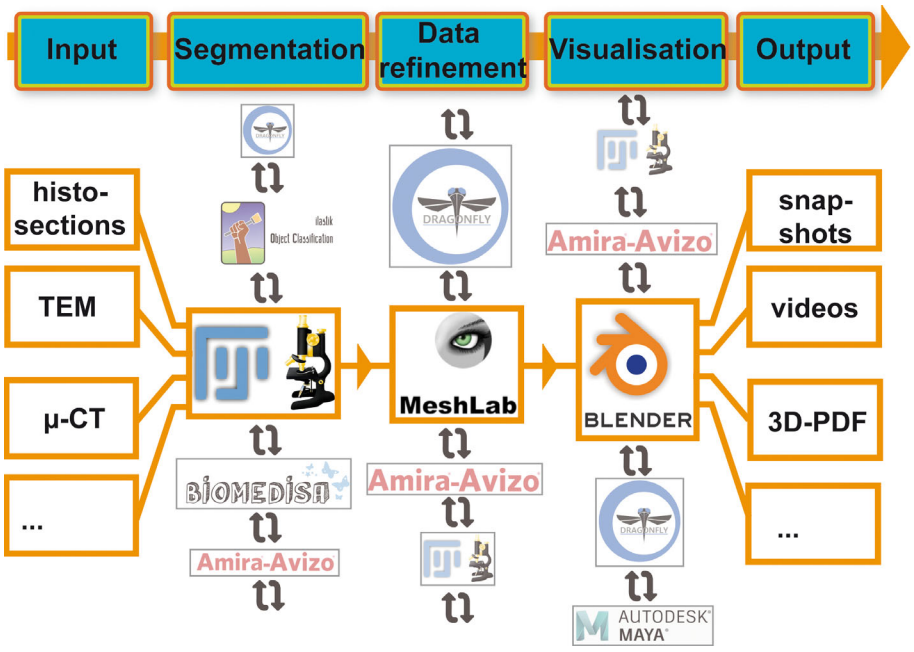

FIGURE 1 Summary of our modular open source solution for high performance 3D-visualization. Please note that all steps from input generation until style of output can be modified according to the respective needs. In our case, we used ultrastructural and serial azan-sections, processed them via ImageJ, MeshLab and Blender, and generated meaningful snapshots as well as video-files. The resulting videos about the amphinomid nuchal organ can be found under S4 video and the video of the anterior nervous system of *Hypania invalida* under S5 video

2 | MATERIALS AND METHODS

2.1 | Software packages

Our Open source workflow represents a combination of three open source software packages, namely ImagesJ (https://imagej.nih.gov/ij/) (see S1), Meshlab (https://www.meshlab.net/) (see S2) and Blender (https://www.blender.org/) (see S3). A detailed step-by-step user manual is provided in the supplement as S1-S3. Furthermore, we show examples of possible data presentation by using the work flow as videos in S4 and S5.

2.2 | Datasets used for 3D-visualizations

The used data sets for the exemplarily presentation of the workflow are a serial-block face SEM (ultrastructual) dataset of the larval nuchal organ of the annelid *Paramphinome jeffreysii* (Amphinomidae, Annelida) (Helm et al., in prep.) and a serial series of AZAN-stained histological sections of the anterior end of the annelid *Hypania invalida* (Terebelliformia, Annelida) (Kalke et al., 2021). The amphinomid larvae were collected in 2017 during the ForBio Field course "International course on annelid systematics, morphology and evolution" at the Espegrend Marine Biological Station (Bergen, Norway). The larvae were collected during plankton sampling in the Raunefjord and brought to the lab for further fixation. Hence, the larvae of *Paramphinome* were relaxed using 3.5% $MgCl_2$ in FSW (filtered sea water) and subsequently fixed for 1 h at room temperature in 2.5% Glutaraldehyde in phosphate buffered saline (PBS) (1xPBS: 0.05 mol L^{-1} PB, 0.3 mol L^{-1} NaCl). Subsequently, the samples were washed several times in 1xPBS and transferred into sodium cacodylate buffer (0.1 mol L^{-1} cacodylate, 0.24 mol L^{-1} NaCl) for further processing according to the protocol mentioned for SBF SEM in (Büsse et al., 2016).

Adult specimens of *Hypania invalida* were collected in the river Rhein in Bonn (Germany) in 2018. Animals were processed as described elsewhere (Kalke et al., 2021). For further information regarding the sample preparation and imaging techniques please check out the original publications.

3 | RESULTS

As the main focus of the manuscript is represented by the open source workflow itself, the results section is mainly dedicated to the step-by-step procedure allowing the 3D-visualization of different morphological datasets. To provide a modularly and easy to adapt tool set for the analyses of any kind of serial morphological datasets/ sections, we came up with a detailed workflow showing a detailed manual for a successful and easy usage. Therefore, we solely used open source solution packages by combining features of ImageJ, MeshLab and Blender (summarized in Figure 1). Aligned data sets were segmented using *TrakEM2* Plugin in ImageJ and the resulting labels/ reconstructed structures were exported as OBJ-files. After importing the data into MeshLab the object meshes were repaired and cleaned, re-meshed, smoothed and simplified. Subsequently, the resulting meshes were exported as .ply-file. In Blender, artificial surface structures, such as for example, muscle fibers or the appearance of the epidermal cells, were added by using the *Sculpting Mode* and the informations of the original-data set as a template. Subsequently, the modified meshes were re-colored, duplicated and cut in half using the *Boolean-modifier*. For a better 3-dimensional performance, camera movements were animated using the *Walk Navigation* and got refined by smoothing the *keyframes* in the *Graphic Editor*. The videos were rendered with the *Workbench* tool using different lightning.

The protocol described in this peer-reviewed article is published on protocols.io,

S1 ImageJ: https://doi.org/10.17504/protocols.io.b2x9qfr6

S2 MeshLab: https://doi.org/10.17504/protocols.io.b2zhqf36 and

S3 Blender: https://doi.org/10.17504/protocols.io.b2ziqf4e and is included for printing as supporting information file 1–3 (S1, S2, and S3) as PDF-files with this article. Additionally, we provide two videos with examples we generated by using our work flow (see S4 and S5).

4 | DISCUSSION

The use of 3D content in science has revolutionized the way how we understand and present morphology (Murienne et al., 2008; Richter & Wirkner, 2014). The advantages of 3D-visualization also lead to rising numbers of available software packages and services, which improved the acquisition, the processing and the visualization of any kind of morphological datasets (Abràmoff et al., 2004; Cignoni et al., 2008; Collins, 2007; Lösel et al., 2020; Rolfe et al., 2021; Schindelin et al., 2012; Sommer et al., 2011; Stalling et al., 2005). In this respect, commercial products like for example, "Amira" or "Imaris" combine a variety of helpful feature such as alignment, reconstruction, data refinement and visualization in one software package. This fact makes them quite convenient to use while the usability gets improved constantly. Nevertheless, this service results in high acquisition and maintenance costs. Furthermore, the flexibility and user-oriented modification of such commercial solutions is quite limited. Especially for researchers with lower budgets or more interdisciplinary teams - which not mainly focus on morphological data but want to include up-to-date 3D-visualizations–commercial packages result in an unsatisfactory trade off. In this respect, open source solutions provide a much better cost–benefit ratio. In our understanding, morphological and anatomical research of nowadays should use open source solutions as many disciplines already do (see introduction). The advantages of open source software packages and the corresponding communities, which are already there, are seductive and could also effect more interdisciplinary collaborations and exchange without the loss of performance. On the other hand, starting to learn new - especially open source - programs is always challenging. Often we observe a non-intuitive way to use open source software, which can be frustrating and needs time as well as persistence to start and master it. The combination of various software packages from different sources is quite demanding and requires stamina - problems which were adressed by allround packages.

Nevertheless, the opportunity to freely exchange software tools in each step of our workflow - from data acquisition to the final presentation - gives rise to more individual and witty solutions, and allows for an optimal modification of the needed outcome according to the respective (research) interests.

Herein, we supply one easy and cheap open source solution for high quality 3D-visualization usable for various morphological datasets. Due to the combination of nicely fitting and modularly features of ImageJ, MeshLab and Blender, our workflow provides a high user friendliness and adaptability, and thus can be adjusted at any step of the process. Additionally, the provided step-by-step guide enables for an easy replication and adaptation. Accordingly, our workflow might represent a useful tool for an interdisciplinary community dealing with different–not only morphological–datasets, and constitutes an alternative solution to expensive commercial work packages.

AUTHOR CONTRIBUTIONS

Paul Kalke: Conceptualization; investigation; methodology; visualization; writing – original draft; writing – review and editing. **Conrad Helm:** Data curation; project administration; resources; supervision; validation; writing – review and editing.

ACKNOWLEDGMENTS

The authors want to thank the working group "Animal Evolution and Biodiversity" and "Evolutionary Biology and Ecology" for the financial and technical support. We are very thankful to Dr. Christian Wirkner, Dr. Torben Göpel and Dr. Jens Runge to share their expertise in using Amira, MashLab and visualization techniques, and Dr. Patrick Beckers to show us the TrakEM2 plug in of ImageJ. Furthermore, we thank Nataliya Budaeva (Bergen, Norway) and ForBio for the invitation to join the annelid course in Espegrend, and Dr. Georg Becker from the Ecological Rhine Station (University of Cologne) for help with the collection of *Hypania*. Open Access funding enabled and organized by Projekt DEAL.

FUNDING INFORMATION

This work was financially supported by the group "Animal Evolution and Biodiversity" of the University of Goettingen. No third party funding was used in addition.

CONFLICT OF INTEREST

The authors do not have any conflicts of interest.

DATA AVAILABILITY STATEMENT

The data that support the findings of this study are openly available in (repository name e.g., "protocols.io") at; https://doi.org/10.17504/protocols.io.b2x9qfr6; https://doi.org/10.17504/protocols.io.b2zhqf36; https://doi.org/10.17504/protocols.io.b2ziqf4e.

ORCID

Paul Kalke https://orcid.org/0000-0003-4138-3426

REFERENCES

Abràmoff, M. D., Magalhães, P. J., & Ram, S. J. (2004). Image processing with ImageJ. *Biophotonics International*, *11*(7), 36–42. https://doi.org/10.1201/9781420005615.ax4

Allentoft-Larsen, M. C., Gonzalez, B. C., Daniels, J., Katija, K., Osborn, K., & Worsaae, K. (2021). Muscular Adaptations in Swimming Scale Worms (Polynoidae, Annelida). *Royal Society Open Science*, *8*(10), 210541. https://doi.org/10.1098/rsos.210541

Berthold, M. R., Cebron, N., Dill, F., di Fatta, G., Gabriel, T. R., Georg, F., Meinl, T., Ohl, P., Sieb, C., & Wiswedel, B. (2006). "KNIME: The Konstanz Information Miner." In 4th International Industrial Simulation Conference 2006, ISC 2006, *11*, 58–61. https://doi.org/10.1145/1656274.1656280.

Bibermair, J., Ostrovsky, A. N., Wanninger, A., & Schwaha, T. (2021). Reproductive biology, embryonic development and Matrotrophy in the Phylactolaemate bryozoan Plumatella Casmiana. *Organisms Diversity & Evolution*, *21*(2), 467–490. https://doi.org/10.1007/s13127-021-00497-w

Boyer, D. M., Gunnell, G. F., Kaufman, S., & McGeary, T. M. (2016). Morphosource: Archiving and sharing 3-D digital specimen data. *The Paleontological Society Papers*, *22*, 157–181. https://doi.org/10.1017/scs.2017.13

Büsse, S., Hörnschemeyer, T., & Fischer, C. (2016). Three-dimensional reconstruction on cell level: Case study elucidates the ultrastructure of the spinning apparatus of Embia Sp. (Insecta: Embioptera). *Royal Society Open Science*, *3*(10), 160563. https://doi.org/10.1098/rsos.160563

Cignoni, P., Callieri, M., Corsini, M., Dellepiane, M., Ganovelli, F., & Ranzuglia, G. (2008). "MeshLab: An Open-Source Mesh Processing Tool." 6th Eurographics Italian Chapter Conference 2008 – Proceedings, 129–136.

Collins, T. J. (2007). ImageJ for microscopy. *BioTechniques*, *43*(1 S), S25–S30. https://doi.org/10.2144/000112517

Dere, S., Sahasrabudhe, S., & Iyer, S. (2010). "Creating open source repository of 3D models of laboratory Equipments using blender." 2010 international conference on Technology for Education, T4E 2010, 149–156. https://doi.org/10.1109/T4E.2010.5550044.

Drummond, A. J., & Rambaut, A. (2007). BEAST: Bayesian evolutionary analysis by sampling trees. *BMC Evolutionary Biology*, *7*(1), 1–8. https://doi.org/10.1186/1471-2148-7-214

Durrant, J. D. (2019). Blendmol: Advanced macromolecular visualization in blender. *Bioinformatics*, *35*(13), 2323–2325. https://doi.org/10.1093/bioinformatics/bty968

Dwivedi, S., Kasliwal, P., & Soni, S. (2016). "Comprehensive Study of Data Analytics Tools (RapidMiner, Weka, R Tool, Knime)." In 2016 Symposium on colossal data analysis and networking (CDAN), IEEE. 1–8, https://doi.org/10.1109/CDAN.2016.7570894.

Handschuh, S., Baeumler, N., Schwaha, T., & Ruthensteiner, B. (2013). A correlative approach for combining MicroCT, light and transmission electron microscopy in a single 3D scenario. *Frontiers in Zoology*, *10*(1), 1–16. https://doi.org/10.1186/1742-9994-10-44

Huk, T. (2006). Who benefits from learning with 3D models? The case of spatial ability. *Journal of Computer Assisted Learning*, *22*(6), 392–404. https://doi.org/10.1111/j.1365-2729.2006.00180.x

Kadam, K., Sahasrabudhe, S., & Iyer, S. (2012). "Improvement of mental rotation ability using blender 3-D." Proceedings - 2012 IEEE 4th international conference on Technology for Education, T4E, 60–66. https://doi.org/10.1109/T4E.2012.28

Kalke, P., Beckers, P., & Helm, C. (2021). May the palps Be with you–New insights into the evolutionary origin of anterior appendages in Terebelliformia (Annelida). *BMC Zoology*, *30*(6), 1–14. https://doi.org/10.1186/s40850-021-00094-6

Kehl, T., van Rüth, V., Weinrich, J. M., & Hübler, M. (2022). Using three-dimensional visualization as an optimal tool to plan and validate an Aortopexy in a congenital heart disease patient with severe tracheal

stenosis. *Interactive Cardiovascular and Thoracic Surgery*, *34*(4), 708–710. https://doi.org/10.1093/icvts/ivab315

Lösel, P. D., van de Kamp, T., Jayme, A., Ershov, A., Faragó, T., Pichler, O., Jerome, N. T., Aadepu, N., Bremer, S., Chilingaryan, S. A., Heethoff, M., Kopmann, A., Odar, J., Schmelzle, S., Zuber, M., Wittbrodt, J., Baumbach, T., & Heuveline, V. (2020). Introducing Biomedisa as an open-source online platform for biomedical image segmentation. *Nature Communications*, *11*(1), 1–14. https://doi.org/10.1038/s41467-020-19303-w

Maddison, W. P., & Maddison, D. R. (2021). Mesquite: A modular system for evolutionary analysis. Version 1.0 *3*.70. http://www.mesquiteproject.org

Markov, Z., & Russell, I. (2006). "An introduction to the WEKA data mining system." In proceedings of the 11th annual SIGCSE conference on innovation and Technology in Computer Science Education - ITICSE '06, 18:367–68. New York, New York, USA: ACM Press. https://doi.org/10.1145/1140124.1140127.

Melzer, R. R., Spitzner, F., Šargač, Z., Hörnig, M. K., Krieger, J., Haug, C., Haug J. T., Kirchhoff, T. Meth, R., Torres, G., & Harzsch, S. (2021). Methods to study organogenesis in decapod crustacean larvae II: Analysing cells and tissues. *Helgoland Marine Research*, *75*(1), 1–37. https://doi.org/10.1186/s10152-021-00547-y

Murienne, J., Ziegler, A., & Ruthensteiner, B. (2008). A 3D revolution in communicating science. *Nature*, *453*(7194), 450. https://doi.org/10.1038/453450d

Naiman, J. P. (2016). AstroBlend: An astrophysical visualization package for blender. *Astronomy and Computing*, *15*, 50–60. https://doi.org/10.1016/j.ascom.2016.02.002

Nasir, M., Prastowo, R. B., & Riwayani, R. (2018). Design and development of physics learning Media of Three Dimensional Animation Using Blender Applications on atomic Core material. *Journal of Educational Sciences*, *2*(2), 23–32. https://doi.org/10.31258/jes.2.2.p.23-32

Noever, C., Keiler, J., & Glenner, H. (2016). First 3D reconstruction of the rhizocephalan root system using MicroCT. *Journal of Sea Research*, *113*(July), 58–64. https://doi.org/10.1016/j.seares.2015.08.002

O'Leary, M. A., & Kaufman, S. (2011). MorphoBank: Phylophenomics in the 'cloud. *Cladistics*, *27*(5), 529–537. https://doi.org/10.1111/j.1096-0031.2011.00355.x

Ravi, M., Paramesh, V., Kaviya, S. R., Anuradha, E., & Paul Solomon, F. D. (2015). 3D cell culture systems: Advantages and applications. *Journal of Cellular Physiology*, *230*(1), 16–26. https://doi.org/10.1002/jcp.24683

Richter, S., & Wirkner, C. S. (2014). A research program for evolutionary morphology. *Journal of Zoological Systematics and Evolutionary Research*, *52*(4), 338–350. https://doi.org/10.1111/jzs.12061

Rolfe, S., Pieper, S., Porto, A., Diamond, K., Winchester, J., Shan, S., Kirveslahti, H., Boyer, D., Summers, A., & Murat Maga, A. (2021). SlicerMorph: An open and extensible platform to retrieve, visualize and analyse 3D morphology. *Methods in Ecology and Evolution*, *12*(10), 1816–1825. https://doi.org/10.1111/2041-210X.13669

Runge, J., & Wirkner, C. S. (2016). The Hemolymph vascular system in a Raneus Diadematus with special focus on intraspecific variability in artery systems. *Journal of Arachnology*, *44*(2), 153–164. https://doi.org/10.1636/JoA-S-16-001

Schindelin, J., Arganda-Carreras, I., Frise, E., Kaynig, V., Longair, M., Pietzsch, T., Preibisch, S., Rueden, C., Saalfeld, S., Schmid, B., Tinevez, J.-Y., White, D. J., Hartenstein, V., Eliceiri, K., Tomancak, P., & Cardona, A. (2012). Fiji: An open-source platform for biological-image analysis. *Nature Methods*, *9*(7), 676–682. https://doi.org/10.1038/nmeth.2019

Smalley, K. S. M., Lioni, M., & Herlyn, M. (2006). Life isn't flat: Taking cancer biology to the next dimension. *In Vitro Cellular and Developmental Biology - Animal*, *42*(8–9), 242–247. https://doi.org/10.1290/0604027.1

Sommer, C., Straehle, C., Kothe, U., & Hamprecht, F. A. (2011). "Ilastik: Interactive learning and segmentation toolkit." Proceedings - International Symposium on Biomedical Imaging, 230–33. https://doi.org/10.1109/ISBI.2011.5872394.

Stalling, D., Westerhoff, M., & Hege, H. C. (2005). Amira: A highly interactive system for visual data analysis. *Visualization Handbook*, *1*, 749–767. https://doi.org/10.1016/B978-012387582-2/50040-X

Verdes, A., Navarro, C., & Álvarez-Campos, P. (2021). Mobile learning applications to improve invertebrate zoology online teaching. *Invertebrate Biology*, *140*(1), 1–12. https://doi.org/10.1111/ivb.12321

Wipfler, B., Bradler, S., Büsse, S., Hammel, J., Müller, B. R., & Pass, G. (2021). Evolutionary morphology of the antennal heart in stick and leaf insects (Phasmatodea) and Webspinners (Embioptera) (Insecta: Eukinolabia). *Zoomorphology*, *140*(3), 331–340. https://doi.org/10.1007/s00435-021-00526-4

Wirkner, C. S., & Richter, S. (2010). Evolutionary morphology of the circulatory system in Peracarida (malacostraca; Crustacea). *Cladistics*, *26*(2), 143–167. https://doi.org/10.1111/j.1096-0031.2009.00278.x

Zilverschoon, M., Vincken, K. L., & Ronald Bleys, L. A. W. (2017). The virtual dissecting room: Creating highly detailed anatomy models for educational purposes. *Journal of Biomedical Informatics*, *65*, 58–75. https://doi.org/10.1016/j.jbi.2016.11.005

Zoppè, M., Porozov, Y., Andrei, R., & Cianchetta, S. (2008). Using blender for molecular animation and scientific representation. *Blender Conference*, *1*, 1–6 http://www.scivis.it/images/stories/PDFarticle/blenderzoppeetal3.pdf

SUPPORTING INFORMATION

Additional supporting information can be found online in the Supporting Information section at the end of this article.

How to cite this article: Kalke, P., & Helm, C. (2023). No cost but high performance–An alternative open source solution for 3D-visualizations in morphology. *Microscopy Research and Technique*, *86*(2), 193–197. https://doi.org/10.1002/jemt.24250

Palps across the tree – the neuronal innervation and development of sensory head appendages in Annelida

Paul Kalke[1]*, Samira S. Linder[1], Patrick Becker[2] & Conrad Helm[1]*

[1]Helm Lab, Johann-Friedrich-Blumenbach-Institute, Animal Evolution and Biodiversity, University of Göttingen,, 37073 Göttingen, Germany
[2]Institute of Evolutionary Biology, University of Bonn, 53121 Bonn, Germany

*** Correspondence:**
Corresponding Author
paul.kalke@uni-goettingen.de

chelm@uni-goettingen.de

Keywords: Polychaeta, Magelonidae, Amphinomidae, Spionidae, Rostraria, ontogeny, larvae

Abstract

Polychaetes inhabit a huge variety of habitats and hence show an even greater morphological diversity. In this context, a key morphological structure to adapt to their individual lifestyles and ecological niches are the prominent head appendages.

In the last years more and more studies focussed on the mainly sensory annelid head appendages – namely the antennae, palps, buccal lips and cirri - to unravel the evolutionary origin and phylogeny of Annelida. Unfortunately, comparable data for most of the polychaete families are lacking so far, especially when it comes to features of the larval anterior nervous system and the related innervation and potential homology of head appendages. In this study, we therefore use an integrative morphological approach including immunohistochemistry and confocal laser scanning microscopy in combination with histological serial sections and 3D-visualisation. With special focus on the palps, this comprehensive dataset is used to provide a closer look into the development of the larval anterior nervous system and the related sensory system of three polychaete families representing major groups of the annelid tree of life. Hence, we investigate Magelonidae - as member of the Paleoannelida - as well as Amphinomidae as representing the sister group of Errantia and Sedentaria (Pleistoannelida), and the derived Spionidae forming a taxon deeply nested within the latter. Our detailed data of larval and adult neuronal features and scaffolds support the homology of feeding palps across the annelid tree. Furthermore, our observations show that larval palps gradually transform into the adult ones while keeping a very similar innervation pattern. Solely for Amphinomidae a loss of larval palps during ontogenesis has to be assumed. Therefore, our investigations enlight important and so far unknown details in terms of structural homology across Annelida and are important for our understanding of annelid evolution.

1 Introduction

Marine polychaetes exhibit a remarkable diversity, both in terms of their morphological adaptations and ecological niches.

In particular the evolution of head appendages in polychaetes has fascinated researchers across the decades and the understanding of these structures remains an ongoing scientific endeavour (Nilsson, 1912; Binard and Jeener, 1928; Orrhage, 1966; Rouse and Fauchald, 1997; Rouse and Pleijel, 2001; Orrhage and Müller, 2005; Purschke, Bleidorn and Struck, 2014; Beckers *et al.*, 2019; Beckers, Helm and Bartolomaeus, 2019; Kalke, Beckers and Helm, 2021). Whereas many aspects of annelid morphology and evolution have been investigated across the years, our knowledge concerning the evolution and putative homology of head appendages in Annelida is still very limited (Purschke, 2016). Head appendages – in particular the so-called palps - play a crucial role in the ecological success and adaptability of marine polychaetes, but their comparability and evolutionary adaptation in different taxa are still not fully elucidated (Rouse and Fauchald, 1997; Rouse and Pleijel, 2001; Beckers *et al.*, 2019; Beckers, Helm and Bartolomaeus, 2019; Kalke, Beckers and Helm, 2021). Hence, palp-bearing members of the annelid tree of life either exhibit slender, elongated feeding-palps or stout and quite immobile sensory palps (Purschke, 2016). However, the question of a possible homology between the different palp types and between the same morphotype of palps in different taxa still remains an open question (Purschke, Bleidorn and Struck, 2014; Kalke, Beckers and Helm, 2021). In particular the comparison and transition of larval towards adult palp-like structures is hardly understood and bears numerous knowledge gaps. In the present investigation we therefore focus on the comparison between larval and adult palps in three annelid taxa – Magelonidae, Amphinomidae, and Spionidae. These particular families are chosen based on their phylogenetic relationship and the presence of elongated palp-like head appendages in at least some of the larval stages (see Fig. 1). Moreover, at least Magelonidae and Spionidae exhibit elongated palps in the adult stage as well.

The basally-branching Magelonidae use their slender palps for the uptake of detritus and organic debris from the inhabited soil (Jones, 1968; Weigert *et al.*, 2014; Helm *et al.*, 2018). It is also mentioned that adult Magelonidae are exceptional flexible in switching from deposit-feeding (Jones, 1968; Jumars, Dorgan and Lindsay, 2015) over subsurface feeding (Jumars, Dorgan and Lindsay, 2015) and suspension feeding (Hartmann-Schröder *et al.*, 1971; Wolff,

1973) to carnivorous feeding by catching veliger-larvae, crustacean larvae and other small animals (Jones, 1968; Wilson, 1982). As shown previously, adult Magelonidae possess true feeding-palps, which are elongated, posses a food-rim, lack cilia but are papillose, and are neuronally innervated by the dorsal and ventral root of the circumoesophageal connectives (Orrhage, 1966; Purschke, 2016; Beckers, Helm and Bartolomaeus, 2019). Comparable adult feeding-palps of other taxa exhibiting a similar innervation pattern are also described e.g., for the basally-branching Oweniidae (Beckers *et al.*, 2019) and Chaetopteriformia (Helm, Schwarze and Beckers, 2022). Therefore, these structures have to be considered being a plesiomorphic character state for annelids (Beckers, Helm and Bartolomaeus, 2019).

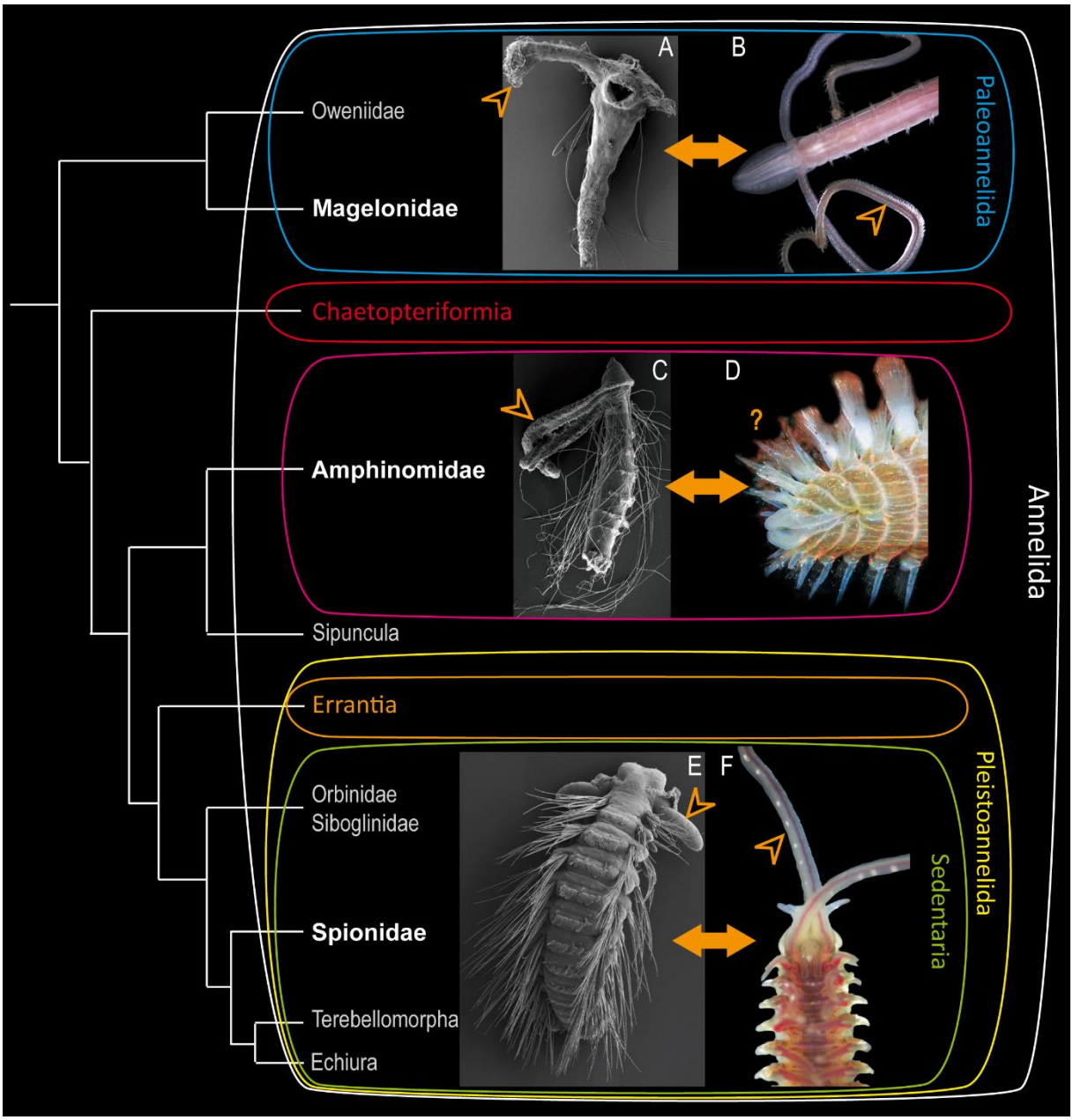

Fig. 1: Modified annelid Phylogeny based on Helm et al. 2018. Larva of *Magelona mirabilis* (A), Rostraria larva of *Paramphinome jeffreysii* (C) and late larva of *Malacoceros fuliginosus* (E) added as SEM-micrographs. Adults of *Magelona mirabilis* (B), *Eurythoe complanata* (D) and *Malacoceros fuliginosus* (F) added as light microscopic micrographs. The respective families are highlighted in bold white letters, arrowheads mark the position of the larval and adult palps.

Interestingly, such slender appendages are not present in adult Sipuncula and Amphinomidae, but are present in many taxa of the sedentary Pleistoannelida, such as adult Sabellariidae (Orrhage, 1980; Faroni-Perez *et al.*, 2016), Siboglinidae (Worsaae, Rimskaya-Korsakova and Rouse, 2016; Rimskaya-Korsakova, Galkin and Malakhov, 2018), Terebllidae (Orrhage, 2001; Kalke, Beckers and Helm, 2021), Spionidae (Orrhage, 1966; Orrhage and Müller, 2005) and

Cirratuliformia (Purschke, 2016). Whereas the data source for adult feeding-palps allows some comparisons across taxa and supports a homology statement, our knowledge concerning the larval head appendages is still very scarce.

Many polychaete larvae are planktotrophic (Rouse, 1999, 2006) and thus spend their developmental time in the water column, where they grow elongated larval palps that help to capture diatoms, flagelattes and other larvae (Wilson, 1936, 1982; Jones, 1968). Although distantly related, taxa such as Magelonidae and Spionidae use their multifunctional elongated larval head appendages for feeding throughout their life stages. Furthermore, other annelid taxa bear slender palp-like appendages only during their larval phase, while the adults no longer have palp-like head structures. The best example for this condition are the fireworms, the Amphinomidae. In this clade a transition from planktotrophic larvae (Rouse, 1999, 2006) to omnivorous scavangers or carnivores adults (Fauchald and Jumars, 1979; Jumars, Dorgan and Lindsay, 2015) can be observed. This change of ecological adaptations goes along with morphological differences e.g., in the arrangement of head appendages, the development of sufficient parapodia and hollow, calcified chaetae (Müller *et al.*, 2021). Rostraria larvae – the unique amphinomid larval type - use their elongated palp-like head appendages to feed using their ciliary bands in a downstream manner (Rouse, 1999, 2006), similar to the larvae of Magelonidae and Spionidae (Lit?). As adults most Amphinomidae have two lateral and one median antennae and - as claimed by other authors - two short “palps” located dorsally of the buccal lips (Orrhage, 1990; Orrhage and Müller, 2005). Therefore, amphinomids are of particular interest when it comes to the evolutionary transition between the different palp types.

By understanding the fate of larval palp-like head appendages and potential transitions towards adult conditions in Magelonidae, Amphinomidae as well as Spionidae, we can elucidate a crucial aspect of the ontogenesis of these enigmatic and ecologically important sensory and feeding structures. By exploring the morphological features and adaptations of palps within and among these families, we aim to shed light on the evolutionary trajectories and developmental changes of these important sensory and feeding structures.

Our study employs an integrative morphological approach, combining various microscopic techniques such as immunohistochemistry, confocal laser-scanning microscopy and Azan-stained histological section stacks and subsequent 3D-visualisation. These methods allow us

to visualize and analyse the morphological characteristics of larval and adult palps in great detail. For a better understanding and comparison of the main findings, we also supply interactive 3D-schemes for the anterior larval neuronal scaffold of all three families.

By doing so we seek to understand the developmental changes and variations in palps during the transition from larvae to adults, which in addition might give a hint towards an evolutionary origin of the enigmatic sensory palps found in Errantia. Furthermore, our data will help to answer the fundamental question concerning the homology of different types of palps and other sensory head appendages throughout Annelida.

2 Materials & Methods

2.1 Specimen collection

Adult specimens of *Magelona mirabilis* (Johnston, 1865) and *Malacoceros fuliginosus* (Claparede, 1868) were collected in Morgat (Brittany, France) in 2015. Specimens were maintained with the collected sediment in an aquarium with a 12h:12h light regime and 3.5% salinity at 17°C at the Michael Sars Centre (Bergen, Norway). Adults were fed a mixture of yeast and grinded fish food. After artificial fertilization in filtered seawater (FSW) the developmental stages were reared at 18 °C in glass bowls containing 0.5 l FSW. The culture was not aerated, set under strict diurnal rhythm (12:12 – light: dark), and fed with a mix of unicellular algae (*Isochrysis*). Water was changed regularly.

Rostraria larvae of *Paramphinome jeffreysii* (McIntosh, 1868) were collected via plankton net close to the Espegrend marine biological field station (Raunefjord, Bergen, Norway) in 2017. Adult specimens of *Eurythoe complanata* (Pallas, 1766) were collected from the private aquarium of Peter Lesny, Bonn (COI barcode sequence available at the NCBI GenBank, Accession number: KY630466*)*.

2.2 Immunohistochemistry

Anatomical details of larvae of *Magelona mirabilis*, *Paramphinome jeffreysii* and *Malacoceros fuliginosus* were investigated using standard immunohistochemical staining protocols. Hence, specimens were relaxed in 7% $MgCl_2$ and subsequently fixed in 4% paraformaldehyde (PFA) in 1x phosphate buffered saline with Tween (PTW = 1x PBS: 0.05 M PB / 0.3 M NaCl / 0.3%

TritonX. Fixation was performed at room temperature (RT) for 2 h. After fixing, the specimens were washed and stored in PTW containing 0,005% NaN_3 until usage at 4 °C. For antibody staining, specimens were rinsed 3 x 10 min in PTW and incubated in 10 µg proteinase K/ml PTW for few minutes according to the larval age. After 2 short rinses in glycine (2 mg glycine/ml PTW), and 3 × 5 min washes in PTW, the specimens were re-fixed using 4% PFA in PTW containing 0.6/0.3 % TritonX for 20 min at RT. Subsequently, the samples were rinsed 2 × 5 min in PTW as well as 2 × 5 min in THT (0.1 M TrisCl, 0.3 TritonX, pH 8,5), and blocked with 5% goat serum (Sigma-Aldrich, Steinheim, 25 µl goat serum in 500 µl THT) for 2 h. Afterwards, specimens were incubated with the primary antibodies against α-tubulin (Anti-acetyl α - tubuline, clone 6-11B-1, Merck, Darmstadt, 2 µl tubulin in 500 µl incl. 5% goat serum) and serotonin (5-HT (serotonin), ImmunoStar Inc., Husk, USA, 1 µl in 500 µl incl. 5% goat serum) in THT for 48-72 h at 4 °C. Afterwards, samples were rinsed 2 × 10 min in 1 M NaCl in THT and washed 5 × 30 min in THT. Subsequently, the samples were incubated in the secondary antibodies goat-anti-mouse 633 (Alexa Fluor® 633 goat-anti-mouse IgG (H + L), Thermo Fisher Scientific Inc., Waltham, USA, 1 µl in 500 µl inlc. 5% goat serum) and goat-anti-rabbit 488 (Alexa Fluor® 488 goat-anti-rabbit IgG (H + L), Thermo Fisher Scientific Inc., Waltham, USA, 1 µl in 500 µl incl. 5% goat serum) in THT for 48-72 h at 4 °C. After staining, specimens were rinsed 5 × 30 min in THT and 2 × 5 min in PTW. Additionally, samples were incubated in DAPI (DAPI, Thermo Fisher Scientific Inc., Waltham, USA, 5 µl in PTW) in PTW overnight at 4 °C. Subsequently, the specimens were dehydrated in an ascending isopropanol series, cleared using Murray's clear (benzyl alcohol & benzyl benzoate, 1:2) and embedded between two cover slips using DPX mounting medium (Merck, Darmstadt, Germany). The specimens were analysed with the confocal laser scanning microscopes Leica TCS SP5 and SP8 (Leica Microsystems, Wetzlar, Germany). The confocal image stacks were processed with Leica AS AF v2.3.5 (Leica Microsystems) and Imaris × 64 9.5.0 (Bitplane AG, Zurich, Switzerland).

2.3 Azan staining, histological sectioning and 3D-reconstruction

Semi-thin sections and AZAN-staining of adult *Eurythoe complanata* were performed as described previously (Beckers, Loesel and Bartolomaeus, 2013). Accordingly, specimens were relaxed in 7% MgCl2 and then fixed in Bouin's fluid for 12 h, dehydrated in an ethanol series and incubated in methylbenzoat and butanol. Afterwards, the samples were pre-incubated in

Histoplast (Thermo Scientific, Dreieich, Germany) and embedded in Paraplast (McCormick Scientific, Richmond, USA). 5 µm thick sections were made using a Reichert-Jung Autocut 2050 microtome (Leica, Wetzlar, Germany). The sections were transferred to albumen-glycerin coated glass slides. Afterwards, sections were stained with Carmalaun, differentiated with sodium phosphotungstate (5%), washed in distilled water, stained in aniline blue orange G and subsequently embedded with Malinol (Waldeck, Münster, Germany). In Azan staining, the neuropil of the nervous system stain gray, the nuclei of cell somata stain red, the extracellular matrix stain the musculature stains orange (Beckers et al. 2013). Each section was digitalized at 40x magnification using a slide scanner (Olympus dotslide (2.2 Olympus, Hamburg)) and aligned using IMOD (Kremer et al. 1996) and imodalign (www.q-terra.de/biowelt/3drekon/guides/imod_first_aid.pdf). For the 3D-visualization, we used a digital workflow using solely open source software like ImageJ, MeshLab and Blender (Kalke and Helm, 2022). For the 3D-schemes we used curve tools in Blender (for a better understanding see: https://www.youtube.com/watch?v=Ve9h7-E8EuM) and for the preparation of 3D-Pdfs deep exploration.

3 Results

For the investigation of larval and adult palp features in marine polychaetes we used 9 days-post -fertilisation (9dpf) larvae of the magelonid *Magelona mirabilis* (Jonston, 1865) (Fig. 2), ~10 as well as ~60 dpf larvae of the spionid *Malacoceros fuliginosus (Claparède, 1868)* (Fig. 3) and Rostraria-larvae of the amphinomid *Paramphinome jeffreysii* (McIntosh, 1868) (Fig. 4). Adult *Eurythoe complanata* (Pallas, 1766) were used for Azan-histological sections (Fig. 5) and subsequent 3D-reconstruction (Fig. 6). For a better understanding of morphological features, we summarized our findings in 3D-schematic drawings, which are shown on the respective figures and are visualized for comparison as interactive 3D-Pdfs in Fig. 6 C - G.

For general terms and annotation of the nervous system, we refer to (Richter *et al.*, 2010), for the anterior nervous system we used the annotations of (Schmidbaur *et al.*, 2020). For the description of adult *E. complanata* please refer to (Beckers and Tilic, 2021).

3.1 Central nervous system and head appendages in larval *Magelona mirabilis* (Magelonidae)

The early larvae of *M. mirabilis* show one prominent palp (Fig. 2A, C), while the other one is still in development and only appears as a palp-bud (Fig. 2A, C). Both structures are randomly ciliated compared to real ciliary bands in other annelid larvae. The anterior central nervous system consists of the ventral (*vrcc*) and dorsal root (*drcc*) of the circumoesophageal connectives and fuse in posterior direction (Fig. 2A - C). The transition of the circumoesophageal connectives (*cc*) into the ventral nerve cord (*vnc*) is fluent (Fig. 2A - D). The *vnc* shows already three commissures (Fig. 2A, C) and terminate posteriorly by giving rise to two pygidial nerves.

The outgrown palp is innervated by at least four neurite bundles, whereas the two most prominent ones (pn2 and pn3) originate from the vrcc and the drcc (Fig. 2A – D). The two more slender palp neurite bundles originate from the lip nerve ring (*linr*) - which surrounds the mouth opening (Fig. 2B) - and from the *cc* more posteriorly (Fig. 2A – D). The serotonin-like immunoreactivity (serotonin-lir) exhibits most structures of the anterior central nervous system excluding the *vrcc*. The lip nerve ring (*linr*) shows a strong serotonergic signal too, crowned by one of two prominent perikarya. The second prominent serotonergic perikaryon is located anterior-most on the *drcc*. Although the *vrcc* shows no serotonergic signal all palp nerves do (Fig. 2D).

For further comparisons, please use the interactive 3D-Pdf (see Fig. 5A).

3.2 Central nervous system and head appendages in larvae of *Malacoceros fuliginosus* (Spionidae)

For *Malacoceros fuliginosus* we describe here a quite early metatrochophore of ~10dpf and a juvenile larva (~60dpf) directly before metamorphosis. The early metatrochophore appears with typical larval features such as a distinct prototroch, gastrotroch and telotroch. Furthermore, the first pair of metanephridia is developed at this stage (Fig. 3A). In this stage

the palp buds are visible posterior to the prototroch by anti-serotonin staining (Fig. 3B; note that the cilia are removed in the image). Despite these larval features, the anterior central nervous system is well-developed. Hence, it exhibits a distinct brain consisting of the ventral (vrcc) and dorsal root (*drcc*) of the circumoesophageal connectives, which fuse posteriorly to the circumoesophageal connectives (*cc*) (Fig. 3B, C). The transition from the *cc* to the ventral nerve cord (*vnc*) is smooth and first slender commissures and segmental nerves appear (Fig. 3A, B).

In juvenile *M. fuliginosus*, the larval ciliary bands are still well-developed but show first signs of reduction due to metamorphosis into the adult stage (Fig. 3D). The *vnc* shows two strong and distinct neurite bundles with α-tubulin-lir bearing hundreds of slender commissures and at least twelve segmental nerves (Fig. 3D). The transition from the *vnc* to the *cc* is distinct and in addition marked by the first two anterior-most segmental nerves (Fig. 3 E, F). In anterior direction, the *cc* split into the *vrcc* and the *drcc* to fuse again forming the juvenile brain (Fig. 3E – G). Dorsally, each root of the *cc* send, most likely, sensorial nerves into the remnants of the prototroch (Fig. 3E, F).

The juvenile palps are innervated by at least five neurite bundles (Fig. 3E - G). Two slender nerves originate anteriorly from the *vrcc*. The *drcc* gives rise to one thick nerve and two slender ones, which – in contrast to the thick one - emerge slightly more posteriorly from the *drcc* (Fig. 3E-F). The serotonin-lir shows the strongest signal in the brain. The palp nerves (*pn3*) originate from the *vrcc* and the stomatogastric nerve loop.

For further comparison, please use the interactive 3D-Pdf (see Fig. 5B).

3.3 Central nervous system and head appendages in Rostraria larvae of *Paramphinome jeffreysii* (Amphinomidae)

Rostraria larvae have two characteristic and strongly ciliated palps (Fig. 4A, B), which extend over the length of its entire body (not shown in full length). Similar to many polychaete larvae, Rostraria-larvae show a posterior telotroch, a ventral gastrotroch and a more anteriorly

arranged meta- and prototroch (Fig. 4A, B). The prototroch – which is situated anterior to the mouth opening-, and the metatroch, in a more posterior position, surround the larval “head” ventrally and form the ciliated food rim of the palps and mouth region (Fig. 4B). The brain consists of the ventral (*vrcc*) and dorsal root (*drcc*) of the circumoesophageal connectives (Fig. 4B - D). The latter form distinct neurite bundles in posterior direction, termed by doing so as circumoesophageal connectives (*cc*) and ventral nerve cord (*vnc*) (Fig. 4A – E). In a regular manner, circular segmental neurites interconnect the neurite bundles of the *vnc* and the dorsal longitudinal neurite bundle (*dln*) (Fig. 4A, C – E). Directly anterior of the segmental neurite bundles, paired parapodial nerves appear with developmental progression in anterior direction (Fig. 4B, D, E). The larval nuchal organs are located anterior to the palps and are innervated by two slender nerves entering the *drcc* dorsally (Fig. 4C – E).

The huge palps are innervated by at least three palp nerves/ neurite bundles (Fig. 4A, C – E). The most prominent palp nerve (pn1) represents the continuation of the prototroch nerve (*prtrn*), which runs along the upper lip (Fig. 4C, D). *Pn1* continues in dorsal direction crossing the *vrcc* and *drcc* (Fig. 4B – D). At this point, slender neurite bundles from both roots fuse with *pn1* (Fig. 4B – D). Additionally, one big neurite bundle (*con*) originates from the *drcc* and fuses with *pn1*, too (Fig. 4C, D). The two slender palp nerves (*pn*) run, like *pn1*, along the palp but split after entering the head region dorsally and fuse next to *pn1* and *con* with the dorsal ring nerve (*drn*) (Fig. C, D, E).

The *drn* is located dorsally (between the palps) and is highly interconnected appearing as a kind of intersection between both sides of the animal (Fig. 4E). Thus, it is connected anteriorly and laterally with the *drcc.* Laterally, there are further interconnections with *con* and *pn1*, and posteriorly with the *dln* and the segmental nerves.

For further comparison, please use the interactive 3D-Pdf (see Fig. 5C).

3.4 Central nervous system and head appendages of adult *Eurythoe complanata* (Amphinomidae)

Adult *E. complanata* possess five antennae - four lateral and one median one (Fig. 6A). Distally, all antennae exhibit circular nerves, which split into two neurite bundles and fuse for the lateral antennae again right after entering the anterior end of *E. complanata* (Fig. 6A). Posterior to the origin of the root of the lip neurite bundles (*rlin*), all six antennal nerves fuse with the anterior main brain mass (Fig. 6 B – D; 7A, B). The paired lobed lips are innervated by at least six longitudinal neurite bundles, which all originate from different locations from the *rlin* and are interconnected by several semi-circular neurite bundles (Fig. 6A, B, D; 7A, B). Anterior of the main brain mass *E. complanata* has two ventral big eyes and two smaller dorsal ones, which are innervated by nerves originating from the antero-dorsal brain (Fig. 6B, D; 7A, B).

The brain itself is huge and highly compressed. Therefore, the assignment of a ventral (*vrcc*) and dorsal root (*drcc*) of the circumoesophageal connectives or their respective tracts is impossible based on our dataset. After the fusion of the *rlin*, the *vrcc* and *drcc* proceed into the central neuropil , which increase in size and become tapered in posterior progression (Fig. 6B – D, G; 7A, B). At the level where the *vrcc* and the *drcc* enter the brain, several rows of dorso and dorso-lateral stalk-like neurite bundles originate from two sack-like clusters of perikarya (Fig. 6E, D – F; 7A). These two rows of clusters on each side are very closely associated with each other and proceed to the posterior end of the brain neuropil (Fig. 6E, D – F; 7A).

The arrangement of the ventral nerve cord (*vnc*) is also quite unique in *Eurythoe*. Like in the Rostraria of *P. jeffreysii* the *vrcc* and *drcc* proceed longitudinally in distinct and separated neurite bundles, although entering the brain simultaneously (Fig. 6D – G; 7A, B). Both neurite bundles are regularly interconnected by the *con1*, which runs from the hemi-ganglion of the *drcc* in posterior direction and fuse with the *vrcc* (Fig. 6D – G; 7A, B). The segmentally arranged hemi-ganglia give rise to the lateral (*lcirn*) and dorsal cirral nerves (*dcirn*) of the parapodia (Fig. 6D, G; 7A, B). From the *dcirn* the nerves of the segmental branchiae split off. The hemi-ganglia of the at least first three segments are interconnected to the paired nuchal organ nerves (*non*) by the hemi-circular segmental nerves (*sn*) (Fig. 6D, F; 7A, B). The huge *non* proceed dorsally along the anterior-posterior axis towards groups of undefined cell clusters (not shown) giving

rise to several slender neurite bundles running into the caruncle (Fig. 6G). The origin of the *non* is posterior, in close vicinity to the dorsal row of stalk-like neurite bundles connecting the two rows of perikarya with the dorsal neuropil of each brain side. In addition to the *vrcc* and the *drcc,* we observe another paired neurite bundle located medially (*sgn*) (Fig. 6D, G; 7B). This stomatogastric nerve innervates the alimentary canal more posteriorly (not shown) and is interconnected with the *vrcc* via the *con2* multiple times (Fig. 6D, F, G; 6B). Anteriorly, the *sgn* fuse with the paired root of the lip nerves (*rlin*), together with at least one longitudinal lip nerve from the opposing side (Fig. 6D; 7B).

For a better understanding of the described structures and a better comparison of the used taxa, please use the interactive 3D-Pdfs (see Fig. 6C, D).

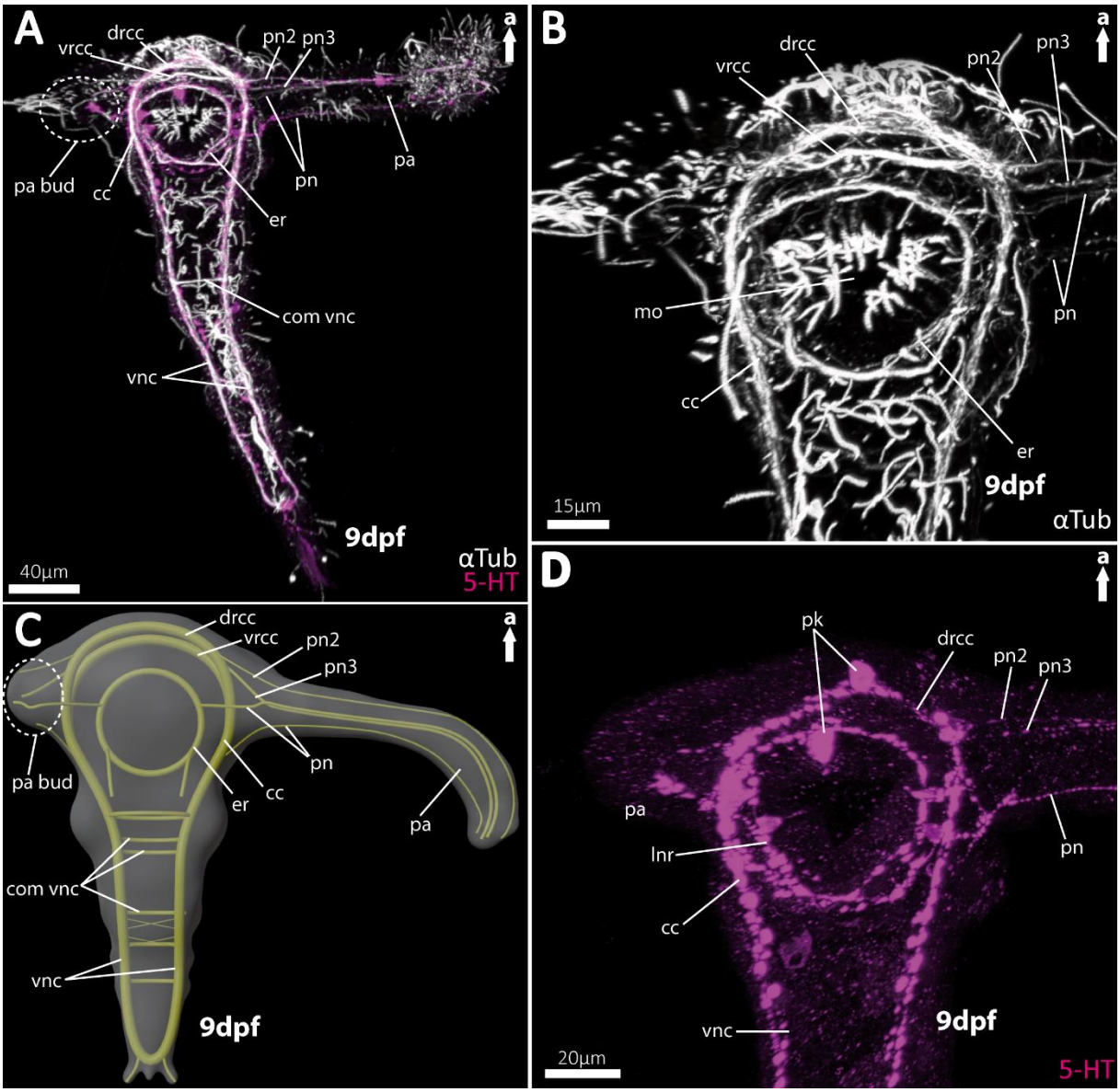

Fig. 2: Nervous system of the larvae (9 dpf) of the magelonid *Magelona mirabilis*. (A) Ventral view of the overall morphology of the nervous system of magelonid larvae stained against acetylated α-tubulin and 5HT-serotonin. The dotted circle marks the growing second palp bud, captured using cLSM micrograph. (B) Magnification of the anterior tubulinergic nervous system in ventral view. (C) 3D-scheme of the nervous system of the larvae of *Magelona mirabilis* in dorsal view. The dotted circle marks the growing second palp bud. (D) Magnification of the serotonergic nervous system in ventral view. ***Abbreviations:*** cc - circumoesophageal connectives, com vnc - commissure of vnc, drcc - dorsal root of cc, er-oesophageal ring, mo - mouth opening, pa - palp, pa bud - palp bud, pn - palp nerves, pn2 - palp nerve of drcc, pn3 - palp nerve of vrcc, pk - serotonin-lir perikarya, vnc - ventral nerve cord, vrcc - ventral root of cc

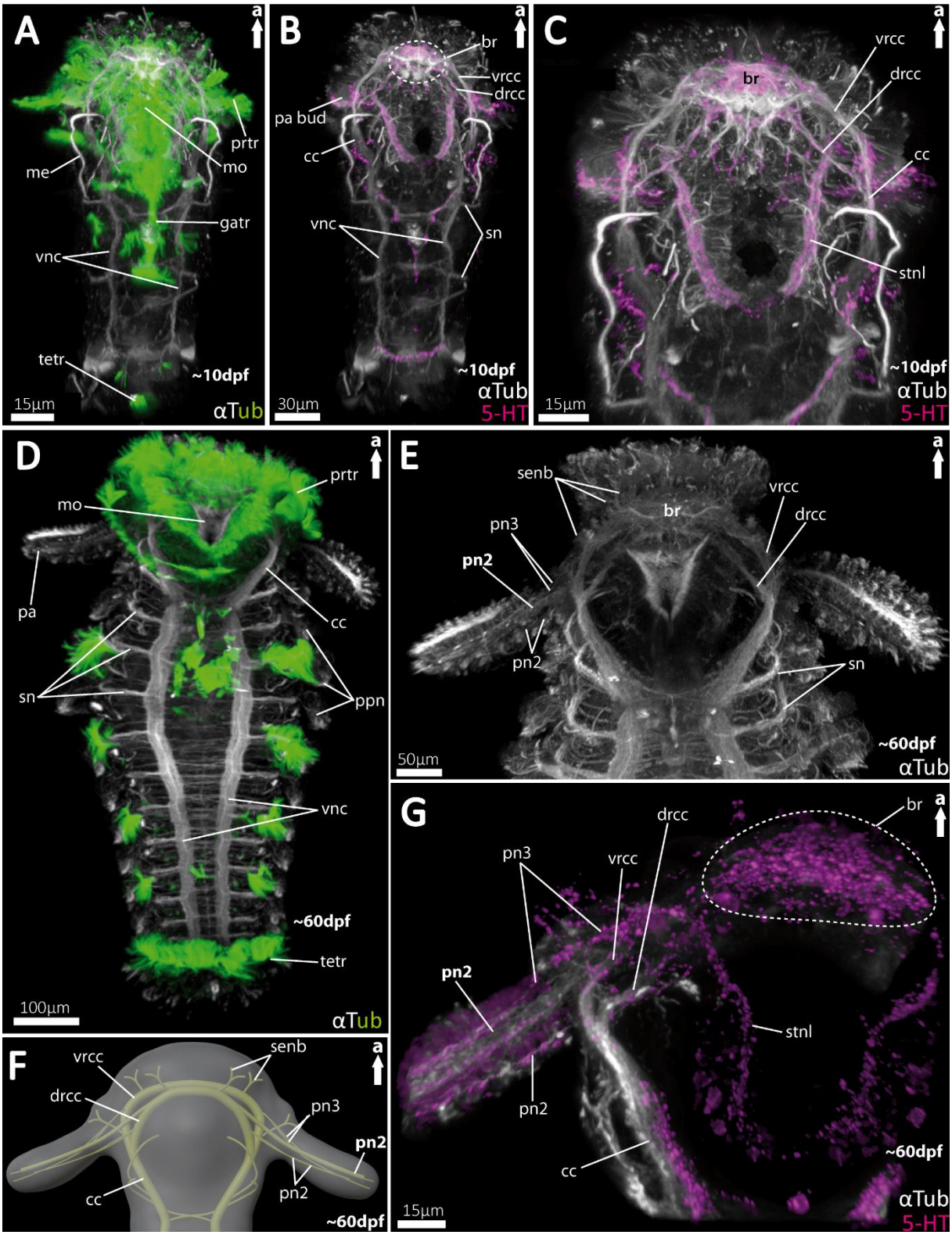

Fig. 3: Nervous system of larvae of the spionid *Malacoceros fuliginosus*. (A) Overall morphology of the tubulinergic nervous system of metatrochophora (~10dpf) in ventral view, with ciliary bands highlighted in green, captured using cLSM micrograph. (B) Overall morphology of the nervous system of a metatrochophore (~10dpf) stained against acetylated α-tubulin and 5HT-serotonin in ventral view. The dotted circle marks the position of the brain, and early palp buds start to develop directly under the prototroch, captured using cLSM micrograph. (C) Magnification of the anterior nervous system of the metatrochophore shown in (B), with the dorsal and ventral aspects of the circumoesophageal

connectives well displayed. (D) Overall morphology of the tubulinergic nervous system and external ciliation (highlighted in green) of a juvenile specimen (~60dpf) of *M. fuliginosus* close to its metamorphosis in ventral view. (E) Magnification of the anterior tubulinergic nervous system with a focus on the brain and innervation of the feeding palps in ventral view. (F) 3D-scheme of the anterior nervous system of a juvenile of the same age in dorsal view. (G) Magnification of the anterior nervous system stained against acetylated α-tubulin and 5HT-serotonin of juvenile *M. fuliginosus* in dorsal view. ***Abbreviations:*** br - brain, cc - circumoesophageal connectives, drcc - dorsal root of cc, gatr - gastrotroch, metr - metatroch, mo - mouth opening, pa - palp, pa bud - palp bud, **pn2 –** thick palp nerve of drcc, pn2 – slender palp nerve of drcc, pn3 - palp nerve of vrcc, ppn - parapodial neurite bundles, prtr - prototroch, senb - sensorial neurite bundles, sn - segmental neurite bundles, stnl – stomatogastric nerve loop, tetr - telotroch, vnc - ventral nerve cord, vrcc - ventral root of cc

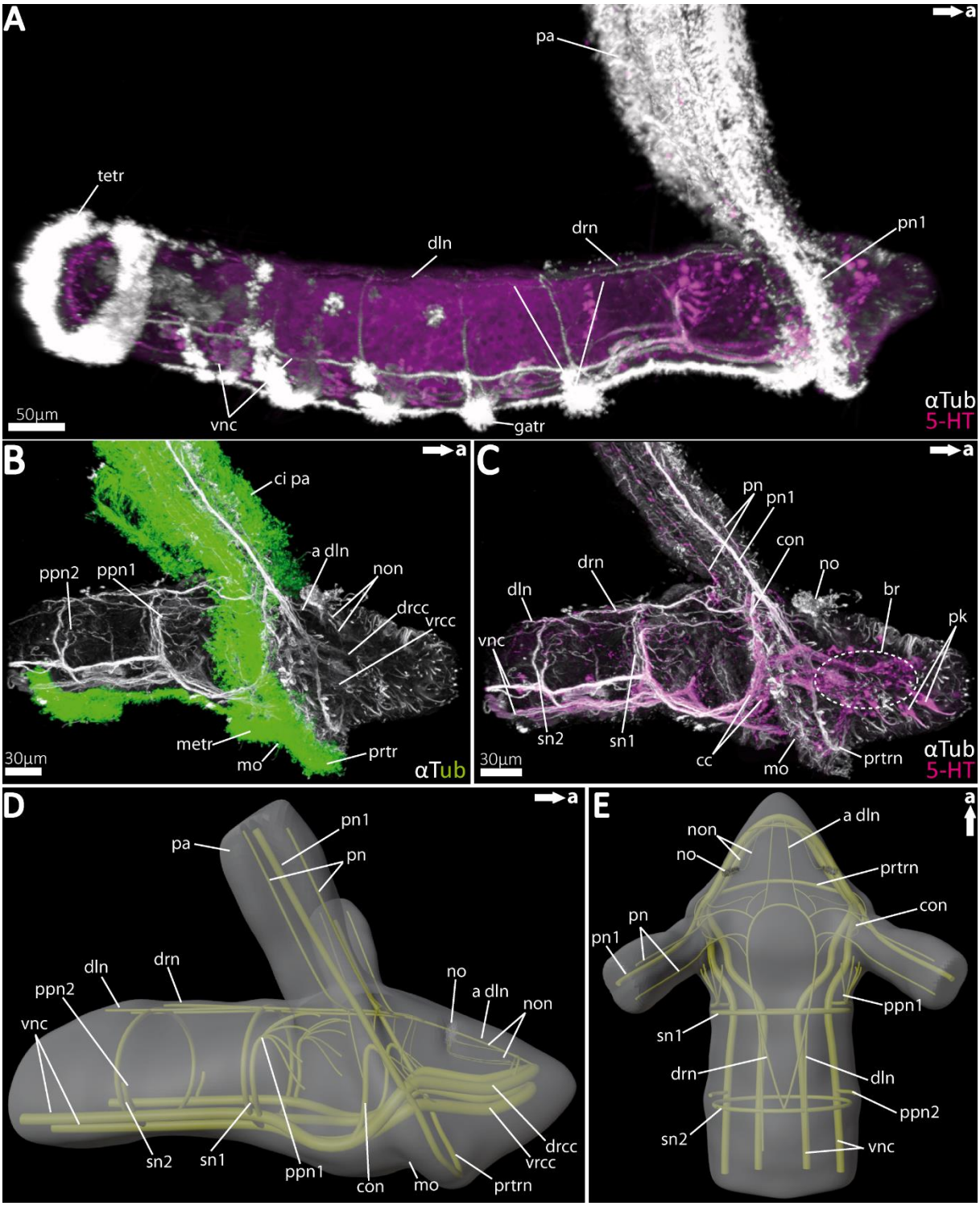

Fig. 4: Nervous system of the Rostraria larva of the amphinomid *Paramphinome jeffreysii*. (A) Overall morphology of the nervous system and ciliation of the Rostraria of Paramphinome jeffreysii stained against acetylated α-tubulin and 5HT-serotonin, showing only one third of the strong ciliated feeding palps. (B) Magnification of the anterior nervous system stained against acetylated α-tubulin, highlighting cilia in green, cLSM micrograph. (C) Same magnification of the anterior nervous system as in (B) stained against acetylated α-tubulin and 5HT-serotonin, omitting the cilia of the elongated feeding palps and the ciliary bands. The dotted circle marks the position of the brain, captured using cLSM micrograph. D, (E) 4D-scheme of the anterior nervous system of the Rostraria. (D) in lateral and

(E) in dorsal view. ***Abbreviations:*** a dln - anterior dorsal longitudinal neurite bundle, br - brain, cc - circumoesophageal connectives, ci pa - cilia of palps, con - drcc + pn1 connecting neurite bundle, dln - dorsal longitudinal neurite bundle, drcc - dorsal root of cc, drn - dorsal ring nerve, gatr - gastrotroch, metr - metatroch, mo - mouth opening, no - nuchal organ, non - nuchal organ nerves, pa - palp, pn - palp nerves, pn1 - main palp nerve interconnected with drcc and vrcc, ppn1 - parapodial neurite bundle of 1st chaetiger, ppn2 - parapodial neurite bundle of 2nd chaetiger, prtr - prototroch, prtrn - prototroch nerve, pk - serotonin-lir perikarya, sn - segmental neurite bundles, sn1 - segmental neurite bundle of 1st chaetiger, sn2 - segmental neurite bundle of 2nd chaetiger, tetr - telotroch, vnc - ventral nerve cord, vrcc - ventral root of cc

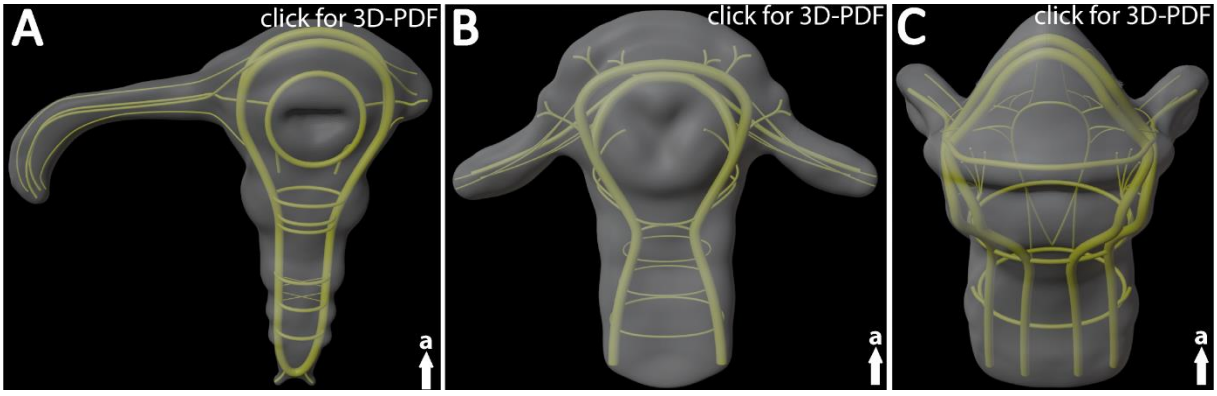

Fig. 5: Comparative 3D-Pdfs of the larvae of all mentioned taxa. (A) 3D-Pdf of 3D-scheme of larva (9dpf) of *Magelona mirabilis*, please click on the image for use. (B) 3D-Pdf of 3D-scheme of Rostraria larva of *Paramphinome jeffreysii*, please click on the image for use. (C) 3D-Pdf of 3D-scheme of juvenile (~60dpf) of *Malacoceros fuliginosus*, please click on it for use.

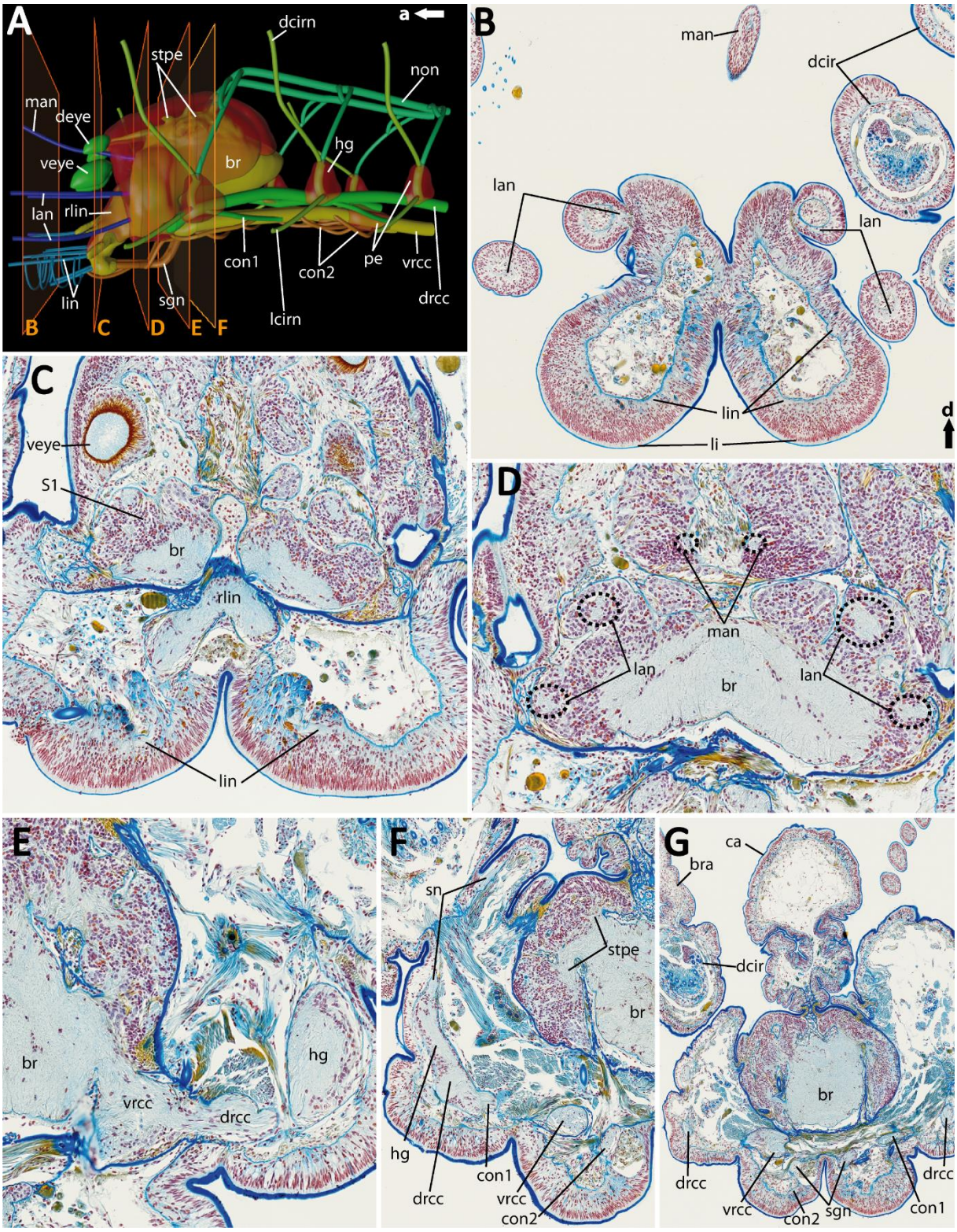

Fig. 6: General anatomy with focus on the nervous system of the anterior end of adult *Eurythoe complanata*, (B-F) 5 µm sections, Azan-staining, light microscopic images. (A) 3D-scheme of the anterior nervous system of adult *E. complanata* in lateral view. The frames show the area of paraffin-sections 6B - 6F. (B) Cross-section through the paired lips and all five antennae, see 6A. (C) Cross-section through the root of the main lip neurite bundles (rlin) and the anterior region of the complex brain, see 6A. (D) Cross-section through the brain region all five antennae nerves originate. (E) Cross-section through area where *vrcc* and *drcc* enter the brain. (F) Cross-section through the first hemi-

ganglion, splitting off. (G) Cross-section through the caruncle and the brain slightly posterior to the area where the nuchal organ nerve (*non*) leaves the brain. ***Abbreviations:*** br - brain, bra - branchiae, ca - caruncle, con1 - neurite bundle connecting drcc and vrcc, con2 - neurite bundle connecting vrcc and sgn, dcir - dorsal cirrus, dcirn, lcirn - nerves of dorsal and lateral cirrus, deye - dorsal eye, drcc - dorsal root of cc, hg - hemi-ganglion, lan – nerve of lateral antenna, li - lips, lin - lip neurite bundle, man – nerve of median antenna, non - nuchal organ nerve (caruncle), pe - perikaria, rlin - root of lip neurite bundle, sn - segmental neurite bundle, sgn - stomatogastric neurite bundles, stpe - stalk of perikaria cluster, veye - ventral eye, vrcc - ventral root of cc, S1 - type 1 neuron refer to Beckers & Tilic (2021)

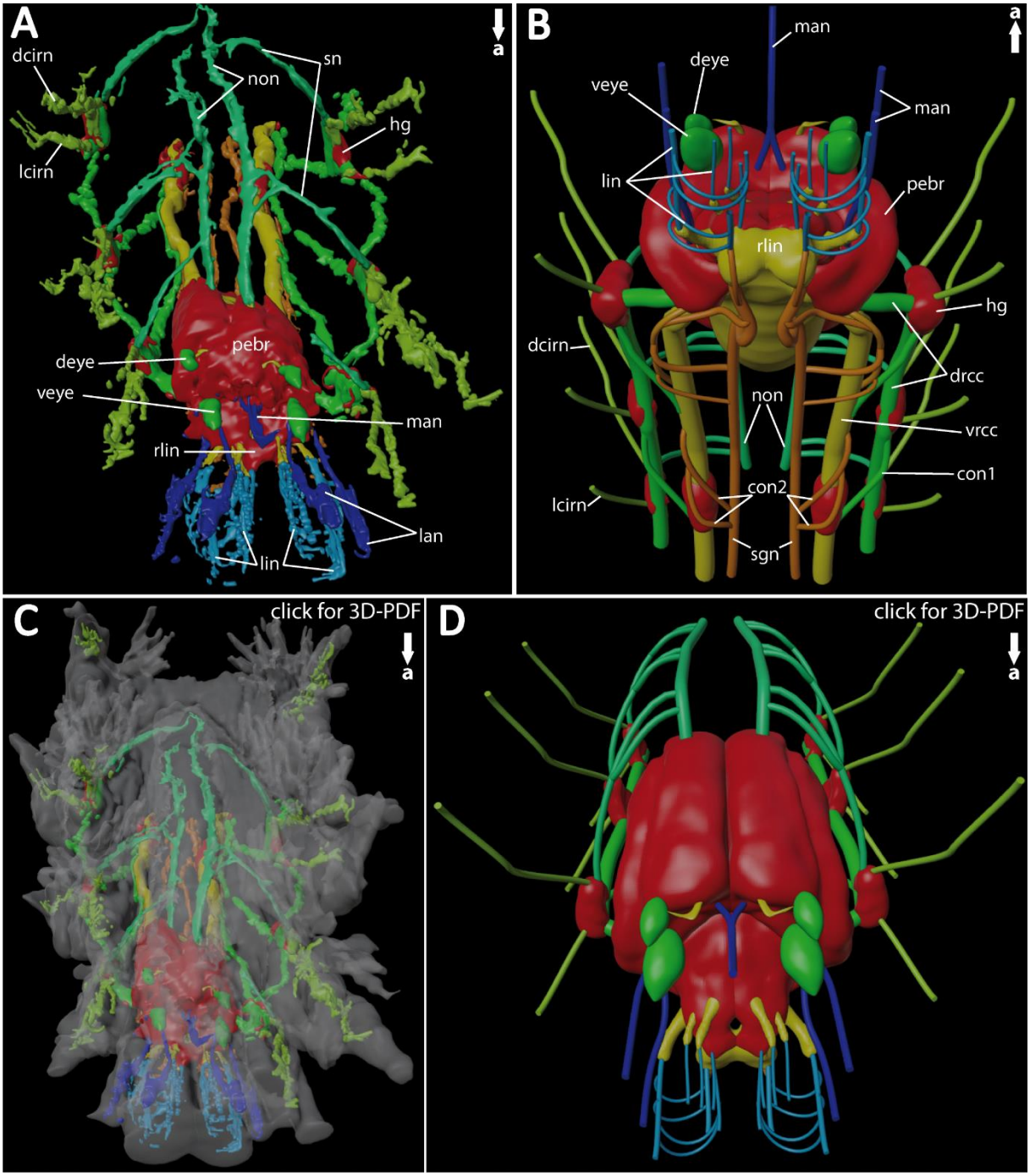

Fig. 7: General anatomy of the anterior nervous system of adult *Eurythoe complanata* and (A) 3D-reconstruction based on Azan-stained paraffin-sections in antero-dorsal view. (B) 3D-scheme of adult *E. complanata* in antero-ventral view. (C) 3D-Pdf of 3D-reconstruction shown in (A), please click on the

image for use. (D) 3D-Pdf of 3D-scheme shown in (B), please click on the image for use. ***Abbreviations:*** br - brain, con1 - neurite bundle connecting drcc and vrcc, con2 - neurite bundle connecting vrcc and sgn, dcirn, lcirn - nerves of dorsal and lateral cirrus, deye - dorsal eye, drcc - dorsal root of cc, hg - hemi-ganglion, lan - lateral antenna, li - lips, lin - lip neurite bundle, man - median antenna, non - nuchal organ nerve (caruncle), pe - perikaria, pebr - perikaria of brain, rlin - root of lip neurite bundle, sn - segmental neurite bundle, sgn - stomatogastric neurite bundles, veye - ventral eye, vrcc - ventral root of cc

4 Discussion

4.1 The larval anterior nervous system and sensory head appendages in Magelonidae, Amphinomidae and Spionidae

The larval anterior nervous systems and head appendages in Magelonidae, Amphinomidae, and Spionidae exhibit several common neuronal characteristics. Hence, one notable feature is the presence of prominent and well-defined lateral circumoesophageal connectives, consisting of a dorsal and ventral root, which are particularly distinct in *Paramphinome jeffreysii*. These connectives fuse at the anterior end and run into the brain. The brain region of the spionid *Malacoceros fuliginosus* shows a quite complex und structured neuropil when compared with *Magelona mirabilis* and *P. jeffreysii*. However, all herein observed larval stages share certain developmental characteristics, such as the presence of the first metanephridia, several larval ciliary bands, and the occurrence of a simple but well-developed ventral nerve cord (*vnc*). Therefore, all investigated larval types and stages are seemingly comparable in terms of complexity and age.

Nevertheless, one interesting ontogenetic aspect is the onset of larval palp development, which varies drastically between the investigated taxa. Notably, the larval feeding palps appear quite late in development in *Malacoceros* when compared to *Magelona*, where the latter are developed in early stages (before 5 dpf), but not at the same time (see also Beckers, Helm and Bartolomaeus, 2019). Hence, solely one larval palp is present in early stages, whereas the second one develops quite late in the planktonic phase. For *P. jeffreysii* it is difficult to classify exactly when the palps appear due to the capture method via plankton net and the longevity of Rostraria larvae (Rouse, 2006; Barroso *et al.*, 2010). However, the external anatomy of the Rostraria defines them as being of a developmental stage comparable to the palp-bearing *Malacoceros* larvae.

Despite these variations in ontogenetic appearance, all examined larvae possess fully developed or – in the case of *Magelona* - partly developed paired feeding-palps. Furthermore, these feeding palps are elongated and well-defined by external morphological features such as a prominent food-rim (Purschke, Bleidorn and Struck, 2014). Additionally, the neuronal innervation of these palps is highly comparable and consistent, with neurite bundles originating from the dorsal (*drcc*) and ventral root (*vrcc*) of the circumoesophageal connectives (Orrhage and Müller, 2005). Regarding the ciliary structure of the feeding-palps, different species display unique adaptations. How these important feeding and sensory structures, especially the food-rim, are equipped - either papillose in magelonids (Jones, 1968; Hernández-Alcántara and Solís-Weiss, 2000), or ciliated in many other species - seems to be of less importance for this question and differences in the ciliature of these feeding palps can be considered as individual adaptations to feeding strategies (Dauer, 1983, 1985, 1987; Dauer and Ewing, 1991).

In contrast to the examined species, the Mitraria, the planktotrophic larva of the basally-branching Owenidae (Rouse, 2006), lacks larval palps (Helm *et al.*, 2016). Even though oweniids represent the putative magelonid sister group, the neurite bundles of the developing adult feeding-palps are missing even in freshly metamorphosed juveniles.

For the basally-branching Chaetopteriformia, larval palp development for e.g. *Chaetopterus variopedatus* starts around 50 days-post-fertilization (dpf) see (Irvine, Chaga and Martindale, 1999; Helm, Schwarze and Beckers, 2022). However, whether these palps are used for larval feeding and their neuronal innervation pattern remain unclear. Notably, the oldest examined *Chaetopteridae* larvae, which were 20 dpf, did not show any palp nerves in anti-tubulin, anti-5HT, nor anti FMRFamid staining see (Helm, Schwarze and Beckers, 2022).

In the sister group of Amphinomidae, the Sipuncula, the larval nervous system differs significantly from what we observe in amphinomids. For instance, there is no prominent sign of immunoreactive neurite bundles running to the prostomial tip similar to palp nerves or other neuronal innervation. Additionally, no distinct nuchal organs and no prominent dorsal longitudinal neurite bundles as seen in *P. jeffreysii* are described for larval Sipuncula (Kristof and Maiorova, 2016).

Whereas the availability of comparable datasets is quite scarce for the basally-branching groups, numerous investigations exist for Pleistoannelida. Interestingly, in pleistoannelid taxa we have a strong bias on the sedentary polychaetes - with detailed investigations of the larval nervous systems of Capitellidae (Meyer *et al.*, 2015), Sabellaridae (Brinkmann and Wanninger, 2008; Faroni-Perez *et al.*, 2016), Serpulidae (McDougall *et al.*, 2006; Nedved, 2010) and Spionidae (Kumar *et al.*, 2020).

In the case of the sedentary *Sabellaria alveolata* (*Sabellaridae*), the early developing prototroch ring nerve is closely associated with the latter developing palp nerves, similar to the herein investigated Rostraria of *P. jeffreysii* and the late metatrochophore of *M. fuliginosus* (Brinkmann and Wanninger, 2008). Moreover, the innervation pattern of the late larval stages of *S. alveolata* – shortly before metamorphosis - reveals two palp nerves. Notably, each of them is interconnected with the ventral and dorsal root of the *cc* and connected to the prototroch nerve ring, similar to the conditions observed in the Rostraria of *Paramphinome* (see (Brinkmann and Wanninger, 2008; Faroni-Perez *et al.*, 2016). Unfortunately, for the so far examined serpulid taxa (McDougall *et al.*, 2006; Nedved, 2010) as well as for *Chaetopterus variopedatus* (see Helm, Schwarze and Beckers, 2022) the ontogenetic stages where in particular the neurogenesis of head appendages should take place lack sufficient data. Additionally, studies on the larval nervous system of errant pleistoannelids with planktonic larvae are scarce as well, and mainly focus on Nereididae and Phyllodocidae see (Voronezhskaya, Tsitrin and Nezlin, 2003; Winchell, Valencia and Jacobs, 2010; Starunov, Voronezhskaya and Nezlin, 2017). For *Phyllodoce maculata* (Voronezhskaya, Tsitrin and Nezlin, 2003) and *Platynereis dumerilii* (Starunov, Voronezhskaya and Nezlin, 2017) we face the same problem of a lack of data concerning palp ontogenesis in the fitting developmental stages.

Finally, other well-studied pleistoannelid taxa such as *Capitella teleta* (Capitellidae) (Meyer *et al.*, 2015), *Platynereis massiliensis* (Helm *et al.*, 2014) and *Neanthes arenaceodenata* (*Nereididae*) (Winchell, Valencia and Jacobs, 2010) show a lecitotrophic development and do not possess typical larval traits making comparisons with planktotrophic larvae ineligible. Furthermore, the mentioned as well as many other investigations mostly focus on other aspects of the ontogenesis and specific stages, and do not highlight sensorial head structure. As a consequence more studies are needed combining different morphological methods to

build up a solid backbone for a better understanding and discussion of the evolutionary history of this diverse and complex head appendages in polychaetes.

4.2 Comparison of the adult anterior nervous system and head appendages of Magelonidae, Amphinomidae and Spionidae

Due to their prominent appearance, the head appendages of adult Magelonidae and Spionidae have been extensively studied. Hence, their elongated feeding-palps fulfil all the morphological criteria to be termed as such (see (Orrhage, 1966; Beckers, Helm and Bartolomaeus, 2019). Externally, in both taxa, the palps are elongated and have a food-rim or are "grooved" (Rouse and Fauchald, 1997; Rouse and Pleijel, 2001; Struck, 2011; Purschke, Bleidorn and Struck, 2014). In addition, the palps of the basally-branching Magelonidae as well as of the deeply nested Spionidae are innervated by distinct neurite bundles originating in the *drcc* and *vrcc* and their respective commissures (Orrhage and Müller, 2005) - criteria which are also fulfilled for the head appendages of adult Owenidae (Beckers *et al.*, 2019) and Chaetopteridae (Orrhage, 1966; Helm, Schwarze and Beckers, 2022). Therefore, this characters can be suggested as being a plesiomorphic character state (Beckers, Helm and Bartolomaeus, 2019). Furthermore, these characteristics are also known for a variety of sedentary pleistoannelids (Orrhage and Müller, 2005; Purschke, 2016; Kalke, Beckers and Helm, 2021). As a consequence, the adult feeding-palps containing a food rim have to be considered as being homologous throughout Annelida. For annelid taxa with a different type of palp the picture is not that homogeneous at a first glance.

The anterior nervous system and the respective head appendages of e.g., *Eurythoe complanata*, present unique characteristics when compared with other polychaetes. Hence, the dorsal (*drcc*) and ventral root (*vrcc*) of the circumoesophageal connectives (*cc*) form distinct neurite bundles, similar to the conditions observed in the Rostraria of *Paramphinome jeffreysii*. Previously, the *drcc* was referred to as the "lateral nerve" (Müller, Berenzen and Westheide, 2003; Helm *et al.*, 2018) or "longitudinal podial nerve" (Orrhage, 1990), but due to the conserved separation of *vrcc* and *drcc* in larvae and adult specimens a change in naming had to be proposed. Our data suggest that the *drcc* contributes to the brain formation by giving rise to the dorsal-most tract or brain commissure (see 3D-pdf Fig. 7C), which interestingly is supported by data of (Orrhage, 1990) as well. Other studies dealing with the

regeneration of the anterior amphinomid nervous system, show that the “lateral nerve” originates from the ventral nerve cord of the amputee and takes part in the formation of the regenerating *drcc* of the brain (Müller, Berenzen and Westheide, 2003; Helm *et al.*, 2018). Nevertheless, in *E. complanata* the *drcc* and *vrcc* never fuse to a common *cc*, despite encircling the oddly posterior located mouth opening and oesophagus (see Fig. 1D).

Exceptional is also the arrangement of the stomatogastric neurite bundles (*sgn*) - a third pair of longitudinal neurite bundles, that run parallel between the strands of the *vrcc*. These bundles innervate the stomatogastric tract further posteriorly (own observation, (Orrhage, 1990) and are connected to the *vrcc* multiple times. In anterior direction, the stomatogastric neurite bundles fuse with the roots of the lip nerves. As mentioned previously, annelid stomatogastric nerves always originate from the *vrcc* – a picture which seems to be true for amphinomids, too (Kalke, Beckers and Helm, 2021).

The buccal lips – structures situated at the anterior tip of the amphinomid head - are innervated from longitudinal nerves solely emanating from distinct lip nerve roots, which are part of the *vrcc*. Although, based on our data we cannot rule out a contribution of nerves emanating from the *drcc* this condition seems to resemble observations described for Eunicidae and *Hyalinoecia tubicola* (Onuphidae) (Zanol, 2010; Kuhl, Bartolomaeus and Beckers, 2022). Nevertheless, further data are needed to support a homology of these structures.

When it comes to the antennae, the neurite bundles of the five antennae of *E. complanata* originate from the main dorsal fibril mass. As described by (Orrhage, 1995; Orrhage and Müller, 2005), the nerves of all antennae originate solely from the dorsal root of the *cc*. For *Eurythoe complanata*, the origin of all antennal nerves from the same brain region in direct vicinity to the dorsal most commissure of the *drcc* can be considered as an additional indicator. The lateral antennae are innervated by only one nerve, whereas the two nerves of the median antennae fuse proximally. However, in our data we do not observe any contribution of nerves or neurite bundles emanating from the *vrcc* and thus, cannot confirm previous investigations describing the ventral-most lateral antennae as being palps innervated by both roots of the circumoesophageal connectives (Orrhage, 1990).

Antennae in general are only described for amphinomids and pleistoannelids, and seem to have evolved in the last common ancestor of both (and Sipuncula) (Purschke, 2016). The presence of five antenna-like appendages appears to be a rare character state, and besides amphinomids, only occurs in certain Eunicida (Zanol, 2010). Nevertheless, so far these eunicid appendages are considered to be three antennae and two palps (Zanol *et al.*, 2021). Notably, recent investigations dealing with the innervation of head appendages of Eunicida support the presence of a maximum of three antennae in Polychaeta (Kuhl, Bartolomaeus and Beckers, 2022). A condition which was previously emphasized by (Orrhage and Müller, 2005) and (Purschke, Bleidorn and Struck, 2014). Consequently and due to our presented data, amphinomids so far seem to be the only examined polychaetes with five antennae, one median and four lateral ones.

Accordingly, we disagree with the use of the term "palps" for the description of the latera-most head appendages in Amphinomidae, as assumed by previous authors (Orrhage, 1990). Instead, our data supports the ontogenetic reduction of palps in amphinomids, a point that will be discussed in the further course.

4.3 The fate of larval head appendages and the homology of annelid feeding palps

The larval neuroanatomy and innervation of head appendages as observed on Magelonidae is highly similar to the larval and/ or adult conditions exhibited by other basally branching taxa, such as Owenidae (Beckers *et al.*, 2019), Chaetopteridae (Helm, Schwarze and Beckers, 2022), Sipuncula (Wanninger *et al.*, 2005; Kristof, Wollesen and Wanninger, 2008; Carrillo-Baltodano *et al.*, 2019) and Amphinomidae (present study). In *Pleistoannelida*, this neuronal pattern is often retained only in adult or late juvenile specimens (Orrhage and Müller, 2005; Purschke, 2016).

Previous studies suggested that magelonid larvae shed their larval palps during metamorphosis and re-grow them as adults (Wilson, 1982). During the larval development of *M. mirabilis* the papillae of the palps develop gradually (own observation, (Beckers, Helm and Bartolomaeus, 2019). Additionally, Wilson mentioned that “very late larval stages taken in plankton hauls often lack larval tentacles these may have been shed as a result of crowded,

sometimes silty, conditions in the tow-net bucket" – a fact which would explain the observation of short, growing palps in adults post-metamorphosis. Based on our observations, the identical innervation pattern in terms of larval and adult palps by nerves of the *drcc* and *vrcc* clearly supports a gradually development of larval towards adult feeding-palps. Therefore, a loss of larval palps during metamorphosis in Magelonidae seems implausible and caused by destructive sampling methods during earlier investigations.

A similar condition with the larval feeding palps sharing exactly the same innervation pattern as described for adult individuals is supported by our data concerning *Malacoceros fuliginosus* and former studies (Orrhage, 1966). As a consequence the same conservation of larval palp innervation and a gradual development of the larval feeding palp into the adult ones has to be assumed for sedentary Annelida. Consequently, the larval and adult palps of magelonids and spionids are homologous to the feeding palps of other annelid taxa, both throughout the annelid tree and the entire ontogeny.

In Amphinomidae, a totally different picture can be observed. The enigmatic Rostraria larvae of *Paramphinome jeffreysii* exhibit true elongated feeding-palps, which are homologous to the feeding palps observed in other annelid taxa.

According to the neuronal innervation patterns described for the anterior end of adult amphinomids (in this case *E. complanata*), no comparable structure resembling the neuronal innervation pattern of the larval feeding-palps can be observed in adult individuals. As a consequence, a reduction or loss of the larval feeding-palps during metamorphosis in Amphinomidae has to be assumed – a finding that changes our understanding in terms of amphinomid morphology as well as the putative homology assumptions that were made in the past. Although adult amphinomid specimens do not possess head appendages that can be homologized with feeding palps of other taxa, the transitional reduction of the respective structures in this annelid family helps to understand the evolutionary adaptive changes in terms of palp morphology throughout annelid taxa. Nevertheless, a comprehensive picture of palp evolution and an integration as well as evolutionary placement of the stout sensory palps within Errantia, needs further investigations due to the lack of comparative data.

Conclusion

Our data nicely illustrate, how drastic the changes during metamorphosis can turn out, if the ecological adaptations of larvae and adults differ.

Nevertheless, our study elucidates that the comparison of larval versus adult morphological features facilitates our understanding in terms of evolutionary transitions of morphological key structures and helps to draw conclusions concerning developmental changes due to ecological adaptations. Therefore, our integrative analyses clearly support a homology of adult and larval feeding palps throughout the annelid tree. Additionally, our observations highlight the adaptive reduction of these feeding palps within amphinomid development and elucidate the immense diversity when it comes to annelid evolution. Nevertheless, more studies are needed to fill the knowledge gaps especially of taxa in key positions within the annelid tree such as Amphinomidae and Sipuncula, as well as for the ontogenetic morphological changes that took place within the branch leading towards Errantia.

Conflict of Interest

The authors declare that the research was conducted in the absence of any commercial or financial relationships that could be construed as a potential conflict of interest.

Author contributions

PK and CH conceived the study and performed the experiments. PB provided the histological datasets. PK analysed the data, performed the 3d visualisations, assembled the figures and drafted the manuscript. All authors read, worked on and approved the final manuscript.

Funding

This work was financially supported by the department “Animal Evolution and Biodiversity” of the University of Goettingen. No third party funding was used in addition. Open Access funding was enabled and organized by the projekt DEAL.

Acknowledgments

The authors want to thank the working group “Animal Evolution and Biodiversity” and “Evolutionary Biology and Ecology” for the financial and technical support. Futhermore, we thank Nataliya Budaeva (University Museum Bergen/ Norway) for help with the collection of

Rostraria larvae as well as the marine biological station Roscoff (Brittany/ France) for help and support during several fieldtrips.

Availability of data

All data analysed in this study are used in the figures of this article. The original confocal image stacks as well as histological data can be made available after personal contact with the corresponding authors.

References

Barroso, R. *et al.* (2010) 'Eurythoe complanata (Polychaeta: Amphinomidae), the "cosmopolitan" fireworm, consists of at least three cryptic species', *Marine Biology*, 157(1), pp. 69–80. Available at: https://doi.org/10.1007/s00227-009-1296-9.

Beckers, P. *et al.* (2019) 'The central nervous system of Oweniidae (Annelida) and its implications for the structure of the ancestral annelid brain', *Frontiers in Zoology*, 16(1), pp. 1–21. Available at: https://doi.org/10.1186/s12983-019-0305-1.

Beckers, P., Helm, C. and Bartolomaeus, T. (2019) 'BMC Evolutionary Biology The anatomy and development of the nervous system in Magelonidae (Annelida) – insights into the evolution of the annelid brain', *BMC Evolutionary Biology* [Preprint].

Beckers, P., Loesel, R. and Bartolomaeus, T. (2013) 'The Nervous Systems of Basally Branching Nemertea (Palaeonemertea)', *PLoS ONE*, 8(6). Available at: https://doi.org/10.1371/journal.pone.0066137.

Beckers, P. and Tilic, E. (2021) 'Fine structure of the brain in Amphinomida (Annelida)', *Acta Zoologica*, 102(4), pp. 483–495. Available at: https://doi.org/10.1111/azo.12383.

Binard, A. and Jeener, R. (1928) *Morphologie du lobe préoral des polychètes*.

Brinkmann, N. and Wanninger, A. (2008) 'Larval neurogenesis in *Sabellaria alveolata* reveals plasticity in polychaete neural patterning', *Evolution & Development*, 10(5), pp. 606–618. Available at: https://doi.org/10.1111/j.1525-142X.2008.00275.x.

Carrillo-Baltodano, A.M. *et al.* (2019) 'Developmental architecture of the nervous system in Themiste lageniformis (Sipuncula): New evidence from confocal laser scanning microscopy and gene expression', *Journal of Morphology*, 280(11), pp. 1628–1650. Available at: https://doi.org/10.1002/jmor.21054.

Dauer, D.M. (1983) 'Functional morphology and feeding behavior of Scolelepis squamata (Polychaeta: Spionidae)', *Marine Biology*, 77(3), pp. 279–285. Available at: https://doi.org/10.1007/BF00395817.

Dauer, D.M. (1985) 'Functional morphology and feeding behavior of Paraprionospio pinnata (Polychaeta: Spionidae)', *Marine Biology*, 85(2), pp. 143–151. Available at: https://doi.org/10.1007/BF00397433.

Dauer, D.M. (1987) ‘Potential systematic significance of spionid polychaete tentacular morphology’, *Proc. Biol. Soc. Wash*, 7, pp. 41–45.

Dauer, D.M. and Ewing, R.M. (1991) ‘FUNCTIONAL MORPHOLOGY AND FEEDING BEHAVIOR OF MALACOCEROS INDICUS (POLYCHAETA: SPIONIDAE)’, *BULLETIN OF MARINE SCIENCE*, 48.

Faroni-Perez, L. *et al.* (2016) ‘Anterior sensory organs in Sabellariidae (Annelida)’, *Invertebrate Biology*, 135(4), pp. 423–447. Available at: https://doi.org/10.1111/ivb.12153.

Fauchald, K. and Jumars, P.A. (1979) ‘The diet of worms: a study of polychaete feeding guilds’, *Oceanography and marine Biology annual review* [Preprint].

Hartmann-Schröder, G. *et al.* (1971) *Die Tierwelt Deutschlands und der angrenzenden Meeresteile nach ihren Merkmalen und nach ihrer Lebensweise: Annelida, Borstenwürmer, Polychaeta; Gesa Hartmann-Schröder*. VEB Gustav Fischer Verlag.

Helm, C. *et al.* (2014) ‘An immunocytochemical window into the development of Platynereis massiliensis (Annelida, Nereididae)’, *International Journal of Developmental Biology*, 58(6–8). Available at: https://doi.org/10.1387/ijdb.140081cb.

Helm, C. *et al.* (2016) ‘Owenia fusiformis - A basally branching annelid suitable for studying ancestral features of annelid neural development’, *BMC Evolutionary Biology*, 16(1). Available at: https://doi.org/10.1186/s12862-016-0690-4.

Helm, C. *et al.* (2018) ‘Convergent evolution of the ladder-like ventral nerve cord in Annelida’, *Frontiers in Zoology*, 15(1). Available at: https://doi.org/10.1186/s12983-018-0280-y.

Helm, C., Schwarze, G. and Beckers, P. (2022) ‘Loss of complexity from larval towards adult nervous systems in Chaetopteridae (Chaetopteriformia , Annelida) unveils evolutionary patterns in Annelida’, *Organisms Diversity & Evolution* [Preprint], (May). Available at: https://doi.org/10.1007/s13127-022-00553-z.

Hernández-Alcántara, P. and Solís-Weiss, V. (2000) ‘MAGELONIDAE FROM THE MEXICAN PACIFIC AND NORTHERN GULF OF MEXICO, WITH THE DESCRIPTION OF A NEW GENUS (MEREDITHIA) AND FOUR NEW SPECIES’, *BULLETIN OF MARINE SCIENCE*, 67.

Irvine, S.Q., Chaga, O. and Martindale, M.Q. (1999) ‘Larval Ontogenetic Stages of Chaetopterus: Developmental Heterochrony in the Evolution of Chaetopterid Polychaetes’, *The Biological Bulletin*, 197(3), pp. 319–331. Available at: https://doi.org/10.2307/1542786.

Jones, M.L. (1968) ‘ON THE MORPHOLOGY, FEEDING, AND BEHAVIOR OF MAGELONA SP’, *The Biological Bulletin*, 134(2), pp. 272–297. Available at: https://doi.org/10.2307/1539604.

Jumars, P.A., Dorgan, K.M. and Lindsay, S.M. (2015) ‘Diet of Worms Emended: An Update of Polychaete Feeding Guilds’, *Annual Review of Marine Science*, 7(1), pp. 497–520. Available at: https://doi.org/10.1146/annurev-marine-010814-020007.

Kalke, P., Beckers, P. and Helm, C. (2021) ‘May the Palps Be With You – New Insights Into the Evolutionary Origin of Anterior Appendages in Terebelliformia (Annelida)’, *BMC Zoology*, 6(30), pp. 1–16. Available at: https://doi.org/10.1186/s40850-021-00094-6.

Kalke, P. and Helm, C. (2022) ‘No cost but high performance–An alternative open source solution for 3D-visualizations in morphology’, *Microscopy Research and Technique* [Preprint]. Available at: https://doi.org/10.1002/jemt.24250.

Kristof, A. and Maiorova, A.S. (2016) '23. Annelida: Sipuncula', *Structure and evolution of invertebrate nervous systems*, pp. 248–253.

Kristof, A., Wollesen, T. and Wanninger, A. (2008) 'Segmental Mode of Neural Patterning in Sipuncula', *Current Biology*, 18(15), pp. 1129–1132. Available at: https://doi.org/10.1016/j.cub.2008.06.066.

Kuhl, S., Bartolomaeus, T. and Beckers, P. (2022) 'How Do Prostomial Sensory Organs Affect Brain Anatomy? Phylogenetic Implications in Eunicida (Annelida)', *Journal of Marine Science and Engineering*, 10(11), p. 1707. Available at: https://doi.org/10.3390/jmse10111707.

Kumar, S. *et al.* (2020) 'The development of early pioneer neurons in the annelid Malacoceros fuliginosus', *BMC Evolutionary Biology*, 20(1), pp. 1–21. Available at: https://doi.org/10.1186/s12862-020-01680-x.

McDougall, C. *et al.* (2006) 'The development of the larval nervous system, musculature and ciliary bands of Pomatoceros lamarckii (Annelida): heterochrony in polychaetes', *Frontiers in Zoology*, 3(1), p. 16. Available at: https://doi.org/10.1186/1742-9994-3-16.

Meyer, N.P. *et al.* (2015) 'Nervous system development in lecithotrophic larval and juvenile stages of the annelid Capitella teleta', *Frontiers in Zoology*, 12(1), pp. 1–27. Available at: https://doi.org/10.1186/s12983-015-0108-y.

Müller, J. *et al.* (2021) '"Brittleworms": Ultrastructure and arrangement of the calcified chaetae of Euphrosine (Amphinomida, Annelida)', *Invertebrate Biology*, 140(4), p. e12353. Available at: https://doi.org/10.1111/ivb.12353.

Müller, M.C.M., Berenzen, A. and Westheide, W. (2003) 'Experiments on anterior regeneration in Eurythoe complanata ("Polychaeta", Amphinomidae): reconfiguration of the nervous system and its function for regeneration', *Zoomorphology*, 122(2), pp. 95–103. Available at: https://doi.org/10.1007/s00435-003-0073-4.

Nedved, B.T. (2010) *NEUROMUSCULAR DEVELOPMENT AND METAMORPHOSIS IN THE SERPULID POLYCHAETE HYDROIDES ELEGANS*. UNIVERSITY OF HAWAI'I.

Nilsson, D. (1912) *Beiträge zur Kenntnis des Nervensystems der Polychaeten*. Almquist & Wiksells.

Orrhage, L. (1966) 'Über die Anatomie des zentralen Nervensystems der sedentaren Polychaeten', *Arkiv för Zoologi*, 19(3), pp. 99–133.

Orrhage, L. (1980) 'On the structure and homologues of the anterior end of the polychaete families sabellidae and serpulidae', *Zoomorphology*, 96(1–2), pp. 113–167. Available at: https://doi.org/10.1007/BF00310081.

Orrhage, L. (1990) 'On the Microanatomy of the Supraoesophageal Ganglion of Some Amphinomids (Polychaeta Errantia), with Further Discussion of the Innervation and Homologues of the Polychaete Palps', *Acta Zoologica*, 71(1), pp. 45–59. Available at: https://doi.org/10.1111/j.1463-6395.1990.tb01180.x.

Orrhage, L. (1995) 'On the Innervation and Homologues of the Anterior End Appendages of the Eunicea (Polychaeta), with a Tentative Outline of the Fundamental Constitution of the Cephalic Nervous System of the Polychaetes', *Acta Zoologica*, 76(3), pp. 229–248. Available at: https://doi.org/10.1111/j.1463-6395.1995.tb00996.x.

Orrhage, L. (2001) ‘On the anatomy of the central nervous system and the morphological value of the anterior end appendages of Ampharetidae, Pectinariidae and Terebellidae (Polychaeta)’, *Acta Zoologica*, 82(1), pp. 57–71. Available at: https://doi.org/10.1046/j.1463-6395.2001.00070.x.

Orrhage, L. and Müller, M.C.M. (2005) ‘Morphology of the nervous system of Polychaeta (Annelida)’, *Hydrobiologia*, 535(1), pp. 79–111. Available at: https://doi.org/10.1007/s10750-004-4375-4.

Purschke, G. (2016) ‘A n n e l i d a : B asa l G roups A n d P l e i s toa n n e l i d a’, in G.P. Andreas Schmidt-Rhaesa, Steffen Harzsch (ed.) *Structure and Evolution of Invertebrate Nervous System*. Oxford University Press, pp. 254–312.

Purschke, G., Bleidorn, C. and Struck, T. (2014) ‘Systematics, evolution and phylogeny of Annelida – A morphological perspective’, *Memoirs of Museum Victoria*, 71, pp. 247–269.

Richter, S. *et al.* (2010) ‘Invertebrate neurophylogeny : suggested terms and definitions for a neuroanatomical glossary.’, *Frontiers in Zoology*, 7(1), pp. 1–49.

Rimskaya-Korsakova, N.N., Galkin, S.V. and Malakhov, V.V. (2018) *The neuroanatomy of the siboglinid Riftia pachyptila highlights sedentarian annelid nervous system evolution*, *PLoS ONE*. Available at: https://doi.org/10.1371/journal.pone.0198271.

Rouse, G.W. (1999) ‘Trochophore concepts: ciliary bands and the evolution of larvae in spiralian Metazoa’, *Biological Journal of the Linnean Society*, 66(4), pp. 411–464.

Rouse, G.W. (2006) ‘Annelid Larval Morphology’, in *Reproductive Biology and Phylogeny of Annelida*. 1st edition. CRC Press, pp. 151–188. Available at: https://doi.org/10.1201/9781482280159-5.

Rouse, G.W. and Fauchald, K. (1997) ‘Cladistics and Polychaetes’, *Zoologica Scripta*, 26(2), pp. 139–204. Available at: https://doi.org/10.1111/j.1463-6409.1997.tb00412.x.

Rouse, G.W. and Pleijel, F. (2001) *Polychaetes*. Oxford, New York: Oxford University Press. Available at: https://doi.org/10.1111/j.1439-0469.2004.00263.x.

Schmidbaur, H. *et al.* (2020) ‘Within-family plasticity of nervous system architecture in Syllidae (Annelida, Errantia)’, *Frontiers in Zoology*, 17(20), pp. 1–44. Available at: https://doi.org/10.1186/s12983-020-00359-9.

Starunov, V.V., Voronezhskaya, E.E. and Nezlin, L.P. (2017) ‘Development of the nervous system in Platynereis dumerilii (Nereididae, Annelida)’, *Frontiers in Zoology*, 14(1), pp. 1–20. Available at: https://doi.org/10.1186/s12983-017-0211-3.

Struck, T.H. (2011) ‘Direction of evolution within Annelida and the definition of Pleistoannelida’, *Journal of Zoological Systematics and Evolutionary Research*, 49(4), pp. 340–345. Available at: https://doi.org/10.1111/j.1439-0469.2011.00640.x.

Voronezhskaya, E.E., Tsitrin, E.B. and Nezlin, L.P. (2003) ‘Neuronal development in larval polychaetePhyllodoce maculata (Phyllodocidae)’, *The Journal of Comparative Neurology*, 455(3), pp. 299–309. Available at: https://doi.org/10.1002/cne.10488.

Wanninger, A. *et al.* (2005) ‘Nervous and muscle system development in Phascolion strombus (Sipuncula)’, *Development Genes and Evolution*, 215(10), pp. 509–518. Available at: https://doi.org/10.1007/s00427-005-0012-0.

Weigert, A. *et al.* (2014) 'Illuminating the base of the Annelid tree using transcriptomics', *Molecular Biology and Evolution*, 31(6), pp. 1391–1401. Available at: https://doi.org/10.1093/molbev/msu080.

Wilson, D.P. (1936) 'Memoirs: The Development of the Sabellid Branchiomma vesiculosum', *Journal of Cell Science*, 2(312), pp. 543–603.

Wilson, D.P. (1982) 'The larval development of three species of Magelona (Polychaeta) from localities near Plymouth', *Journal of the Marine Biological Association of the United Kingdom*, 62(2), pp. 385–401.

Winchell, C.J., Valencia, J.E. and Jacobs, D.K. (2010) 'Confocal analysis of nervous system architecture in direct-developing juveniles of Neanthes arenaceodentata (Annelida, Nereididae)', *Frontiers in Zoology*, 7(1), pp. 1–19. Available at: https://doi.org/10.1186/1742-9994-7-17.

Wolff, W.J. (1973) 'The estuary as a habitat an analysis of data on the soft-bottom Macrofauna of the Estuarine area of the rivers rhine, Meuse, and Scheldt', *Zoologische verhandelingen*, 126(1), pp. 1–242.

Worsaae, K., Rimskaya-Korsakova, N.N. and Rouse, G.W. (2016) 'Neural reconstruction of bone-eating Osedax spp. (Annelida) and evolution of the siboglinid nervous system', *BMC Evolutionary Biology*, 16(1). Available at: https://doi.org/10.1186/s12862-016-0639-7.

Zanol, J. (2010) 'Homology of prostomial and pharyngeal structures in eunicida (Annelida) based on innervation and morphological similarities', *Journal of Morphology*, 271(9), pp. 1023–1043. Available at: https://doi.org/10.1002/jmor.10843.

Zanol, J. *et al.* (2021) 'The Current State of Eunicida (Annelida) Systematics and Biodiversity', *Diversity*, 13(2), p. 74. Available at: https://doi.org/10.3390/d13020074.

Palps are homologous among Annelida – Lessons from Nereididae

Paul Kalke[1,*], Nils Wietoska[1], Patrick Beckers[2], Sebastian Klußmann-Fricke[3] & Conrad Helm[1,*]

Affiliations

[1]Helm Lab, Johann-Friedrich-Blumenbach-Institute, Animal Evolution and Biodiversity, University of Göttingen,, 37073 Göttingen, Germany
[2]Institute of Evolutionary Biology, University of Bonn, 53121 Bonn, Germany
[3]Abberior Instruments, Hans-Adolf Krebs Weg 6, 37077 Göttingen, Germany

* corresponding author

Paul.kalke@uni-goettingen.de

chelm@uni-goettingen.de

Keywords: Polychaetes, Errantia, Platynereis, Head appendages, Antennae, tentacular cirri

Abstract

The diversity and evolutionary history of annelid head appendages has long captivated researchers. But, whether slender feeding-palps common in Paleoannelida and sedentary pleistoannelids, and stout, sensory palps are prominent in Errantia are homologous among annelid taxa has remained elusive. Early attempts to unravel the evolutionary transitions of annelid head appendages and the homology of palps focussed on the examination of the anterior nervous system in various annelid families. However, these efforts were hampered by a lack of a proper phylogeny and lead to misinterpretations and unresolved questions. Recent investigations have revisited previous observations, in paleoannelids, as well as in

Chaetopteriformia, Amphinomidae, and Sedentaria. These studies have shed new light on questions concerning the relations of annelid head appendages. However, comprehensive studies to resolve the evolutionary origins of sensory palps in Errantia remained scarce. In this study, we employ an integrative morphological and focus is on different ontogenetic stages of *Platynereis* species. *Platynereis* encompasses all conceivable types of annelid head appendages (excluding feeding palps), making it an ideal candidate for our analyses. Through integrative investigations, we aim to shed light on the evolution of annelid head appendages in general, with a specific focus on their neuronal innervation across various ontogenetic stages of both *Platynereis* species. In comparison with former studies concerning feeding-palps our data support the idea of the homology of different palp types in Annelida.

Introduction

Annelida represent a widely-spread and morphologically very diverse taxon (Purschke, 2015; Rouse, Pleijel and Tilic, 2022).Based on the fact, that annelids populate almost all habitats on our planet, evolutionary adaptations caused highly variable body plans across the different families (Weigert and Bleidorn, 2016). Hence within Annelida, e.g., filter feeders with large tentacular crowns, errant predators with massive jaws, tube inhabiting groups with slender head appendages or ground-dwelling taxa without any appendages can be found (Rouse and Pleijel, 2001; Purschke, Bleidorn and Struck, 2014; Rouse, Pleijel and Tilic, 2022). In this context, in particular the variability of annelid head appendages has fascinated generations of researchers and was always an important tool for annelid systematics (Purschke, Bleidorn and Struck, 2014). Nevertheless, phylogenetic comparison of the head appendages in polychaetes were hard to handle so far (Rouse and Fauchald, 1997; Rouse and Pleijel, 2001, 2003) – not at least due to a lack of comparative investigations besides sheer external characteristics of the latter. (Schmidbaur *et al.*, 2020) nicely summarize the Annelida with the words "….a clade, which occupies such diverse niches as the Annelida, we find similar patterns in phylogenetically widely separated species in similar niches and a high degree of modularity within a family". In terms of the palps – the probably best-documented and most popular head appendage in Annelida – two different main types can be found in different annelid taxa. Hence, several families possess slender elongated so-called feeding palps, which are mainly used for food uptake, whereas other taxa exhibit stout and short so-called sensory palps

(Purschke, 2015). And, although often used for annelid systematics and species descriptions, the question concerning the homology of both palp types across Annelida was hardly possible so far.

Early on, several investigations tried to answer the evolutionary transition of annelid head appendages and in particular the putative homology of the palps by investigating the anterior nervous system of various annelid families (Orrhage, 1966, 1980, 1990, 1991, 1993, 1995, 1999, 2001; Orrhage and Eibye-Jacobsen, 1998; Orrhage and Müller, 2005). The resulting definitions based on the innervation patterns of the respective head appendages by the neuronal roots and the respective neuronal commissures represented the first potential tool to deal with this problem (Rouse and Fauchald, 1997; Rouse and Pleijel, 2001; Purschke, Bleidorn and Struck, 2014).

Unfortunately, the morphological assumptions based on the existence of potential 12 palp nerve roots and the lack of phylogenomic analyses resulted in misinterpretations and caused even more questions.

Therefore, recent investigations re-evaluated previous observations, e.g. studies of the paleoannelid families Magelonidae (Beckers, Helm and Bartolomaeus, 2019) and Owenidae (Beckers *et al.*, 2019), and of Chaetpterifomia (Helm, Schwarze and Beckers, 2022), Amphinomidae (Kalke et al. submitted) and Sedentaria (Kalke, Beckers and Helm, 2021).

As a consequence, the larval and adult feeding-palps of annelid taxa such as Paleoannelida and Chaetopteriformia (Helm, Schwarze and Beckers, 2022) as well as the larval palps of Amphinomidae (Kalke et al., unpublished) have to be considered as being homologous to the elongated feeding-palps of sedentary taxa such as Terebelliformia (Kalke, Beckers and Helm, 2021), Spionidae (Orrhage, 1966, Kalke et al. submitted) and Sabellariidae (Brinkmann and Wanninger, 2008; Faroni-Perez *et al.*, 2016). This homology statement is mainly based on comparisons of the neuronal scaffolds innervating the feeding palps. However, when it comes to recent investigations about errant Polychaetes, comprehensive studies that would help to solve the question concerning the evolutionary origin of sensory palps are scarce and further datasets are needed for solving the question of palp type homology (Schmidbaur *et al.*, 2020; Kuhl, Bartolomaeus and Beckers, 2022).

Therefore, in this study we use an integrative morphological approach including immunohistochemistry and confocal laser scanning microscopy of whole mount and sectioned

samples combined with Azan-stained histological serial section and subsequent 3D-visualizations to describe the anterior morphology of larval and adult head appendages in Errantia. In our comprehensive analyses we will focus on the errant annelid family Nereididae, in particular on the genus *Platynereis* (Kinberg, 1865). The latter taxon with the sibling species *Platynereis massiliensis* (Moquin-Tandon, 1869) and *Platynereis dumerilii* (Audouin & Milne Edwards, 1833) can without exaggeration be named as the most extensive studied polychaete taxon (Jekely, Keijzer and Godfrey-Smith, 2015; Kuehn *et al.*, 2019; Williams and Jékely, 2019). Especially, due to the establishment of *P. dumerilii* as the spiralian model organism, recent studies touch a vast number of biological disciplines ranging from molecular, towards morphological, behavioural as well as developmental approaches (Özpolat *et al.*, 2021). Therefore, *Platynereis* also represents a suitable taxon for our analyses, which will later enable to embed our results in various contexts.

Furthermore, Nereididae and in particular *Platynereis* exhibit all possible types of annelid head appendages (excl. feeding palps). Hence, integrative analyses will help to gain important analyses into the evolution of annelid head appendages in general.

Our data will therefore focus on the head appendages and their respective neuronal innervation in different ontogenetic stages of both *Platynereis* species to elucidate the question of a potential homology of different palp types in Annelida.

Material and Methods

Specimen collection

Adult specimens of *Platynereis massiliensis* (Moquin-Tandon, 1869) were collected in Roscoff (Brittany, France) in June 2019. The resulting culture was established in Göttingen keeping several individuals in plastic boxes with a 12h:12h light regime and 3.5% salinity at 18°C. A culture of *Platynereis dumerilii* was acquired from the Tomancak lab at the Max Planck Institute of molecular cell biology and genetics Dresden (Germany). The culture was maintained according to Özpolat et al. (2021), with a 12h:12h light regime and a salinity of 3,5% at 18 °C.

Immunohistochemistry for whole mount samples

Anatomical details of adult *Platynereis massiliensis* and larvae of *Platynereis dumerilii* were investigated using standard immunohistochemical staining protocols. Specimens were relaxed using 7% $MgCl_2$ and subsequently fixed in 4% paraformaldehyde (PFA) in 1x phosphate buffered saline with TritonX (PTW = 1x PBS: 0.05 M PB / 0.3 M NaCl / 0.3% TritonX). Fixation was performed at room temperature (RT) for 2 h. After fixing, the specimens were washed and stored in PTW containing 0,005% NaN3 until usage at 4 °C. For antibody staining, specimens were rinsed 2 × 5 min in PTW at RT and permeabilized in 1% (10mg/1 ml PTW) Collagenase D (Roche Diagnostics GmbH) between 1 h for adult specimens and 30 min for larvae. Subsequently, samples were rinsed 3 x 10 min in PTW and incubated in 10 µg proteinase K/ ml PTW for at least 30 min for adults and 5 min for larvae. After 2 short rinses in glycine (2 mg glycine/ ml PTW), and 3 × 5 min washes in PTW, the specimens were re-fixed using 4% PFA in PTW containing 0.6/0.3 % TritonX for 10 min at RT. Subsequently, the samples were rinsed 2 × 5 min in PTW, 2 × 5 min in THT (0.1 M TrisCl, 0.3 TritonX, pH 8,5) and blocked with 5% goat serum (Sigma-Aldrich, Steinheim, 25 µl goat serum in 500 µl THT) for 2 h. Afterwards, specimens were incubated with the primary antibodies against α-tubulin (Anti-acetylated α -tubulin, clone 6-11B-1, Merck, Darmstadt, 2 µl tubulin in 500 µl incl. 5% goat serum) and serotonin (5-HT, ImmunoStar Inc.,Hudson, USA, 1 µl in 500 µl incl. 5% goat serum) in THT for 48-72 h at 4 °C. Afterwards, samples were rinsed 2 × 10 min in 1 M NaCl in THT and washed 5 × 30 min in THT. Subsequently, the samples of adult *P. massiliensis* were incubated in the secondary antibodies goat-anti-mouse Alexa 633 (Alexa Fluor® 633 goat-anti-mouse IgG (H + L), Thermo Fisher Scientific Inc., Waltham, USA, 1 µl in 500 µl inlc. 5% goat serum) and goat-anti-rabbit Alexa 488 (Alexa Fluor® 488 goat-anti-rabbit IgG (H + L), Thermo Fisher Scientific Inc., Waltham, USA, 1 µl in 500 µl incl. 5% goat serum) in THT for 48-72 h at 4 °C. Alternatively, larvae of *P. dumerilii* were incubated using secondary antibodies coupled to goat anti-mouse IgG Abberior Star Red (1 µl in 200 µl incl. 5% goat serum, Göttingen, Germany) and goat-anti-rabbit IgG Abberior Star Orange (1 µl in 200 µl incl. 5% goat serum, Abberior, Göttingen, Germany) in THT for 48-72 h at 4 °C. After the staining, specimens were rinsed 5 × 30 min in THT and 2 × 5 min in PTW. Additionally, samples were incubated in DAPI (DAPI, Thermo Fisher Scientific Inc., Waltham, USA, 5 µl in PTW) in PTW overnight at 4 °C. Subsequently, the adult specimens were dehydrated in an ascending isopropanol series, cleared using Murray's clear (benzyl alcohol & benzyl benzoate, 1:2) and embedded between

two cover slips using DPX mounting medium (Merck, Darmstadt, Germany). Alternatively, the larvae were directly mounted in RapiClear 1.49 (SunjinLabs, Taiwan) in combination with 100 µm iSpacers (SunjinLabs, Taiwan) on standard microscope slides and covered with # 1.5H coverslips. The adult specimens were analysed with a confocal laser scanning microscope Leica TCS SP8 (Leica Microsystems, Wetzlar, Germany). The confocal image stacks were processed with Leica AS AF v2.3.5 (Leica Microsystems). Additionally, *P. dumerilii* at 6 days past fertilization (dpf) were analysed using an Abberior Facility Line Microscope (Abberior Instruments, Göttingen, Germany). For deconvolution, image stacks were acquired using optimized imaging parameters and deconvolution was carried out using Huygens Professional (Scientific Volume Imaging, Hilversum, Netherlands). Detailed 3D-analyses of all image stacks were carried out using Imaris 64 9.5.0 (Bitplane AG, Zurich, Switzerland).

Immunohistochemistry for sections

Semi-thin immunohistological sections were processed as described in Beckers et al. (2020). Hence, animals were fixed for 20h in 7% Formol-solution in ultrafiltrated seawater. Fixative was removed by rinsing the specimens six times in phosphate buffer (PBS), followed by washing them 6 x 30 min in PBS on a shaker. Afterwards, the specimens were transferred to 40% EtOH with three media changes and subsequently transferred to 70% EtOH to prepare them for standard paraffin embedding. Afterwards, specimens were transferred to 80%, 90%, 95% EtOH for 30min each, followed by transferring them to 100% EtOH 3 x 30min. Subsequently, animals were rinsed in methyl benzoate for 72h with several media changes in between and then washed 2 x 12h in butanol. The butanol was heated up in an oven to 60°C and then replaced with 1/3 paraffin wax mixture 2 x 12h (Histoplast, Thermo Scientific, Dreieich, Germany). Subsequently, the mixture was replaced with 2/3 Histoplast mixture and 3 x 12h with Histoplast at 60°C. Embedding was conducted in pre-heated casting molds with Paraplast (McCormick Scientific, Richmond, IL, USA) in the orientation of the preferred section angle for cross- or longitudinal sections. 10µm sections were performed with a Leica RM 2165 microtome (Leica, Wetzlar, Germany). The sections were placed on slides coated with 0,06% Poly-L-Lysin and de-paraffinised by rinsing the slides three times in Xylene for 2,5min. The slides were transferred to a Xylene/Ethanol solution (100%, 1:1), then washed in a descending EtOH series (100%, 95%, 90%, 80%, 70%, 40%), followed by rinses with distilled water, each 2

x 2.5min. Subsequently, the water was removed from the slides using lens cleaning tissues without touching the sections. To prevent antibody solutions to run off from the object slide, a liquid barrier marker (Roti® Liquid Barrier Marker, Carl Roth GmbH + Co. KG, Karlsruhe, Germany) was applied to create a border around the sections. Afterwards, PBS was applied to the section two times, followed by two times THT (0.1 M TrisCl, 0.3 TritonX, pH 8,5), each for 15min at RT. Slides were incubated for 2h in a wet chamber at RT, using blocking solution with goat serum (5% goat serum, Sigma-Aldrich Chemie GmbH, Steinheim, 25µl goat serum in 500 µl THT), before applying primary antibodies against serotonin (5-HT, ImmunoStar, Hudson, WI, USA, 10µl in 500 µl) and acetylated α-tubulin (Anti-acetyl α -tubulin, clone 6-11B-1, Merck, Darmstadt, 2µl in 500µl) in blocking solution in blocking solution for 24h in a wet chamber at 4°C. Slides were then rinsed 4 x 15min with THT at RT, before applying the secondary antibodies goat-anti-mouse Alexa 633 (Alexa Fluor® 633 goat-anti-mouse IgG (H + L), Thermo Fisher Scientific Inc., Waltham, USA, 1 µl in 500 µl inlc. 5% goat serum) and goat-anti-rabbit Alexa 488 (Alexa Fluor® 488 goat-anti-rabbit IgG (H + L), Thermo Fisher Scientific Inc., Waltham, USA, 1 µl in 500 µl incl. 5% goat serum) for 2h in blocking solution in a wet chamber at RT. The slides were then washed 2 x with THT followed by 2 x PTW for 15min at RT each. Subsequently, the slides were incubated for 2h with DAPI (4',6-diamidino-2-phenylindole, DAPI, Thermo Fisher Scientific Inc., Waltham, USA, 5µl in 500µl). Afterwards, the slides were washed twice with PTW and twice with PBS for 15min each. For mounting, the liquid barrier marker was removed by carefully peeling it of the slides and the latter covered with 90% glycerol/ 10% 10x PTW containing DABCO (1,4-diazabicyclo[2.2.2]octane) (250mg/10ml PTW). The cover slip was sealed using clear nail polish and the slides were stored at RT to prevent air from entering the slides. The slides were analysed using the same procedures as described for the whole mounts.

Histological sectioning, Azan-staining and 3D-reconstruction

For semi-thin sections and Azan-staining adult *Platynereis massiliensis* were processed as described in Beckers et al. (2013). Accordingly, specimens were relaxed in 7% MgCl2 and then fixed in Bouin's fluid for 12 h, dehydrated in an ascending ethanol series and incubated in methylbenzoat and butanol. Afterwards the samples were pre-incubated in Histoplast (Thermo Scientific, Dreieich, Germany) and embedded in Paraplast (McCormick Scientific,

Richmond, USA). 5 µm thick sections were made using a Reichert-Jung Autocut 2050 microtome (Leica, Wetzlar, Germany). The sections were transferred to albumen-glycerin coated glass slides. Afterwards, sections were stained with Carmalaun, differentiated with sodium phosphotungstate (5%), washed in distilled water, stained in aniline blue orange G and subsequently embedded with Malinol (Waldeck, Münster, Germany). In Azan-staining, the neuropil of the nervous system stains gray, the nuclei of cell somata stain red, the extracellular matrix stains blue and the musculature stains orange (Beckers et al. 2013). Each section was digitalized at 40x magnification using a slide scanner (Olympus dotslide (2.2 Olympus, Hamburg)) and aligned using IMOD (Kremer et al. 1996) and imodalign (www.q-terra.de/biowelt/3drekon/guides/imod_first_aid.pdf). For the 3D-visualization we used a digital workflow using solely open source software like ImageJ, MeshLab and Blender (Kalke and Helm 2022). For the 3D-schemes we used the curve tool implemented in Blender (for a better understanding see: https://www.youtube.com/watch?v=Ve9h7-E8EuM) and for the preparation of 3D-Pdfs deep exploration.

Results

For the investigation of the anatomy of adult and larval *Platynereis* we used a comparative approach (Fig. 1). Details of the developing larval head appendages are shown as cLSM-micrographs of 6dpf larvae of *Platynereis dumerilii* (Audouine & Milne Edwards, 1833) (Fig. 2). The anatomy of the head appendages, such as antennae (Fig. 3), short sensorial palps (Fig. 4) and cirri (Fig. 5) are visualized by a combination of immunohistochemistry and confocal laser scanning microscopy, Azan-histology and subsequent 3D-reconstruction. For a better understanding, we also supply 3D-schematic drawings on each figure and interactive 3D-Pdfs of the schematic visualisation of the anterior nervous system (Fig. 1D), musculature (Fig. 1E) as well as 3D-vizualizations of the latter (Fig. 1F).

For general terms and annotations we refer to the vocabulary used by (Richter *et al.*, 2010), concerning the anterior nervous system, we refer to (Schmidbaur *et al.*, 2020) if not stated otherwise.

The central anterior nervous system of adult *Platynereis massiliensis*

The central neuropil of the brain is fully encapsulated in several perikarya clusters (Fig. 1A, F and G). These clusters can be divided in the largest central perikarya cluster, which is surrounded by smaller ones and the anterior and posterior eyes (when viewed from dorsal) (Fig. 1A). Anteriorly these clusters can be differentiated into the smallest apical cluster, which is located in close vicinity to the ventral and dorsal mushroom body, laterally into the lateral perikarya cluster and posteriorly the cluster of the posterior neurite bundle of the brain (*pon*) (Fig. 1A). The somata of the perikarya clusters are rich in cell plasma and the nucleus is less stained (Fig. 1J and also 5E). The calyx of mushroom bodies consist of densely packed globuli cells with the characteristic small amount of plasma and the lack of glia cell processes enwrapping the soma. (Fig. 1I and J). The peduncle of the bigger ventral mushroom body consists of at least five smaller ones fusing distally, whereas the dorsal one shows two neurite bundles fusing to the peduncle (Fig. 1F, I and J). The peduncle of both mushroom bodies crosses the anterior dorsal and ventral commissure of the *vrcc* (ventral root of *cc*) and can be traced deep in the unstructured central areas of the central neuropil (see also Fig. 3G, H and 4H). Another cluster of perikarya (*pkcc*) is located ventro-laterally on the circumoesophageal connectives (*cc*) in direct vicinity to the splitting point of the inter-cirral neurite bundle (*icin*) (Fig. 1F and G).

The central neuropil is composed of centrally located, less structured areas. At least three commissures of the ventral (*vrcc*) and dorsal root (*drcc*) of the circumoesophageal connectives (Fig. 1C and D) are exhibited. Commissures of the ventral root are the anterior dorsal commissure (*acvr*), the medium dorsal commissure (*mcvr*) and the ventral commissure (*vcvr*) (Fig. 1C and D). The commissures of the *drcc* are the dorsal commissure (*dcdr*), the median dorsal commissure (*mcdr*) and the ventral commissure (*vcdr*) (Fig. 1 C and D).

The musculature of the anterior end of adult *Platynereis massiliensis*

The musculature of the adult peristomium consists of two dorsal and two ventral longitudinal muscle bundles, which are encapsulated by a rather thin layer of circular muscles. The latter form - together with the epidermis - the cutaneous muscle tube (Fig. 1E, H). Muscular elements crossing the peristomium and prostomium are two lateral longitudinal muscle bundles, which are attached to the circular muscles of the peristomium and terminate at the `cirral base` (Fig. 1E, Hand 5D). The other one is the pharynx muscle (*phm*) which is attached ventrally to the dorsal longitudinal muscles of the peristomium and dorsally to the pharynx

(Fig. 1E, H and 5E). In the prostomium only muscles associated with the head appendages can be differentiated, such as a prominent transversal muscle proceeding from one `cirral base` (*cib*) to the other (Fig. 1E, H and 5E). In addition, three muscle bundles of each lateral antennae (Fig. 3), nine palp muscles (Fig. 4) and two types of cirral muscles (Fig. 5) can be investigated.

The larval anterior nervous system and innervation of the head appendages in *Platynereis dumerilii*

The larval anterior nervous system is composed of two circumoesophageal connectives (*cc*) consisting of neurite bundles of its dorsal (*drcc*) and ventral root (*vrcc*). These neurite bundles emanate from the ventral nerve cord (*vnc*) and fuse anteriorly while running into the larval brain (Fig. 2A, F and H). The serotonergic (5-HT) part of the nervous system is distributed in separated areas of the *vrcc* and *drcc*. A strong serotonergic immunoreactivity is concentrated in the dorso-median apical organ and three huge neurons are associated with it (Fig. 2B). In close vicinity, two pairs of ciliary photoreceptor cells (*crpc*) are located and send slender nerves into the dorsal brain region next to the posterior neurite bundle of the brain (*pon)*. The nuchal organs are innervated by this dorsal brain region (Fig. 2B). From the ventral brain region two distinct neurite bundles emanate, which innervate the anterior stomatogastric nervous system (*stgns*) (Fig. 2A, B, E and F). After the split of the *drcc* and *vrcc*, neurite bundles originating in both roots form the main palp nerve (*pn1*) (Fig. 2C-H). The *pn1* proceeds in anterior direction by splitting off into more slender neurite bundles, which converge again distally (Fig. 2B, F and H). An additional, distinct palp nerve originates solely from the *vrcc* (*pn3*) and terminates distally in the palp (Fig. 2A, B, D-H). The neurite bundles of the lateral antennae arise solely from the dorsal brain region of the *drcc* and proceed parallel to the main palp nerve in anterior direction (Fig. 2A, F and H).

The neuronal innervation and musculature of the head appendages of adult *Platynereis massiliensis*

The paired neurite bundles of the lateral antennae originate at the base of the dorsal root of the circumoesophageal connectives (*drcc*) (Fig. 3A, C). Subsequently the antennal nerve proceeds in anterior direction passing the central optic neuropil (*con*) and the anterior median commissure of the *vrcc* (*acvr*) dorsally (Fig. 3A – D, G and H). Afterwards, a small nerve splits off the main antennal nerve and runs into a potentially glandular area at the anterior tip of

the prostomium (Fig. 3A). The neurites of the main nerve split off as well, but terminate in putatively sensory antennal cells (Fig. 3A).

The musculature of the lateral antennae is very simple. Hence, it consists of three longitudinal muscles wrapped spirally around each antennal nerve (Fig. 3E, F). They are all attached to the dorsal prostomium and reach the antennal base.

The main palp nerve (*pn1*) originates from the point where the ventral root and the dorsal root - after splitting from each other - fuse again and proceed into the brain. Thus, it is innervated by both roots (Fig. 4A, B, D; see also 1F and G). Before entering the brain, at least three lateral and one ventral palp nerve from the periphery of the palps fuse with *pn1* (Fig. 4F, G, H). Another palp nerve originates from the median dorsal commissure of the *vrcc* (*pn3*) and fuses with *pn1,* too. Distally, *pn1* splits off and its neurites terminate like a brush in the putative sensorial cells at the wide tip of the short sensorial palps.

The musculature of the palps is quite complex when compared with the other head appendages. Around the distal part of the palps, five longitudinal muscle bundles are located - two paired inner lateral, one anterior muscle and two outer lateral bundles, which are herein called palp framing muscles (*fpm*) (Fig. 4E, also 1E). The inner lateral palp framing muscles are connected to the four anchor muscles (*aom*), located between the antennal bases (Fig. 4E, also 1E and 3F). Posterior, at the tip of the palp, two additional longitudinal muscles are attached. The latter proceed unilateral to the `cirral base` of each side (Fig. 4C, E and 1E). The transversal palp muscle is located ventrally to the base of each palp (Fig. 4C, E and 1E). The biggest muscles of the palps are the contralateral palp muscles, which proceed from each `cirral base` to the ventral base of the palp of the opposite side (Fig. 4C, D and 1E).

The four tentacular cirri on each side of the anterior end can be divided into two ventral and two dorsal ones and are each innervated by one dorsal tentacular cirri nerve (*dtcn*) or one ventral tentacular cirri nerve (*vtcn*) (Fig. 5A and B; see also 1B and F). The *dtcn* originates distally from the dorsal cirral neurite bundle (*dcin*), which emanates from the ventral nerve cord lateral to the circumoesophageal connectives (*cc*) and proceed parallel to it. The *cc* and the *cin* are connected to each other by the inter-cirral neurite bundle (*icin*) (Fig. 5A, B and E). The ventral tentacular cirral nerves emanate directly from the *cc* in close vicinity to the origin of the *icin* (Fig. 5A and B). The only perikarya cluster of the *cc* (*pkcc*) is located at the same spot (see also 1F and G).

The musculature of the tentacular cirri can be divided into two components. A longitudinal tentacular cirral muscle, which is attached to circular muscles of the cutaneous muscle tube of the peristomium and the `Helmsche Umbogen` (Fig. 5C, D and E). The `Helmsche Umbogen` is composed of longitudinal muscle fibers oriented as a collar around the first proximal part of the tentacular cirri (Fig. 5C, D and E).

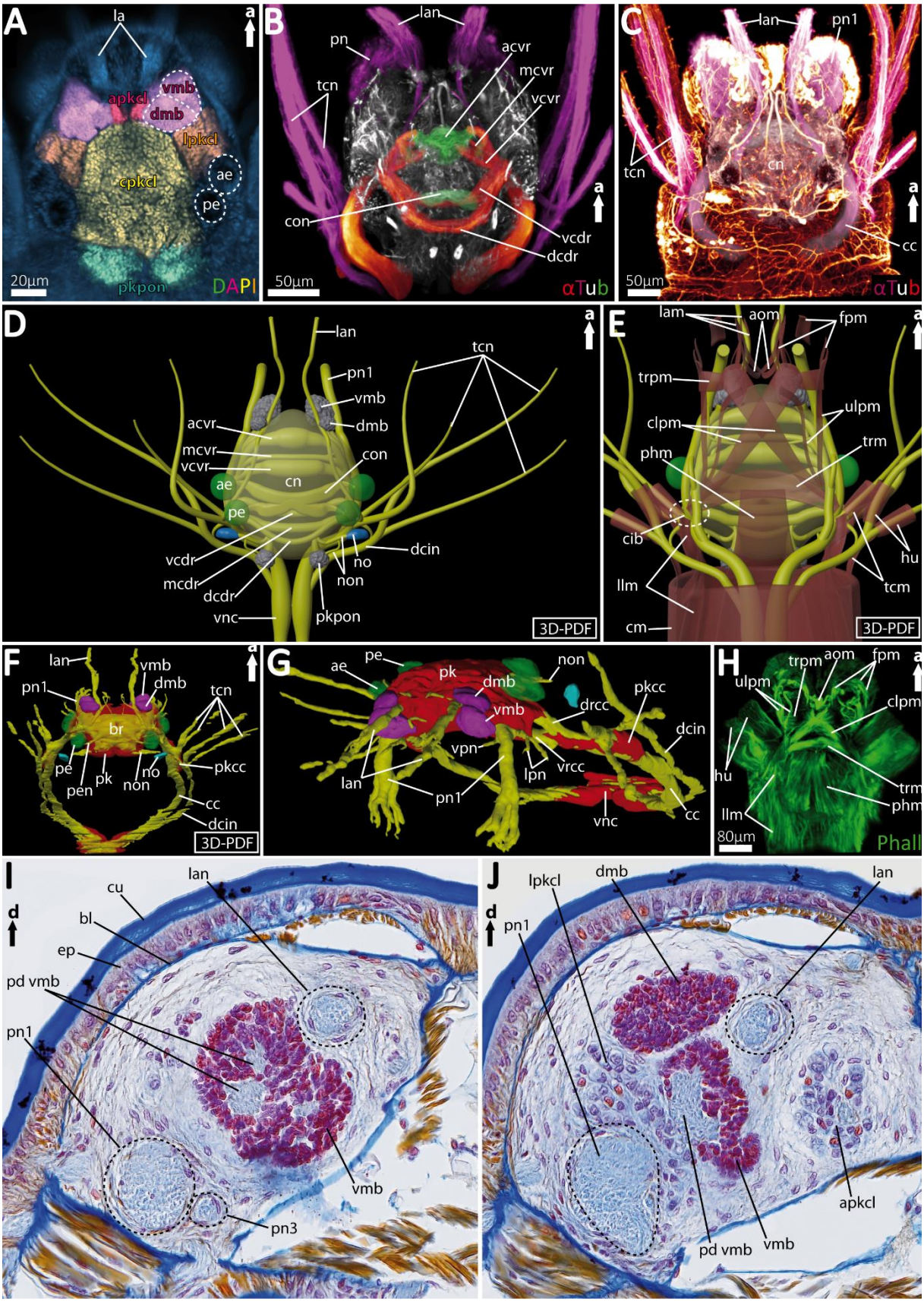

Fig. 1: Overview about the anterior morphology of adult *Platynereis massiliensis*. Orientation of the specimen is implemented via the white arrow, with a = anterior.A: Dorsal view of the color coded perikarya clusters of the brain of *P. massiliensis*, captured using cLSM micrograph. Dotted circles mark the position of the anterior and posterior eyes and the mushroom bodies. B: Morphology of the

anterior nervous system in dorsal view using cLSM micrograph. The peripheral nervous system is omitted, the head appendages are color coded in pink, the central neuropil in white and specialized neuropils and commissures of the brain in red and green C:. Dorsal view of the overall morphology of the acetylated α-tubulinergic anterior nervous system using cLSM. The peripheral nervous system is color coded in red, the central neuropil in white and the head appendages: the lateral antennae, the palps and the tentacular cirri in pink. D: Schematic drawing of the anterior nervous system (yellow) in dorsal view, eyes are highlighted in green and perikarya in gray. By clicking on it you activate the interactive 3D-PDF. E: Schematic drawing of the anterior nervous system (yellow) and musculature (red) in ventral view. By clicking on it you activate the interactive 3D-PDF. F: Dorsal view of a 3D-rekonstruction of the anterior nervous system (yellow) based on Azan-histology, perikarya are red and translucent, eyes in green, nuchal organ in cyan and mushroom bodies in magenta and pink. By clicking on it you activate the interactive 3D-PDF. G: Fronto-lateral view of the same reconstruction. H: Dorsal view of the anterior musculature with a focus on the muscular system of the head appendages, captured using anti-f-actin phalloidin cLSM micrograph. I: Magnification of an Azan-stained histological cross section with focus on the ventral mushroom body, dotted circles mark two palp nerves and the antennal nerve. J: Magnification of an Azan-histological cross section posterior to (I) with focus on the ventral and dorsal mushroom body, dotted circles mark the fused palp nerves and the antennal nerve. **Abbreviations:** acvr – anterior dorsal commissure of the vrcc, ae – anterior eye, aom – anchor muscles, apkcl – apical cluster of perikaria, bl – basal lamina, br – brain, cc – circumoesophageal connectives, cib – cirral base, clpm – contralateral palp muscles, cm – circular musculature of body wall, cn – central neuropil of brain, con - central optical neuropil, cpkcl – central cluster of perikaria, cu – cuticle, dcdr - dorsal commissure of the drcc, dcin – dorsal cirri neurite bundle, dmb – dorsal mushroom body, drcc – dorsal root of cc, ep – epidermis, fpm – palp framing muscles, hu – Helmsche Umbogen, icin – intercirral neurite bundle, la – lateral antennae, lam – lateral antennae muscles, lan – lateral antennae nerves, llm – lateral longitudinal muscles, lpkcl - lateral cluster of perikaria, lpn – lateral palp nerves, mcdr - median commissure of the drcc, mcvr - median dorsal commissure of the vrcc, no – nuchal organ, non – nuchal organ nerves, pd vmb – peduncle of vmb, pe – posterior eye, pen – posterior eye nerve, phall – phalloidin-rhodamin, phm – pharynx muscle, pk – perikaria, pkcc – perikaria cluster of cc, pkpon – perikaria of pon, pn – palp nerves, pn 1 – main palp nerve, pn3 – palp nerve originating from the vrcc, pon – posterior neurite bundle of brain, tcm – tentacular cirri muscles, tcn – tentacular cirri nerves, trm – transversal muscle, trpm – transversal palp muscles, ulpm – unilateral palp muscles, vcdr - ventral commissure of the drcc, vcvr – ventral commissure of the vrcc, vmb – ventral mushroom body, vnc – ventral nerve cord, vpn – ventral palp nerves, vrcc – ventral root of cc, α-tub - α-tubulin

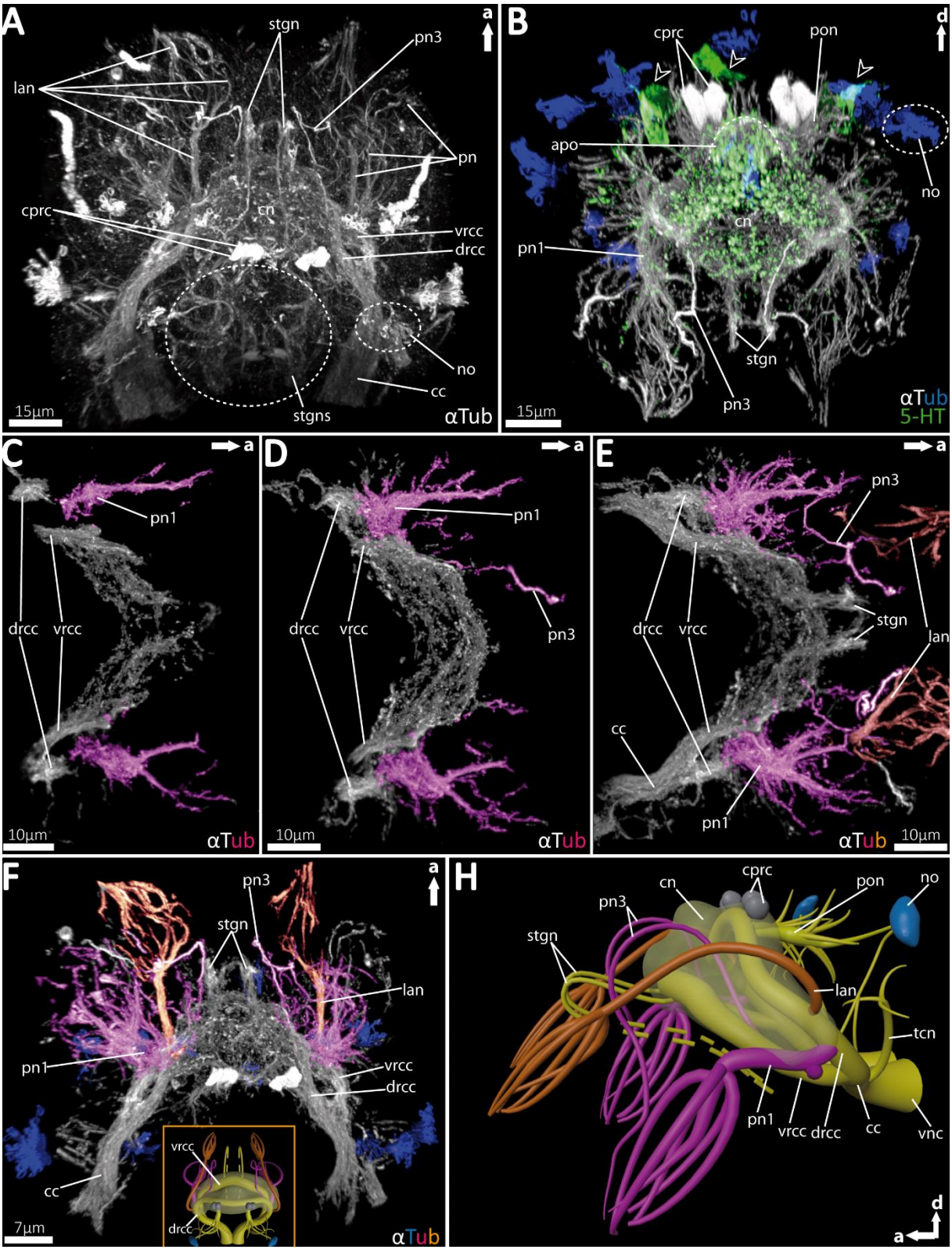

Fig. 2: Overview about the morphology of the anterior nervous system of 6 dpf (days-post-fertilisation) nectochaete larva of *Platynereis dumerilii* with focus on the palps. Orientation of the specimen is implemented via the white arrow, with a = anterior & d = dorsal. A: Dorsal view of the tubulinergic anterior nervous system. Dotted circles mark the position of the nuchal organ and the anterior stomatogastric nervous system. B: Frontal view on the tubulinergic anterior nervous system. Serotonergic parts of the nervous system highlighted in green and cilia in blue. The apical organ is marked by the dotted line, surrounded by its three serotonergic neurons (arrowheads). C, D, E: Digital

longitudinal sections through the anterior nervous system in ventro-dorsal progression. The main palp nerve (*pn1*) and *pn3* are highlighted in pink, the nerves of the antennae in orange. F: Dorsal view of the acetylated α-tubulinergic anterior nervous system, anterior stomatogastric nervous system omitted, nerves of palps are highlighted in pink, antennal nerves in orange and cilia in blue. The orange frame show a 3D-shematic drawing of the larval anterior nervous system in the same orientation, also shown in (H). H: Lateral view of the 3D-schematic drawing of the anterior nervous system (yellow), the central neuropil is translucent and the palp nerves are highlighted in pink, the antennal nerves in orange, the nuchal organ in blue and the *cprc* in gray. **Abbreviations:** 5-HT - serotonin (receptor), apo – apical organ, cc – circumoesophageal connectives, cn – central neuropil of brain, cprc – ciliary photoreceptor cell, drcc – dorsal root of cc, lan – lateral antennae nerves, no – nuchal organ, pn 1 – main palp nerve, pn3 – palp nerve originating from the vrcc, pon – posterior neurite bundle of brain, stgn – stomatogastric neurite bundles, stgns – stomatogastric nervous system, tcn – tentacular cirri nerves, vnc – ventral nerve cord, vrcc – ventral root of cc, α-tub - α-tubulin

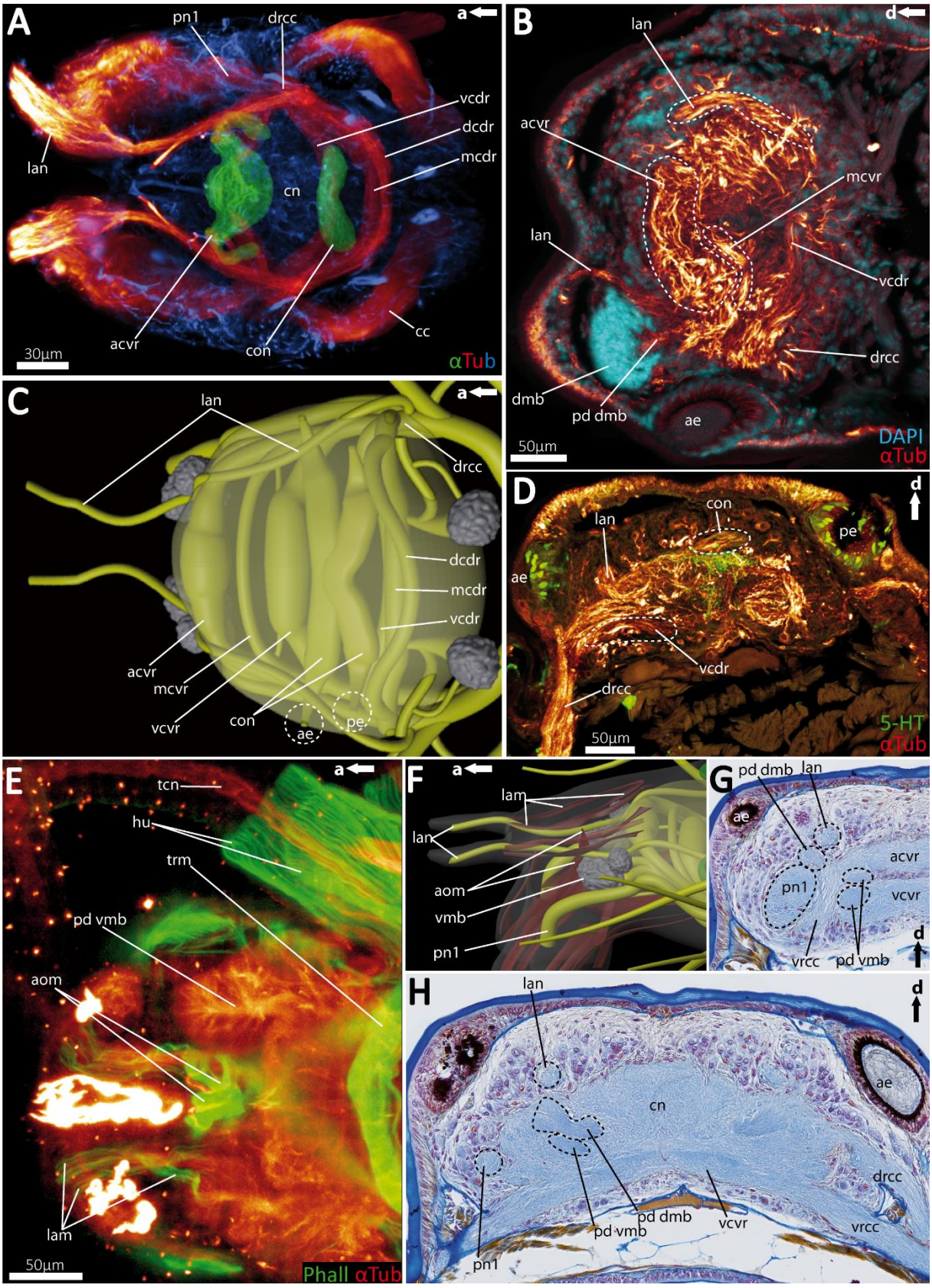

Fig. 3: Morphology of the antennae and the anterior end of *Platynereis massiliensis*. A: Dorsal view of the acetylated α-tubulinergic anterior nervous system with focus on the antennae, using cLSM micrograph. The central nervous system, the antennal and palp nerves are shown in red, the rest in blue, the cirri are omitted. B: Longitudinal paraffin section through the brain, stained against Dapi (cyan) and tubulin (red). Dotted lines mark the position of antennal nerve and commissures of the vrcc.

C: Schematic drawing of the anterior nervous system (yellow) with focus on the antennae, perikaria highlighted in gray. D: Paraffin diagonal-cross section in between the anterior and posterior eyes, stained against acetylated α-tubulin (red) and 5HT-serotonin (green). Dotted lines mark the location of the central optic neuropil and *vcdr*. E: Dorsal view of the antennal musculature and anterior brain region stained against anti-f-actin phalloidin (green) and acetylated α-tubulin (red), ventral structures omitted. F: Lateral view of a schematic drawing of the innervation (yellow) and musculature (red) of the antennae. G, H: Azan-histological cross sections visualize the pathway of the antennal nerve dorsally through the brain. Dotted circle mark the pathway of antennal and palp nerves, and the peduncles of the mushroom bodies. **Abbreviations:** 5-HT - serotonin (receptor), acvr – anterior dorsal commissure of the vrcc, ae – anterior eye, aom – anchor muscles, cc – circumoesophageal connectives, cn – central neuropil of brain, con - central optical neuropil, dcdr - dorsal commissure of the drcc, dmb – dorsal mushroom body, drcc – dorsal root of cc, hu – Helmsche Umbogen, lam – lateral antennae muscles, lan – lateral antennae nerves, mcdr - median commissure of the drcc, pd dmb – peduncle of dmb, pd vmb – peduncle of vmb, pe – posterior eye, phall – phalloidin-rhodamin, pn 1 – main palp nerve, tcn – tentacular cirri nerves, trm – transversal muscle, vcdr - ventral commissure of the drcc, vcvr – ventral commissure of the vrcc, vmb – ventral mushroom body, vrcc – ventral root of cc, α-tub - α-tubulin

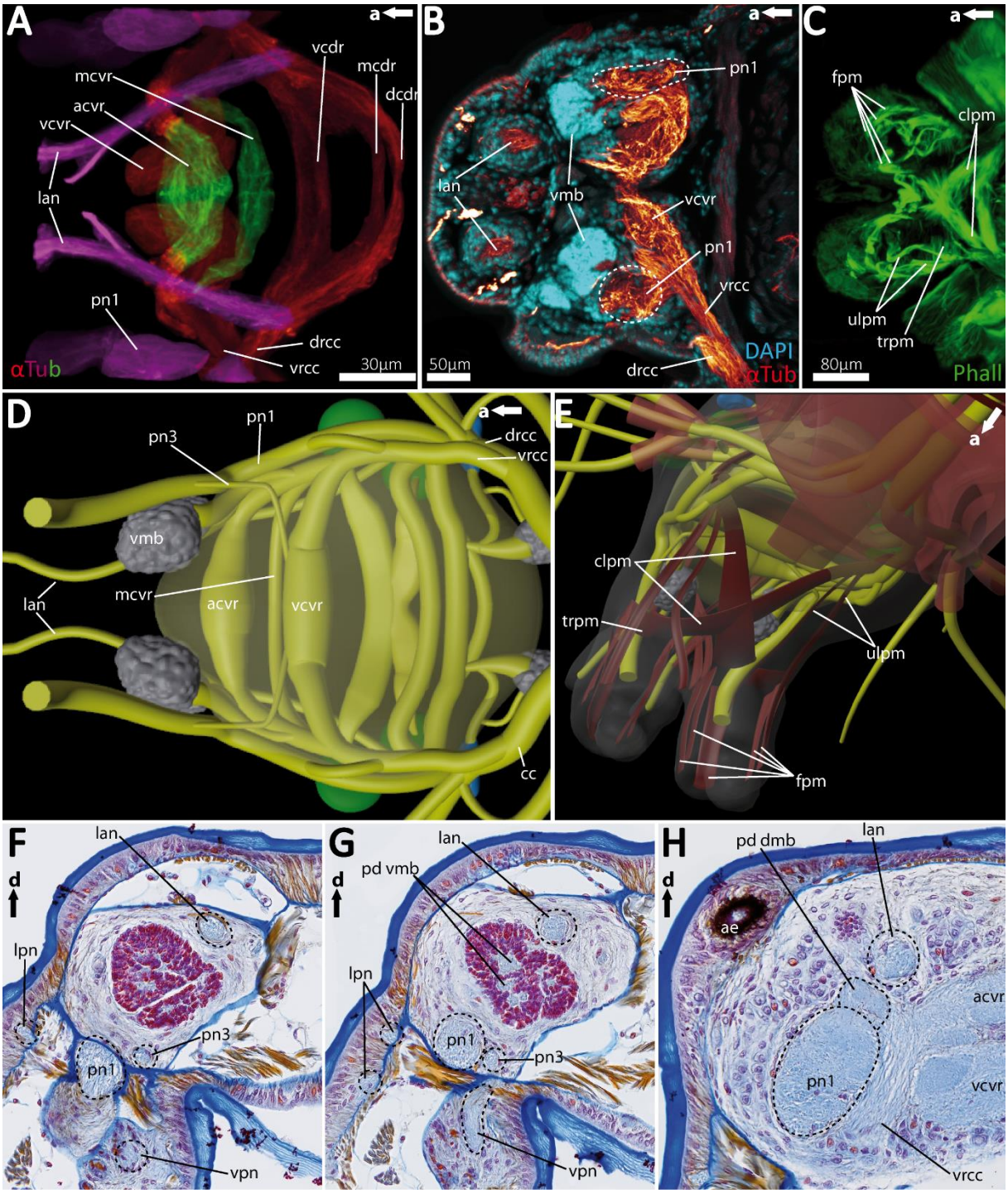

Fig. 4: Morphology of the palps and associated structures of the anterior end of *Platynereis massiliensis*. Orientation of the specimen is implemented via the white arrow, with a = anterior. A: Dorsal view of cLSM micrograph of the brain region stained against acetylated α-tubulin, the main palp nerve (*pn1*) and nerves of antennae are color coded in pink, dorsal and ventral root and their commissure in red and green. B: Longitudinal paraffin section stained against acetylated α-tubulin (red) and DAPI (cyan) through the brain showing the origin of *pn1*. C: Dorsal view of palp musculature stained against anti-f-actin phalloidin, captured in cLSM micrograph. D: Schematic drawing of the anterior nervous system (yellow) in ventral view, with focus on the palp innervation, eyes colored in green and perikarya in gray. E: Schematic drawing of the anterior nervous system (yellow) and musculature (red) in ventro-lateral view with a focus on the palp musculature. F, G, H: Magnification

of Azan-stained histological cross sections through the brain in anterior-posterior progression, showing the pathway and fusion of palp nerves. **Abbreviations:** acvr – anterior dorsal commissure of the vrcc, ae – anterior eye, cc – circumoesophageal connectives, clpm – contralateral palp muscles, dcdr - dorsal commissure of the drcc, dmb – dorsal mushroom body, drcc – dorsal root of cc, fpm – palp framing muscles, lan – lateral antennae nerves, lpn – lateral palp nerves, phall – phalloidin-rhodamin, mcdr - median commissure of the drcc, mcvr - median dorsal commissure of the vrcc, pd dmb – peduncle of dmb, pd vmb – peduncle of vmb, pn 1 – main palp nerve, pn3 – palp nerve originating from the vrcc, trpm – transversal palp muscles, ulpm – unilateral palp muscles, vcdr - ventral commissure of the drcc, vcvr – ventral commissure of the vrcc, vmb – ventral mushroom body, vpn – ventral palp nerves, vrcc – ventral root of cc, α-tub - α-tubulin

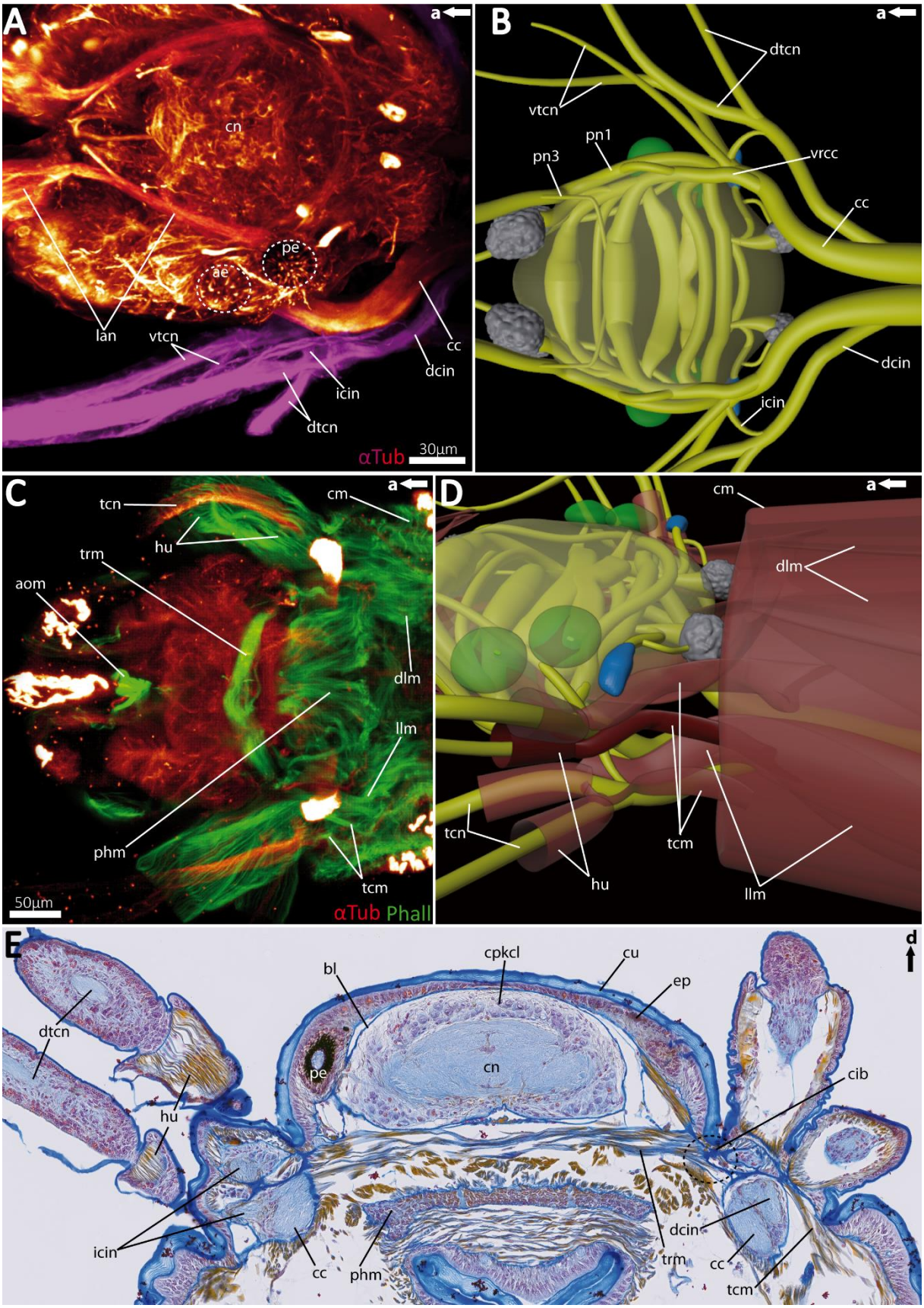

Fig. 5: Overview of the morphology of the tentacular cirri and the anterior end of *Platynereis massiliensis*. Orientation of the specimen is implemented via the white arrow, with a = anterior & d = dorsal.A: Magnification of the acetylated α-tubulinergic nervous system of the tentacular cirri and the brain in dorsal view, cirri highlighted in pink. Dotted circles mark the position of the eyes. B: Schematic

drawing of the anterior nervous system (yellow) in ventral view, with focus on the innervation of the cirri, eyes are highlighted in green, perikarya in gray. C: Dorsal view of the musculature of the tentacular cirri and anterior brain region stained against anti-f-actin phalloidin (green) and acetylated α-tubulin (red), ventral structures omitted. D: Schematic drawing of the nervous system (yellow) and musculature (red) of the anterior end with focus on the tentacular cirri, in dorso-lateral view, eyes in green, nuchal organ in blue and perikarya in gray. E: Azan-histological cross section through the region of the *icin* (intercirral neurite bundle)-region. **Abbreviations:** ae – anterior eye, aom – anchor muscles, bl – basal lamina, cc – circumoesophageal connectives, cib – cirral base, cm – circular musculature of body wall, cn – central neuropil of brain, cpkcl – central cluster of perikaria, cu – cuticle, dcin – dorsal cirri neurite bundle, dlm – dorsal longitudinal musculature of body wall, dtcn – dorsal tentacular cirri nerves, ep – epidermis, hu – Helmsche Umbogen icin – intercirral neurite bundle, lan – lateral antennae nerves, llm – lateral longitudinal muscles, pe – posterior eye, phall – phalloidin-rhodamin, phm – pharynx muscle, pn 1 – main palp nerve, pn3 – palp nerve originating from the vrcc, tcm – tentacular cirri muscles, tcmn – tentacular cirri muscle nerve, tcn – tentacular cirri nerves, trm – transversal muscle, vrcc – ventral root of cc, vtcn – ventral cirri nerves, α-tub - α-tubulin

Discussion

The question of palp homology

The definition of the enigmatic head appendages fascinated and puzzled researchers over several decades (Hanström, 1927; Binard and Jeener, 1928; Wilson, 1936, 1982; Rouse and Pleijel, 2001; Orrhage and Müller, 2005). Nevertheless, so far a consistent homology statement and evolutionary scenario for the evolution of head appendages was difficult. One approach with a huge impact on the understanding of annelid evolution, is the theory of the 12 palp nerve roots (Orrhage and Müller, 2005). This systematic study of the innervation patterns of polychaete head appendages represented a potential tool to facilitate the definition of head appendages. Unfortunately and despite highly detailed and stunning descriptions of the anterior nervous system of a huge diversity of annelid families, not at least the lack of a proper molecular backbone concerning the annelid tree of life lead to misinterpretations (Beckers, Helm and Bartolomaeus, 2019; Kalke, Beckers and Helm, 2021). Therefore, recent investigations e.g., dealing with the paleoannelid *Magelona mirabilis*, lead to a closer examination of these previous studies and to a re-evaluation of annelid key taxa in this respect (Beckers *et al.*, 2019, 2019; Kalke, Beckers and Helm, 2021; Helm, Schwarze and Beckers, 2022). As a result and thanks to recent phylogenomic studies (Weigert *et al.*, 2014; Helm *et al.*, 2018), our understanding of annelid evolution changed dramatically within the last years.

Nevertheless, the old question concerning the homology of annelid head appendages – in particular of the different types of palps – remains unanswered so far, due to the lack of comparative morphological data. While the sister groups to the Pleistoannelida, such as the Paleoannlida with Magelonidae and Oweniidae, or Chaetopterifomia and Amphinomidae as well as sedentary families are well-covered (Orrhage, 1980; Orrhage and Müller, 2005; Brinkmann and Wanninger, 2008; Purschke, 2015; Faroni-Perez *et al.*, 2016; Worsaae, Rimskaya-Korsakova and Rouse, 2016; Rimskaya-Korsakova, Galkin and Malakhov, 2018) comprehensive analyses dealing with errant annelid taxa are scarce. But, although previous investigations focussing on neuronal innervations and general histology already highlighted a homology of elongated feeding palps throughout the annelid phylogeny, the question

concerning the evolutionary origin of the stout sensory errant palps and their potential homology stayed open so far.

Head appendages of Errantia

With focus on nereidid taxa, our investigations therefore highlight the development and anatomy of larval as well as adult sensory palps to uncover the potential evolutionary origin. And although the used taxa differ in several ontogenetic features, *P. massiliensis* and *P. dumerilii* develop the head appendages similar in timing with respect to the number of chaetigerous segments (Helm *et al.*, 2014; Starunov, Voronezhskaya and Nezlin, 2017) and are highly comparable to the direct development of *Neanthes arenacoedentata* (Winchell, Valencia and Jacobs, 2010). For all species, a quite early and simultaneous development of all three major types of head appendages can be examined. Unfortunately, all previous studies solely focussed on the overall development of the species and thus do not allow an application of the innervation pattern tool and its definition of the head appendages. Our herein presented data supports the early and simultaneous development of all types of head appendages. Interestingly, our data exhibit that the larval innervation pattern of lateral antennae, palps and the first pair of tentacular cirri reflects the pattern that can be observed in adult specimens.

Thus, the lateral antennae are each innervated by one nerve, which originates from the base of the dorsal root of the circumoesophageal connectives in the brain. A similar pattern is reported for other Phyllodocida, like Syllidae (Schmidbaur *et al.*, 2020), Hesionidae, Acoetidae, Polynoidae and Sigalionidae (Orrhage, 1991), and Onuphidae, Eunicidae, Dorvilleidae and Histriobdellidae (Orrhage, 1995; Kuhl, Bartolomaeus and Beckers, 2022). Although, for Nereididae no median antennae is present, this head appendage can be called homologous across Errantia based on the available data as well (Orrhage, 1991, 1995; Orrhage and Eibye-Jacobsen, 1998; Schmidbaur *et al.*, 2020; Kuhl, Bartolomaeus and Beckers, 2022).

The tentacular cirri differ strongly in numbers among errant taxa, but share a similar innervation pattern (Orrhage and Eibye-Jacobsen, 1998). As already stated by other authors, tentacualr cirri represent transformed parapodial structures, with a simplified innervation

due to ontogenetic cephalisation, but with a neuronal innervation pattern comparable with the one of parapodia (Winchell, Valencia and Jacobs, 2010).

When it comes to the most prominent type of errant head appendage – the sensory, stout palps – the source of available datasets is very limited. The short sensorial palps of herein investigated taxa are innervated by putative sensory neurite bundles originating distally, than fuse into one main palp nerve (*pn1*). At the point where the ventral (*vrcc*) and dorsal root (*drcc*) of the circumesophageal connective run into the central neuropil of the brain, *pn1* splits off and proceeds in each root, similar to the situation described for Syllidae (Schmidbaur *et al.*, 2020). *Pn3* – also mentioned for syllids - originates in larval and adult *Platynereis* from the *vrcc*. *Pn2,* which is solely innervated by the *drcc* and mentioned in Syllidae, is not present in our data. A similar innervation of the errant palps by at least one nerve of the *vrcc* and the *drcc* or their commissures is described for syllids, hesionids, trochochaetids, acoetids, polynoids, sigalionids, other nereidids (Orrhage, 1991; Orrhage and Eibye-Jacobsen, 1998; Schmidbaur *et al.*, 2020) and eunicidan families like Onuphidae, Eunicidae, Dorvilleidae and Histriobdellidae (Orrhage, 1995; Kuhl, Bartolomaeus and Beckers, 2022). Furthermore, Glyceridae and Goniadidae show a comparable innervation pattern, with five pairs of prostomial nerves resembling the innervation pattern of the palps in other errant taxa (Orrhage, 1999).

As several authors reported frictions/discrepancies in their findings when comparing them with the detailed descriptions of Orrhage (Beckers, Helm and Bartolomaeus, 2019; Schmidbaur *et al.*, 2020; Kalke, Beckers and Helm, 2021), the “12 palp root theory” appears superseded and not supported by recent findings. Thus, the approach of (Schmidbaur *et al.*, 2020), which was also used herein, focussing on the differentiation of palp nerves in main palp nerves (pn1) innervated by both roots, palp nerves innervated solely by the dorsal root (pn2) and palp nerves innervated solely by the ventral root (pn3), should be used in the future.

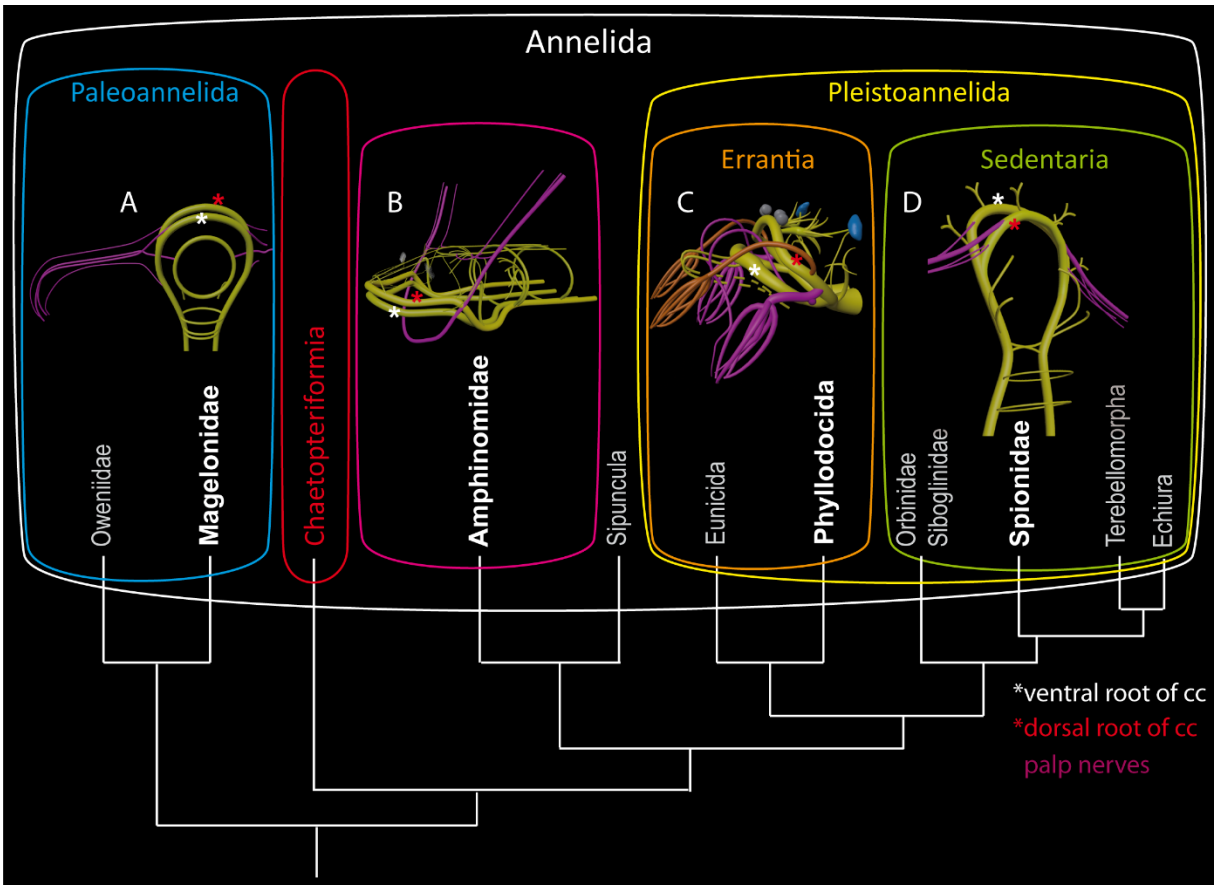

Fig. 6: Annelid phylogeny based on Helm et al. (2018) including 3D-shematic drawings of the larval anterior nervous system with focus on the palp innervation. A: 9dpf (days-post-fertilisation) larva of *Magelona mirabilis* (Magelonidae). B: Rostraria larva of Paramphinome jeffreysii (Amphinomidae). C: Nectochaete larva (6dpf) of *Platynereis dumerilii* (Nereididae). D: ~60 dpf larva of *Malacoceros fuliginosus* (Spionidae). The asterisks mark the position of the ventral (white asterisk) and dorsal root (red asterisk) of the circumoesophageal connectives, palp nerve are highlighted in pink. All palps in the shown annelid taxa exhibit a similar neuronal innervation pattern.

Homology of palps in Annelida

Previous investigations, focussing on the larval and adult feeding-palps of three annelid key taxa – the Magelonidae, Amphinomidae and Spionidae – already showed that the palps of *Magelona mirabilis* (Magelonidae) and *Malacoceros fuliginosus* (Spionidae) transform gradually into the adult palps, whereas the larval palps of amphinomids get reduced (Kalke et al., submitted). Nevertheless, these comparative investigations highly supported a homology of larval and adult feeding palps throughout the annelid tree, based on neuronal innervation patters as well as the general anatomy of the latter (Kalke et al., submitted).

The herein presented comparison between larval and adult innervation patterns of nereidids results in a similar observation. Hence, the larval palps get transferred into adult structures,

but still share the same neuronal innervation pattern. Whereas the neuronal innervation pattern of adult errant palps complicates of homology statement due to fusions and ontogenetic transformations throughout development, the larval conditions differ. Notably, in particular the larval neuronal scaffold is highly comparable to the conditions observed in taxa bearing elongated feeding-palps. As a consequence, elongated feeding-palps and the stout sensorial palps of Errantia have to be considered as being homologous structures sharing a comparable neuronal innervation by neurite bundles originating from the *drcc* and the *vrcc* (see Fig. 6).

Furthermore, the adaptive transformation from slender feeding-palps towards short sensorial palps took place in the last common ancestor of errant Pleistoannelida, - a hypothesis already previously mentioned for the stem linage of Eunicida (Kuhl, Bartolomaeus and Beckers, 2022).

Although shown to be homologous based on the neuronal scaffold, future observations will benefit from including the musculature of head appendages into the comparison of annelid head appendages. Such an additional character system will help to understand the adaptive transformations that happened in various annelid families and will therefore deepen our knowledge concerning annelid evolution.

Conclusion

This study addresses the long-standing question of palp homology in annelids. Over decades, researchers grappled with defining head appendages, with the "12 palp root theory" of Orrhage and Co-workers being a notable attempt. Recent investigations, including paleoannelids, Chaetopteriformia and Pleistoannelida, prompted a re-evaluation of previous research, leading to a significant transformation in our understanding of annelid evolution. Our focus on nereidid taxa revealed that they exhibit an early and simultaneous development of head appendages, with larval innervation patterns closely resembling those in adults. The innervation pattern of their antennae, palps and tentacular cirri, in comparison with former studies, suggests the homology of head appendages across Errantia.

Comparative investigations in other annelid taxa further support the homology of feeding palps throughout the annelid tree, emphasizing the similarities in neuronal innervation patterns between larval and adult stages. This suggests that elongated feeding-palps and stout sensorial palps of Errantia share a common origin. In addition, we propose that the transformation from slender feeding-palps to short sensorial palps occurred in the last common ancestor of errant Pleistoannelida. While this study advances our understanding of palp homology, future research should consider head appendage musculature to deepen our knowledge of annelid evolution.

Conflict of Interest

The authors declare that the research was conducted in the absence of any commercial or financial relationships that could be construed as a potential conflict of interest.

Funding

This work was financially supported by the group “Animal Evolution and Biodiversity” of the University of Goettingen. No third party funding was used in addition. Open Access funding enabled and organized by Projekt DEAL.

Acknowledgments

The authors want to thank the working group “Animal Evolution and Biodiversity” and “Evolutionary Biology and Ecology” for the financial and technical support.

Availability of data

All data analysed in this study are used in figures of this article. The original 3D confocal image stacks can be made available after personal contact with the corresponding authors.

References

Beckers, P. *et al.* (2019) 'The central nervous system of Oweniidae (Annelida) and its implications for the structure of the ancestral annelid brain', *Frontiers in Zoology*, 16(1), pp. 1–21. Available at: https://doi.org/10.1186/s12983-019-0305-1.

Beckers, P., Helm, C. and Bartolomaeus, T. (2019) 'BMC Evolutionary Biology The anatomy and development of the nervous system in Magelonidae (Annelida) – insights into the evolution of the annelid brain', *BMC Evolutionary Biology* [Preprint].

Binard, A. and Jeener, R. (1928) *Morphologie du lobe préoral des polychètes*.

Brinkmann, N. and Wanninger, A. (2008) 'Larval neurogenesis in *Sabellaria alveolata* reveals plasticity in polychaete neural patterning', *Evolution & Development*, 10(5), pp. 606–618. Available at: https://doi.org/10.1111/j.1525-142X.2008.00275.x.

Faroni-Perez, L. *et al.* (2016) 'Anterior sensory organs in Sabellariidae (Annelida)', *Invertebrate Biology*, 135(4), pp. 423–447. Available at: https://doi.org/10.1111/ivb.12153.

Hanström, B. (1927) 'DAS ZENTRALE UND PERIPHERE NERVENSYSTEM DES KOPFLAPPENS EINIGER POLYCHÄTEN', *Zeitschrift für Morphologie und Ökologie der Tiere*, 7(4), pp. 543–596. Available at: https://www.jstor.org/stable/43261104.

Helm, C. *et al.* (2014) 'An immunocytochemical window into the development of Platynereis massiliensis (Annelida, Nereididae)', *International Journal of Developmental Biology*, 58(6–8). Available at: https://doi.org/10.1387/ijdb.140081cb.

Helm, C. *et al.* (2018) 'Convergent evolution of the ladder-like ventral nerve cord in Annelida', *Frontiers in Zoology*, 15(1). Available at: https://doi.org/10.1186/s12983-018-0280-y.

Helm, C., Schwarze, G. and Beckers, P. (2022) 'Loss of complexity from larval towards adult nervous systems in Chaetopteridae (Chaetopteriformia , Annelida) unveils evolutionary patterns in Annelida', *Organisms Diversity & Evolution* [Preprint], (May). Available at: https://doi.org/10.1007/s13127-022-00553-z.

Jekely, G., Keijzer, F. and Godfrey-Smith, P. (2015) 'An option space for early neural evolution', *Philosophical Transactions of the Royal Society B: Biological Sciences*, 370(1684). Available at: https://doi.org/10.1098/rstb.2015.0181.

Kalke, P., Beckers, P. and Helm, C. (2021) 'May the Palps Be With You – New Insights Into the Evolutionary Origin of Anterior Appendages in Terebelliformia (Annelida)', *BMC Zoology*, 6(30), pp. 1–16. Available at: https://doi.org/10.1186/s40850-021-00094-6.

Kuehn, E. *et al.* (2019) 'A scalable culturing system for the marine annelid Platynereis dumerilii', *PLoS ONE*, 14(12). Available at: https://doi.org/10.1371/journal.pone.0226156.

Kuhl, S., Bartolomaeus, T. and Beckers, P. (2022) 'How Do Prostomial Sensory Organs Affect Brain Anatomy? Phylogenetic Implications in Eunicida (Annelida)', *Journal of Marine Science and Engineering*, 10(11), p. 1707. Available at: https://doi.org/10.3390/jmse10111707.

Orrhage, L. (1966) 'Über die Anatomie des zentralen Nervensystems der sedentaren Polychaeten', *Arkiv för Zoologi*, 19(3), pp. 99–133.

Orrhage, L. (1980) ‘On the structure and homologues of the anterior end of the polychaete families sabellidae and serpulidae’, *Zoomorphology*, 96(1–2), pp. 113–167. Available at: https://doi.org/10.1007/BF00310081.

Orrhage, L. (1990) ‘On the Microanatomy of the Supraoesophageal Ganglion of Some Amphinomids (Polychaeta Errantia), with Further Discussion of the Innervation and Homologues of the Polychaete Palps’, *Acta Zoologica*, 71(1), pp. 45–59. Available at: https://doi.org/10.1111/j.1463-6395.1990.tb01180.x.

Orrhage, L. (1991) ‘On the Innervation and Homologues of the Cephalic Appendages of the Aphroditacea (Polychaeta)’, *Acta Zoologica*, 72(4), pp. 233–246. Available at: https://doi.org/10.1111/j.1463-6395.1991.tb01201.x.

Orrhage, L. (1993) ‘On the Microanatomy of the Cephalic Nervous System of Nereidae (Polychaeta), with a Preliminary Discussion of Some Earlier Theories on the Segmentation of the Polychaete Brain’, *Acta Zoologica*, 74(2), pp. 145–172.

Orrhage, L. (1995) ‘On the Innervation and Homologues of the Anterior End Appendages of the Eunicea (Polychaeta), with a Tentative Outline of the Fundamental Constitution of the Cephalic Nervous System of the Polychaetes’, *Acta Zoologica*, 76(3), pp. 229–248. Available at: https://doi.org/10.1111/j.1463-6395.1995.tb00996.x.

Orrhage, L. (1999) ‘On the morphological value of the glycerid-goniadid prostomium and its appendages (Polychaeta)’, *Acta Zoologica*, 80(3), pp. 251–264. Available at: https://doi.org/10.1046/j.1463-6395.1999.00025.x.

Orrhage, L. (2001) ‘On the anatomy of the central nervous system and the morphological value of the anterior end appendages of Ampharetidae, Pectinariidae and Terebellidae (Polychaeta)’, *Acta Zoologica*, 82(1), pp. 57–71. Available at: https://doi.org/10.1046/j.1463-6395.2001.00070.x.

Orrhage, L. and Eibye-Jacobsen, D. (1998) ‘On the Anatomy of the Central Nervous System of Phyllodocidae (Polychaeta) and the Phylogeny of Phyllodocid Genera: a New Alternative’, *Acta Zoologica*, 79(3), pp. 215–234. Available at: https://doi.org/10.1111/j.1463-6395.1998.tb01160.x.

Orrhage, L. and Müller, M.C.M. (2005) ‘Morphology of the nervous system of Polychaeta (Annelida)’, *Hydrobiologia*, 535(1), pp. 79–111. Available at: https://doi.org/10.1007/s10750-004-4375-4.

Özpolat, B.D. *et al.* (2021) ‘The Nereid on the rise: Platynereis as a model system’, *EvoDevo*, 12(1), p. 10. Available at: https://doi.org/10.1186/s13227-021-00180-3.

Purschke, G. (2015) ‘24 Annelida: basal groups and Pleistoannelida’, *Structure and evolution of invertebrate nervous systems*, p. 254.

Purschke, G., Bleidorn, C. and Struck, T. (2014) ‘Systematics, evolution and phylogeny of Annelida – A morphological perspective’, *Memoirs of Museum Victoria*, 71, pp. 247–269.

Richter, S. *et al.* (2010) ‘Invertebrate neurophylogeny : suggested terms and definitions for a neuroanatomical glossary.’, *Frontiers in Zoology*, 7(1), pp. 1–49.

Rimskaya-Korsakova, N.N., Galkin, S.V. and Malakhov, V.V. (2018) *The neuroanatomy of the siboglinid Riftia pachyptila highlights sedentarian annelid nervous system evolution*, *PLoS ONE*. Available at: https://doi.org/10.1371/journal.pone.0198271.

Rouse, G., Pleijel, F. and Tilic, E. (2022) *Annelida*. Oxford University Press.

Rouse, G.W. and Fauchald, K. (1997) 'Cladistics and Polychaetes', *Zoologica Scripta*, 26(2), pp. 139–204. Available at: https://doi.org/10.1111/j.1463-6409.1997.tb00412.x.

Rouse, G.W. and Pleijel, F. (2001) *Polychaetes*. Oxford, New York: Oxford University Press. Available at: https://doi.org/10.1111/j.1439-0469.2004.00263.x.

Rouse, G.W. and Pleijel, F. (2003) 'Problems in polychaete systematics', *Hydrobiologia*, 496, pp. 175–189.

Schmidbaur, H. *et al.* (2020) 'Within-family plasticity of nervous system architecture in Syllidae (Annelida, Errantia)', *Frontiers in Zoology*, 17(20), pp. 1–44. Available at: https://doi.org/10.1186/s12983-020-00359-9.

Starunov, V.V., Voronezhskaya, E.E. and Nezlin, L.P. (2017) 'Development of the nervous system in Platynereis dumerilii (Nereididae, Annelida)', *Frontiers in Zoology*, 14(1), pp. 1–20. Available at: https://doi.org/10.1186/s12983-017-0211-3.

Weigert, A. *et al.* (2014) 'Illuminating the base of the Annelid tree using transcriptomics', *Molecular Biology and Evolution*, 31(6), pp. 1391–1401. Available at: https://doi.org/10.1093/molbev/msu080.

Weigert, A. and Bleidorn, C. (2016) 'Current status of annelid phylogeny', *Organisms Diversity and Evolution*, 16(2). Available at: https://doi.org/10.1007/s13127-016-0265-7.

Williams, E.A. and Jékely, G. (2019) 'Neuronal cell types in the annelid Platynereis dumerilii', *Current Opinion in Neurobiology*, 56, pp. 106–116. Available at: https://doi.org/10.1016/j.conb.2018.12.008.

Wilson, D.P. (1936) 'Memoirs: The Development of the Sabellid Branchiomma vesiculosum', *Journal of Cell Science*, 2(312), pp. 543–603.

Wilson, D.P. (1982) 'The larval development of three species of Magelona (Polychaeta) from localities near Plymouth', *Journal of the Marine Biological Association of the United Kingdom*, 62(2), pp. 385–401.

Winchell, C.J., Valencia, J.E. and Jacobs, D.K. (2010) 'Confocal analysis of nervous system architecture in direct-developing juveniles of Neanthes arenaceodentata (Annelida, Nereididae)', *Frontiers in Zoology*, 7(1), pp. 1–19. Available at: https://doi.org/10.1186/1742-9994-7-17.

Worsaae, K., Rimskaya-Korsakova, N.N. and Rouse, G.W. (2016) 'Neural reconstruction of bone-eating Osedax spp. (Annelida) and evolution of the siboglinid nervous system', *BMC Evolutionary Biology*, 16(1). Available at: https://doi.org/10.1186/s12862-016-0639-7.

Chapter VI: General Discussion

A short statement about Homology

Homology is a tricky and elusive concept, and although Remane´s "Criteria of homology" (Remane, 1952) gave us a tool to develop homology hypotheses, homology itself is difficult to determine precisely (Stach and Starck, 2023). The latter fact even resulted in the suggestion of not using the term homology in comparative biological approaches (Cracraft, 2023). The herein presented investigations do not aim to participate in the ongoing discussions about potential concepts and putative attempts to face homology (see e.g., (Scholtz, 2005; Szucsich and Wirkner, 2007; DiFrisco, Wagner and Love, 2023; Göpel and Richter, 2023; Minelli, 2023; Schlosser, 2023)). Nevertheless, the presented dissertation intends to formulate a homology hypothesis based on our morphological descriptions of annelid head appendages in the light of the recent molecular phylogenies (Weigert *et al.*, 2014; Weigert and Bleidorn, 2016). Nevertheless, with our sole morphological dataset, our perspective is limited to biological homology, which we understood as morphological features of different, related taxa with the same evolutionary origin, thus the so-called phylogenetic or evolutionary homology between species, and the serial or iterative homology within individuals (Müller, 2003; Wagner, 2014). For the herein presented observations and discussions, we used the perspective of general neuronal innervation patterns, which are assumed to be more conserved than other organ systems (Bullock and Horridge, 1965; Rouse and Fauchald, 1997). Furthermore, these datasets have been shown to provide potential for assessing the homology of anterior appendages (Orrhage, 1980; Orrhage and Müller, 2005). In addition, the investigations aim to include the ontogenetic developmental patterns of the head appendages in addition to their neuronal as well as muscular innervation patterns. The latter approach was chosen to gain additional comparable data and another perspective that helps to minimize the possibility that the presented findings are caused by functional constraints (Tilic *et al.*, 2015; Beckers, Pein and Bartolomaeus, 2022).

Definition of the head appendages in Annelida

The annelid head appendages have fascinated generations of scientists, but their shear morphological diversity and baffling distribution among polychaete families have hampered

cladistics attempts based on morphology (Rouse and Fauchald, 1997; Rouse and Pleijel, 2001, 2003). The external morphology of head appendages has been extensively discussed in the past and has contributed to their definition and classification (Rouse and Pleijel, 2003; Struck, 2011; Purschke, Bleidorn and Struck, 2014; Purschke, 2015). However, the definitions of palps, antennae, tentacular cirri, and buccal lips, summarizing the actual diversity of head appendages, are difficult to differentiate solely by external morphological traits.

In the following, I give three short examples of external character traits of members of the Oweniidae (Paleoannelida), Eunicida (Errantia), and Glyceriformia (Phylodocoda, Errantia), that can be misleading for our understanding of homologous characters within Annelida. In Oweniidae, species of *Myriowenia* sp. exhibit elongated feeding-palps, containing a coelomic cavity and a ciliated food-rim, and thus exhibit a classic feeding-palp reflecting the feeding-palps of Magelonidae - the sister group to Oweniidae (Weigert and Bleidorn, 2016; Beckers *et al.*, 2019). *Owenia fusiformis*, on the other hand, has a large terminal `tentacular crown` (see (Beckers *et al.*, 2019)). Due to their innervation patterns, both anterior appendages are homologous to feeding-palps, although they differ strongly externally. In Eunicida, we have the opposite case where e.g. five (Eunicidae & Onuphidae) of the most anterior head appendages look externally identical, but when comparing internal morphological features and their neuronal innervation, three antennae and a pair of palps (most ventrally located) are present (Kuhl, Bartolomaeus and Beckers, 2022). In Glycerifomia, solely the neuronal innervation pattern illuminates a fusion of palps to the conical prostomium (Orrhage, 1999).

These three examples nicely illustrate, that an additional observation of the neuronal innervation patterns and hence of the highly conserved nervous system scaffold (Bullock and Horridge, 1965; Rouse and Fauchald, 1997) - besides external features - is necessary to define and differentiate between head appendages in Annelida. This fact was already proposed by Orrhage (Orrhage and Müller, 2005). However, the herein presented analyses suggest an adjustment of this valid and powerful tool to examine evolutionary old character traits such as head appendages. Notably, Orrhage's theory of the `12 palp nerve roots` could neither conform to recent observations concerning the neuronal scaffolds of Magelonidae, Amphinomidae, Nereididae, Spionidae, and Terebelliformia (ChapterII, VI and V) nor the neuronal innervations observed in Oweniidae, Eunicida (Beckers *et al.*, 2019; Kuhl, Bartolomaeus and Beckers, 2022) and Syllidae (Schmidbaur *et al.*, 2020). A simplification of his findings, e.g., a differentiation only between palp nerves innervated by both roots (*pn1*)

and palp nerves innervated solely by the ventral (*pn3*) or dorsal root (*pn2*) of the circumoesophageal connectives, as stated by Schmidbaur et al., (2020), seems more reasonable and replicable, without losing discernment (Chapter V).

Are feeding-palps of Paleoannelida and Sedentaria (distantly related taxa) homologous

The similarity of feeding-palps of Paleoannelida and Sedentaria always inspired cladistics attempts before the era of molecular phylogenies and lead to the assumption that Magelonidae and Spionidae represent closely related taxa (Spionida) (Rouse and Fauchald, 1997). Although recent investigations highlighted discrepancies concerning the neuronal architecture of the brain by investigating the anterior nervous system of adult *Magelona mirabilis* and compared to Orrhage´s findings, the general neuronal innervation pattern of the feeding-palps coincided in both studies (Orrhage, 1966; Beckers, Helm and Bartolomaeus, 2019) and our own observations (Chapter IV)). Based on the latter and subsequent observations focussing on basally-branching taxa such as Oweniidae (Beckers *et al.*, 2019) and Chaetopteridae (Helm, Schwarze and Beckers, 2022), putative plesiomorphic character states for Annelida were formulated. Hence, a medullary, simplified central nervous system and feeding-palps innervated by the ventral and dorsal part of the brain seemingly represent a character already present in the last common annelid ancestor.

To test whether these findings can be broadened to a higher taxonomic level, we therefore investigated the innervation patterns of larval feeding-palps of annelid key taxa – the Magelonidae, Amphinomidae and Spionidae – and compared them with the neuronal innervation pattern of adult specimens of the same families (Chapter IV). As a result, we can suggest a homology of larval feeding-palps of Paleoannelida, Amphinomidae, and Spionidae, based on the same neuronal innervation by neurite bundles of the ventral and dorsal root of the circumosophageal connectives. Interestingly both, the basally-branching Magelonidae as well as the deeply nested Spionidae, gradually transfer their larval feeding-palps into adult ones. Consequently, the larval and adult feeding-palps of both families share the same neuronal innervation pattern. In contrast, adult Amphinomidae do not exhibit the neuronal innervation pattern described for the feeding-palps of their Rostraria larvae. Due to a drastic metamorphosis and a change of lifestyle from planktonic filter feeding (Barroso *et al.*, 2010) towards a life as benthic scavengers (Fauchald and Jumars, 1979; Jumars, Dorgan and Lindsay,

2015) even remnants of the larval pattern are missing. Nevertheless, the larval feeding palps in all three families – as well as the adult ones in magelonids and spionids – share the same neuronal innervation pattern and can therefore be called homologous.

Another intensively discussed group are the Terebelliformia – a taxon deeply nested within the Sedentaria. Their `buccal tentacles` were homologised with all kind of anterior annelid appendages, reaching from rudiments of antennae to independent outgrowths of the alimentary canal or a similarity to palps (Nilsson, 1912; Binard and Jeener, 1928; Holthe, 1986; Rouse and Fauchald, 1997; Orrhage, 2001; Zhadan and Tzetlin, 2002; Orrhage and Müller, 2005). Interestingly, the main argument to suggest the `buccal tentacles` as outgrowth of the alimentary canal was the close association with the ventral brain part, and thus the ventral origin of the innervating neurite bundles proceeding into them (Orrhage, 2001). This hypothesis could be rejected by uncovering a typical annelid pattern of neuronal innervation of the stomatogastric system by solely the ventral root of the circumosophageal connectives. Furthermore, a close association of the palp innervation and the alimentary canal seems to be the rule and not the exception for Terebelliformia and Annelida in general (Chapter II). In addition, the herein presented data demonstrate the neuronal innervation of the `buccal tentacles` by both roots of the circumoesophageal connectives based on observations of the simplified adult and the less condensed and more complex larval anterior nervous system. Our discernment therefore profited from the additional perspective on larval versus adult neuronal architectures (Chapter II & IV).

Because the innervation patterns of larval and adult Magelonidae, Spionidae, and Terebelliformia as well as larval Amphinomidae follow the same neuronal innervating scaffold formed of the ventral and dorsal root of the circumoesophageal connectives, homology of the latter structures among the investigated taxa can be proposed. As a consequence, feeding-palps across Annelida can be considered as being homologous.

Are palps in general homologous among Annelida?

As mentioned above, data concerning the putative homology of head appendages across the annelid tree of life are available for basally branching groups such as Oweniidae, Magelonidae, and Chaetpteridae and sedentary annelids such as Terebelliformia, Spionidae, Siboglinidae, Sabellaridae…. However, a lack of comparative morphological studies in particular for errant

taxa, such as those for Eunicidae (Kuhl, Bartolomaeus and Beckers, 2022) and Syllidae (Schmidbaur *et al.*, 2020), complicates a final homology hypothesis.

A perfect group to fill this gap of knowledge are the Phyllodocida, which exhibit all types of the most common head appendages among annelid families - palps, antennae, and tentacular cirri (Purschke, 2015). Nevertheless, the condensed neuronal architecture of adult Nereididae, as mentioned for Terebelliformia, hampered observations of the exact neuroanatomical origin of especially the main palp nerve (*pn1*) which would e.g., help to clarify the contribution of the dorsal and ventral root in the innervation of the short sensorial palps. Notably, by including 6dpf (days-post-fertilisation) old larvae of *P. dumerilii* in our comparison, the herein presented investigations confirm the neuronal pattern observed for adult *P. massiliensis* (Chapter V). Consequently, the lateral and median (if present) antennae of Phyllodocida (Orrhage, 1991; Schmidbaur *et al.*, 2020) and Eunicida (Orrhage, 1995; Kuhl, Bartolomaeus and Beckers, 2022), which are innervated solely by the dorsal root of the circumoesophageal connectives, as well as the tentacular cirri among Phyllodocida (Orrhage and Eibye-Jacobsen, 1998; Winchell, Valencia and Jacobs, 2010) can be called homologous. Tentacular cirri can strongly differ in numbers with up to eight pairs in *Leocrates* (Hesionidae) (Orrhage, 1991) and are assumed to be simplified, transformed parapodia, which fuse to the anterior end by cephalization during ontogenesis (Winchell, Valencia and Jacobs, 2010), own observation. Although their number was used as an argument not to be homologous structures (Orrhage and Eibye-Jacobsen, 1998), their neuronal innervation pattern, as observed for *Platynereis,* resembles that of simplified parapodia. Furthermore duplications, such as in the second ventral and dorsal tentacular cirrus in *Platynereis*, can be assumed and represent a serial homology when compared to the first one.

Last but not least, all phyllodocid and eunicid taxa examined so far share the same neuronal innervation pattern when observing the most prominent type of errant head appendages - the stout sensorial palps (Orrhage, 1991, 1995; Orrhage and Eibye-Jacobsen, 1998; Schmidbaur *et al.*, 2020; Kuhl, Bartolomaeus and Beckers, 2022). In addition, even in palp-less taxa such as Glyceriformia, five pairs of prostomial nerves comparable to the conditions observed in other phyllodocid taxa have been described (Orrhage, 1991). These nerves seem to resemble the same innervation pattern, suggesting a fusion of palps toward the conical prostomium. Therefore, we propose that short sensorial palps as well as their neuronal

innervation pattern already evolved in the stem lineage of Errantia, a hypothesis already proposed for Eunicia (Kuhl, Bartolomaeus and Beckers, 2022) (Chapter V).

Interestingly, by comparing the larval neuronal innervation pattern of *Platynereis dumerilii*, we found the same conserved innervating scaffold formed of neurite bundles of the ventral and dorsal root of the circumoesophageal connectives, that was already described in Magelonidae, larval Amphinomidae, and Spionidae (Fig. 6 of Chapter V).

Consequently, our investigations highly support a homology of the different palp types across the annelid tree of life based on the neuronal innervation patterns of annelid feeding-palps and the short sensorial palps. Furthermore, the importance of palps for the evolutionary success of this old and diverse group of invertebrates is shown by the high conservation of this puativley plesiomorph and the evolutionarily old character trait.

Nevertheless, latest investigation of the anterior nervous system and the respective neuronal innervation patters of Scalibregmatidae, suggest the first putative sign of convergent evolution of palps in annelids (unpublished data). Hence, the neuronal innervation patterns and the lack of the latter in closely related taxa (Martínez, Di Domenico and Worsaae, 2014) suggest a parallel evolution of palp-like appendages, that can not be homologized with that of the remaining Annelida. However, further analyses are needed to back up this assumption.

In summary, Orrhage´s descriptions are mostly congruent with the findings of recent investigations and the data presented herein. Nevertheless, major discrepancies can be observed in terms of the neuronal architecture of the brain. In particular, the presence and distribution of commissures he described in most of his investigated taxa as well as the presence of important neuronal patterns could not be validated by our investigations and other studies (Beckers, Helm and Bartolomaeus, 2019; Schmidbaur *et al.*, 2020).

Distribution of the head appendages in Annelida

In the following passage, I will not list all the knowledge about the distribution of head appendages among annelid families, but the paragraph intends to embed our contribution into the current knowledge and to present the consequences of these findings on the understanding of the evolution of head appendages in Annelida.

Previous studies of adult Amphinomidae have proposed two to three antennae and the most ventrally located pair of appendages as being palps (Orrhage, 1990). However, our investigations of larval and adult Amphinomidae (Chapter IV) could not validate former observations. Instead, our studies concludes a homologation of larval feeding-palps of the amphinomid Rostraria larvae with the feeding-palps of the Paleoannelida and supports a subsequent metamorphic reduction in Amphinomidae. Consequently, two pairs of lateral and one median antennae have to be considered as representing the various head appendages in adult *Eurythoe complanata*. Interestingly, we showed that the innervation pattern of the buccal lips in adult Amphinomidae reflects the neuronal innervation pattern observed for Eunicida (Errantia), in particular the innervating neurite bundles solely emanating from the ventral root of the circumoesophageal connectives (Kuhl, Bartolomaeus and Beckers, 2022).

Our findings therefore suggest a different evolutionary scenario for the evolution of short sensorial palps and buccal lips than previously suggested. The transformation from feeding-palps to short sensorial palps occurred in the last common ancestor of Errantia, but the buccal lips have already evolved in the common ancestor of Amphinomidae (+Sipuncula) and Pleistoannelida. In addition, although our findings propose five antennae for adult Amphinomidae, the results of previous studies support the idea of the evolutionary origin of antennae in annelids in the last common ancestor of Amphinomidae (+Sipuncula) and Pleistoannelida (Chapter IV).

With our observation of the anterior nervous system of adult and larval Terebelliformia, we furthermore support the homology of the `buccal tentacles` with feeding-palps in other sedentary taxa such as Spionidae and Paleoannelida (Oweniidae, Magelonidae) (Chapter II & IV). Therefore, all slender annelid head appendages used for feeding as well as the stout anterior-most sensory head structures in Errantia have to be called homologous across different ontogenetic stages. This homology assumption is based on their neuronal (as well as muscular) innervation patterns and the related neurodevelopmental patterns. Hence, the herein presented analyses solve an everlasting scientific discussion concerning the evolution of an annelid key character and propose important comparative investigations that will contribute to our understanding of evolutionary scenarios within Annelida.

Conclusion

This thesis has provided crucial insights into the classification and homology of head appendages in Annelida. The morphological diversity and distribution of these structures have posed challenges for previous classifications based on external traits. However, our research has revealed that considering the neuronal innervation patterns alongside external features is essential for accurate differentiation and definition of these appendages. We have also addressed the question of homology among feeding-palps in Paleoannelida and Sedentaria. Despite their evolutionary distance, we have found evidence supporting the notion that the innervation pattern of feeding-palps is conserved, suggesting a common origin in the last common annelid ancestor. Furthermore, we have explored the homology of head appendages across various annelid taxa, including Phyllodocida, and errant taxa such as Eunicida and Syllidae. While we have strong evidence for the homology of palps, antennae, and tentacular cirri in Phyllodocida and Eunicida, further comparative morphological studies are necessary for a complete understanding. Regarding Amphinomidae, our research challenges previous hypotheses, suggesting a different evolutionary scenario. We propose that the transformation from feeding-palps to short sensorial palps occurred in the last common ancestor of Errantia, while buccal lips evolved earlier, in the common ancestor of Amphinomidae (+Sipuncula) and Pleistoannelida. In summary, our study refines the classification of head appendages in Annelida, emphasizes the importance of incorporating neuronal innervation patterns, and proposes homology hypotheses that will guide future research in evolutionary biology within Annelida. Our findings highlight the complexity of these structures and the need for a multifaceted approach to uncover their evolutionary history.

References

Barroso, R. *et al.* (2010) 'Eurythoe complanata (Polychaeta: Amphinomidae), the "cosmopolitan" fireworm, consists of at least three cryptic species', *Marine Biology*, 157(1), pp. 69–80. Available at: https://doi.org/10.1007/s00227-009-1296-9.

Beckers, P. *et al.* (2019) 'The central nervous system of Oweniidae (Annelida) and its implications for the structure of the ancestral annelid brain', *Frontiers in Zoology*, 16(1), pp. 1–21. Available at: https://doi.org/10.1186/s12983-019-0305-1.

Beckers, P., Helm, C. and Bartolomaeus, T. (2019) 'The anatomy and development of the nervous system in Magelonidae (Annelida) – insights into the evolution of the annelid brain', *BMC Evolutionary Biology*, 19, p. 173. Available at: https://doi.org/10.1186/s12862-019-1498-9.

Beckers, P., Pein, C. and Bartolomaeus, T. (2022) 'Fine structure of mushroom bodies and the brain in Sthenelais boa (Phyllodocida, Annelida)', *Zoomorphology*, 141(1), pp. 19–36. Available at: https://doi.org/10.1007/s00435-021-00546-0.

Binard, A. and Jeener, R. (1928) *Morphologie du lobe préoral des polychètes*.

Bullock, T. and Horridge, G.A. (1965) *Structure and function in the nervous systems of invertebrates.*

Cracraft, J. (2023) 'It is time to move on from homology in comparative biology', *Journal of Morphology*, 284(1), p. e21530. Available at: https://doi.org/10.1002/jmor.21530.

DiFrisco, J., Wagner, G.P. and Love, A.C. (2023) 'Reframing research on evolutionary novelty and co-option: Character identity mechanisms versus deep homology', *Seminars in Cell & Developmental Biology*, 145, pp. 3–12. Available at: https://doi.org/10.1016/j.semcdb.2022.03.030.

Fauchald, K. and Jumars, P.A. (1979) 'The diet of worms: a study of polychaete feeding guilds', *Oceanography and Marine Biology Annual Review*, 17, pp. 193–284.

Göpel, T. and Richter, S. (2023) 'Homologues and homology and their related terms in phylogenetic systematics', *Cladistics*, 39(3), pp. 240–248. Available at: https://doi.org/10.1111/cla.12526.

Helm, C., Schwarze, G. and Beckers, P. (2022) 'Loss of complexity from larval towards adult nervous systems in Chaetopteridae (Chaetopteriformia , Annelida) unveils evolutionary patterns in Annelida', *Organisms Diversity & Evolution*, 22, pp. 631–647. Available at: https://doi.org/10.1007/s13127-022-00553-z.

Holthe, T. (1986) 'Evolution, systematics, and distribution of the Polychaeta Terebellomorpha, with a catalogue of the taxa and a bibliography', *Gunneria*, 55, pp. 1–236.

Jumars, P.A., Dorgan, K.M. and Lindsay, S.M. (2015) 'Diet of Worms Emended: An Update of Polychaete Feeding Guilds', *Annual Review of Marine Science*, 7(1), pp. 497–520. Available at: https://doi.org/10.1146/annurev-marine-010814-020007.

Kuhl, S., Bartolomaeus, T. and Beckers, P. (2022) 'How Do Prostomial Sensory Organs Affect Brain Anatomy? Phylogenetic Implications in Eunicida (Annelida)', *Journal of Marine Science and Engineering*, 10(11), p. 1707. Available at: https://doi.org/10.3390/jmse10111707.

Martínez, A., Di Domenico, M. and Worsaae, K. (2014) 'Gain of palps within a lineage of ancestrally burrowing annelids (Scalibregmatidae)', *Acta Zoologica*, 95(4), pp. 421–429. Available at: https://doi.org/10.1111/azo.12039.

Minelli, A. (2023) 'A refreshed approach to homology—Prioritizing epistemology over metaphysics', *Journal of Morphology*, 284(1), p. e21533. Available at: https://doi.org/10.1002/jmor.21533.

Müller, G.B. (2003) 'Homology: the evolution of morphological organization', in G.B. Müller and S.A. Newman (eds) *Origination of organismal form: Beyond the gene in developmental and evolutionary biology*. MIT Press Cambridge, MA, pp. 51–69.

Nilsson, D. (1912) *Beiträge zur Kenntnis des Nervensystems der Polychaeten*. Almquist & Wiksells.

Orrhage, L. (1966) 'Über die Anatomie des zentralen Nervensystems der sedentaren Polychaeten', *Arkiv för Zoologi*, 19(3), pp. 99–133.

Orrhage, L. (1980) 'On the structure and homologues of the anterior end of the polychaete families sabellidae and serpulidae', *Zoomorphology*, 96(1–2), pp. 113–167. Available at: https://doi.org/10.1007/BF00310081.

Orrhage, L. (1990) 'On the Microanatomy of the Supraoesophageal Ganglion of Some Amphinomids (Polychaeta Errantia), with Further Discussion of the Innervation and Homologues of the Polychaete Palps', *Acta Zoologica*, 71(1), pp. 45–59. Available at: https://doi.org/10.1111/j.1463-6395.1990.tb01180.x.

Orrhage, L. (1991) 'On the Innervation and Homologues of the Cephalic Appendages of the Aphroditacea (Polychaeta)', *Acta Zoologica*, 72(4), pp. 233–246. Available at: https://doi.org/10.1111/j.1463-6395.1991.tb01201.x.

Orrhage, L. (1995) 'On the Innervation and Homologues of the Anterior End Appendages of the Eunicea (Polychaeta), with a Tentative Outline of the Fundamental Constitution of the Cephalic Nervous System of the Polychaetes', *Acta Zoologica*, 76(3), pp. 229–248. Available at: https://doi.org/10.1111/j.1463-6395.1995.tb00996.x.

Orrhage, L. (1999) 'On the morphological value of the glycerid-goniadid prostomium and its appendages (Polychaeta)', *Acta Zoologica*, 80(3), pp. 251–264. Available at: https://doi.org/10.1046/j.1463-6395.1999.00025.x.

Orrhage, L. (2001) 'On the anatomy of the central nervous system and the morphological value of the anterior end appendages of Ampharetidae, Pectinariidae and Terebellidae (Polychaeta)', *Acta Zoologica*, 82(1), pp. 57–71. Available at: https://doi.org/10.1046/j.1463-6395.2001.00070.x.

Orrhage, L. and Eibye-Jacobsen, D. (1998) 'On the Anatomy of the Central Nervous System of Phyllodocidae (Polychaeta) and the Phylogeny of Phyllodocid Genera: a New Alternative', *Acta Zoologica*, 79(3), pp. 215–234. Available at: https://doi.org/10.1111/j.1463-6395.1998.tb01160.x.

Orrhage, L. and Müller, M.C.M. (2005) 'Morphology of the nervous system of Polychaeta (Annelida)', *Hydrobiologia*, 535(1), pp. 79–111. Available at: https://doi.org/10.1186/s40850-021-00094-6.

Purschke, G. (2015) '24 Annelida: basal groups and Pleistoannelida', *Structure and evolution of invertebrate nervous systems*, p. 254.

Purschke, G., Bleidorn, C. and Struck, T. (2014) 'Systematics, evolution and phylogeny of Annelida – A morphological perspective', *Memoirs of Museum Victoria*, 71, pp. 247–269. Available at: https://doi.org/10.24199/j.mmv.2014.71.19.

Rouse, G.W. and Fauchald, K. (1997) 'Cladistics and Polychaetes', *Zoologica Scripta*, 26(2), pp. 139–204. Available at: https://doi.org/10.1111/j.1463-6409.1997.tb00412.x.

Rouse, G.W. and Pleijel, F. (2001) *Polychaetes*. Oxford, New York: Oxford University Press. Available at: https://doi.org/10.1111/j.1439-0469.2004.00263.x.

Rouse, G.W. and Pleijel, F. (2003) 'Problems in polychaete systematics', *Hydrobiologia*, 496, pp. 175–189. Available at: https://doi.org/10.1023/A:1026188630116.

Schlosser, G. (2023) 'Rebuilding ships while at sea—Character individuality, homology, and evolutionary innovation', *Journal of Morphology*, 284(1), p. e21522. Available at: https://doi.org/10.1002/jmor.21522.

Schmidbaur, H. *et al.* (2020) 'Within-family plasticity of nervous system architecture in Syllidae (Annelida, Errantia)', *Frontiers in Zoology*, 17(20), pp. 1–44. Available at: https://doi.org/10.1186/s12983-020-00359-9.

Scholtz, G. (2005) 'Homology and ontogeny: Pattern and process in comparative developmental biology', *Theory in Biosciences*, 124(2), pp. 121–143. Available at: https://doi.org/10.1016/j.thbio.2005.09.002.

Stach, T. and Starck, M. (2023) 'Can you tell me anything about homology? Any one thing that is new?', *Journal of Morphology*, 284(5), p. e21578. Available at: https://doi.org/10.1002/jmor.21578.

Struck, T.H. (2011) 'Direction of evolution within Annelida and the definition of Pleistoannelida', *Journal of Zoological Systematics and Evolutionary Research*, 49(4), pp. 340–345. Available at: https://doi.org/10.1111/j.1439-0469.2011.00640.x.

Szucsich, N.U. and Wirkner, C.S. (2007) 'Homology: A synthetic concept of evolutionary robustness of patterns.', *Zoologica Scripta*, 36(3), pp. 281–289. Available at: https://doi.org/10.1111/j.1463-6409.2007.00275.x.

Tilic, E. *et al.* (2015) 'Phylogenetic significance of chaetal arrangement and chaetogenesis in Maldanidae (Annelida)', *Zoomorphology*, 134(3), pp. 383–401. Available at: https://doi.org/10.1007/s00435-015-0272-9.

Wagner, G.P. (2014) 'A Conceptual Roadmap to Homology', in *Homology, Genes, and Evolutionary Innovation*. Princeton University Press, Princeton; Oxford, 2014, pp. 38–89.

Weigert, A. *et al.* (2014) 'Illuminating the base of the Annelid tree using transcriptomics', *Molecular Biology and Evolution*, 31(6), pp. 1391–1401. Available at: https://doi.org/10.1093/molbev/msu080.

Weigert, A. and Bleidorn, C. (2016) 'Current status of annelid phylogeny', *Organisms Diversity and Evolution*, 16(2), pp. 345–362. Available at: https://doi.org/10.1007/s13127-016-0265-7.

Winchell, C.J., Valencia, J.E. and Jacobs, D.K. (2010) 'Confocal analysis of nervous system architecture in direct-developing juveniles of Neanthes arenaceodentata (Annelida, Nereididae)', *Frontiers in Zoology*, 7(1), pp. 1–19. Available at: https://doi.org/10.1186/1742-9994-7-17.

Zhadan, A.E. and Tzetlin, A.B. (2002) 'Comparative morphology of the feeding apparatus in the Terebellida (Annelida: Polychaeta).', *Cahiers de Biologie Marine*, 43(2), pp. 149–164.